MODELING, SIMULATION AND OPTIMIZATION OF GROUND SOURCE HEAT PUMP SYSTEMS

By

MUHAMMAD HAIDER KHAN

Bachelor of Science in Mechanical Engineering

University of Engineering and Technology

Lahore, Pakistan

2000

Submitted to the Faculty of the
Graduate College of the
Oklahoma State University
in partial fulfillment of
the requirements for
the Degree of
MASTER of SCIENCE
December, 2004

MODELING, SIMULATION AND OPTIMIZATION OF GROUND SOURCE HEAT PUMP SYSTEMS

Thesis Approved:

Dr. J.D. Spitler
Thesis Advisor

Dr. D.E. Fisher

Dr. R.D. Delahoussaye

Dr. A. Gordon Emslie
Dean of the Graduate College

ACKNOWLEDGEMENTS

First and foremost, I am thankful to my God for bestowing me with patience and ability to complete this task.

I feel deeply gratified to my advisor Dr. J.D. Spitler, his intelligence and insight into the subject is unparalleled. I feel like I can spend a life time learning from him. I extend my sincere gratitude to my committee members for their advice on improving upon my work.

This work wouldn't have been possible without sacrifices made by my wife and my mother. They have always been there for me.

Last but not the least I would like to thank my fellow research assistants and friends, especially Mohammad, Shankar, Calvin, Diego, Aditya, and Liu for there help and advice.

TABLE OF CONTENTS

Chapter Page

Chapter Page

LIST OF FIGURES

Figure Page

Figure Page

LIST OF TABLES

CHAPTER 1

Introduction

1.1 Overview of Ground Source Heat Pump Systems

Currently, ground-source heat pump (GSHP) systems are perhaps one of the most widely used renewable energy resources. GSHP systems use the earth's relatively constant temperature as a heat sink for cooling and a heat source for heating. From a thermodynamic perspective, using the ground as a heat source or sink makes more sense than the ambient air because the temperature is usually much closer to room conditions. The use of liquid instead of air as the source/sink fluid for the heat pump also promotes higher efficiency, which can be attributed to the decrease in difference between the source/sink temperature and the refrigerant temperatures. In addition, the specific heat of water is more than four times greater than that of air.

Besides providing the advantage of having lower energy costs, GSHP systems have also proved to have lower maintenance costs, presumably due to not requiring outdoor equipment (Cane, et al. 1998). Water source heat pumps tend to have a longer service life, as they are not subjected to refrigerant pressures as high or low as those of conventional air source heat pumps. These benefits apparently result in high owner satisfaction, as shown by a survey (DOE 1997), 95% of GSHP system owners were completely satisfied.

GSHP systems are categorized by ASHRAE (1995) based on the heat source or sink used. These categories are: (1) ground-water heat pump (GWHP) systems, (2)

surface water heat pump (SWHP) systems, and (3) ground-coupled heat pump (GCHP) systems.

Ground water heat pump (GWHP) systems utilize water wells. Water from the well is usually circulated to a central water-to-water heat exchanger. On the other side of the water-to-water heat exchanger is a closed loop that is connected to the heat pump(s) or chiller(s). The water-to-water heat exchanger isolates the heat pumps from ground water that may cause corrosion and fouling. For a large building, GWHP systems are lower in cost as compared to GCHP because a single high volume well can serve an entire building, which might require many GCHP boreholes (Rafferty, 1995). Local environmental regulations and factors may be the deciding factor in choosing GWHP.

Surface water heat pump (SWHP) systems typically consist of a Slinky®-type coil located in a water body (lake, pond etc.), water-to-water or water-to-air heat pump and circulating pump. SWHP systems can also be either closed loop or open loop systems, though open loop GWHP systems require an isolating water-to-water heat exchanger to prevent corrosion and fouling. Open loop systems cannot be used in colder climates as antifreeze mixtures are required to prevent freezing of the fluid.

Ground-coupled heat pump (GCHP) systems are often referred to as closed-loop GSHP systems. At a minimum, a GCHP system consists of a water-to-water or water-to-air heat pump, a circulating pump and a ground loop heat exchanger (GLHE). The GLHE can be of two configurations; (i) vertical, and (ii) horizontal. The vertical configuration is typically constructed by placing two high-density polyethylene tubes thermally fused at the bottom to form a U-bend in a vertical borehole. The advantages of using the vertical

configuration include smaller surface area requirements, less adverse variations in performance due to seasonal temperature fluctuations, and higher thermal conductivity for depths below the water table. On the other hand, installation of a horizontal system often costs less than the vertical system because of ease of installation.

The focus of this study is the GSHP system with vertical GLHE configuration. In general, the potential for widespread acceptance of GSHP systems is limited by high first cost, ground area requirement, and lack of designers/design guidelines. The process for GSHP system design is complicated by the large number of degrees-of-freedom. Interacting design parameters include GLHE length, equipment capacity, control strategy, grout type, borehole diameter, U-tube diameter, and circulating fluid. Sizing the GLHE using rules of thumb has been effectively used in the past for residential buildings, but in large-scale commercial and institutional applications, some GSHP systems have failed to meet the design loads after few years of operation. The continuously changing environmental conditions and building loads combined with the very large time constant of the GLHE make it difficult to design without the aid of system simulation. Knowledge of significance of each parameter on the design is very important, as this will indicate which parameters should be changed to get a better design, and can be used as the basis for an optimal design procedure.

The accurate prediction of performance for a GSHP system is not possible without taking into account the variation in thermophysical properties caused by using an antifreeze mixture instead of water. Antifreeze mixtures are used as heat transfer fluid in colder climates. They take place of water as the heat transfer fluid because of their low freezing point. Modeling of antifreeze mixtures is necessary in order for them to be

incorporated in thermal system simulation. The most commonly used antifreeze mixtures are aqueous mixtures of propylene and ethylene glycol and methyl and ethyl alcohol. Thermal conductivity, specific heat capacity, viscosity and density are the thermophysical properties for antifreeze mixtures that are of interest to engineers.

Two variations of the GSHP system are the particular focus of this study. Residential GSHP system with vertical GLHE in cold climatic conditions is studied. A variation of the GSHP system used in cooling-dominated commercial buildings is the hybrid ground source heat pump (HGSHP) system. Commercial buildings are usually cooling dominated, resulting in an imbalance between heat extracted from the ground and heat rejected to the ground. Over time, this imbalance raises the loop temperatures and reduces the heat pump COP. To rectify this problem, either the ground loop heat exchanger size can be increased and/or a supplemental heat rejecter such as cooling tower, pavement heating system, or shallow cooling pond can be added. Increasing the size of the ground loop heat exchanger (GLHE) increases the capital cost and may exceed space constraints. The use of a supplemental heat rejecter may allow the GLHE size to be kept relatively small, and allow for lower fluid temperatures, and, hence, higher heat pump COP. GSHP systems that use a supplemental heat rejecter are known as hybrid ground source heat pump (HGSHP) systems.

1.2 Thesis Objective and Scope

This study aims at developing and using procedures for modeling, simulating and optimizing ground source heat pump systems. It builds on past work performed at

Oklahoma State University by Yavuzturk and Spitler (1999), Chiasson, et al. (2000a,b), Yavuzturk and Spitler (2000), and Ramamoorthy, et al. (2001). Each of the following chapters describes a unique contribution towards a better understanding of GSHP systems, used both in commercial and residential applications. The related literature review is included in each chapter.

Chapter 2 deals with modeling of thermophysical properties of aqueous mixtures of propylene and ethylene glycol and methyl and ethyl alcohol used as antifreeze mixtures. The thermophysical properties modeled are thermal conductivity, specific heat capacity, viscosity, and density. A thorough literature review was done to collect previously published measured data existing for these thermophysical properties for the four antifreeze mixtures. A range of mixing rules from the literature were used to fit the data. The results of the equations were compared and the best equation form for each property was chosen. In some cases, it was necessary to modify existing equation forms to obtain satisfactory fits.

Chapter 3 of the thesis explains different component models that were developed or modified for use in HVACSIM+ (Clark 1985). An overview of developing a system simulation using a graphical user interface for HVACSIM+ (Varanasi 2002) is also presented. Experiences gained in developing improved modeling techniques in HVACSIM+ for fluid flow networks are also discussed. The tool developed for running multiyear simulation is also described.

Chapter 4 of the thesis describes a detailed simulation of a residential GSHP system with antifreeze mixtures. The antifreeze mixture type and concentration have a

number of effects. These include the required ground loop heat exchanger length, the capacity and energy consumption of the heat pump, the circulating pump selection and pumping energy, the flow rate required to maintain turbulent flow in the loop, and the first cost of the system. The complex interaction between all of the design variables is illustrated with a sensitivity analysis for each of the variables. Life cycle cost analysis is carried out based on the electricity costs for the heat pump and circulating pump and first costs for the heat pump, circulating pump, grout, borehole drilling, pipe, and antifreeze.

Chapter 5 describes optimization of the GSHP system design using GenOpt (Wetter, 2000) coupled with HVACSIM+. The buffer program, which mediates between GenOpt and HVACSIM+, is also discussed. The optimization methodology and algorithm used to get the 'best' design is explained.

Chapter 6 describes an HGSHP system simulation. This study applies simulation methodology to predict the performance of HGSHP systems with pavement heating system as the supplemental heat rejecter. The life cycle cost is computed based on the electricity costs for the heat pump and circulating pumps, and first costs for the heat pump, circulating pump, pavement heat rejecter, grout, borehole drilling, and pipe.

Conclusions and recommendations for future work are given in Chapter 7.

CHAPTER 2

Modeling of Thermophysical Properties of Antifreeze Mixtures for Ground Source Heat Pump System Application

2.1 Introduction

Antifreeze mixtures are often used as circulating fluids in ground source heat pump (GSHP) systems to prevent freezing. The most commonly used antifreeze mixtures for GSHP systems are aqueous mixtures of propylene and ethylene glycol and methyl and ethyl alcohol.

Thermal conductivity, specific heat capacity, viscosity, density, and freezing point are the thermophysical properties of antifreeze mixtures that are of interest to engineers. High thermal conductivity and specific heat capacity are desirable as they contribute to good heat transfer and thereby decrease the temperature difference between the fluid and the tube wall. Viscosity is important for two reasons; it determines the pressure drop and it influences the type of flow (laminar or turbulent) that will occur in the heat exchanger. The type of flow is important as it is desirable to have turbulent flow for better heat transfer and a higher flow rate may be required to achieve turbulent flow with higher viscosity fluids. Freezing point temperature is an important thermophysical property to be considered when designing GSHP system, as freezing of the circulating fluid can damage the system and result in costly repairs.

The purpose of this study is to develop models of these thermophysical properties that can be utilized in HVACSIM+. The modeling was done using a mix of analytical and statistical methods. Mixing rule correlations, which use the constituents' pure properties and coefficients calculated by the method of least squares, were found to be appropriate for the application in terms of speed and accuracy. A thorough literature review was done to collect previously published measured data existing for ethyl alcohol and methyl alcohol.

A number of mixing rule correlations from the literature was used to fit the data. In some cases, it was necessary to modify existing equation forms to obtain satisfactory fits. The results of the equation fits were compared and the best equation form for each property was chosen.

2.2 Literature Review

The literature review for this study began with the references provided in Thermophysical Properties Research Literature Retrieval Guide (Chaney et al. 1982) and, Thermal Conductivity and Viscosity Data of Fluid Mixtures (Stephan and Heckenberger 1988) and Thermophysical Properties of Liquid Secondary Refrigerants (Melinder 1997) for experimental data. Where the desired data were not found in the above references reverse and forward citation searches were performed. Data for the desired range for Propylene and Ethylene Glycol mixtures was found in ASHRAE Handbook, Fundamentals (ASHRAE 2001), so further search for glycol properties was not conducted.

The thermophysical properties for the pure substances were taken from Physical and Thermodynamic Properties of Pure Chemicals (Daubert and Danner 1989), Recommended Data of Selected Compounds and Binary Mixtures (Stephan and Hildwein 1987), Specific Heat, Non Metallic Liquids and Gases, Thermophysical Properties of Matter (Touloukian and Makita 1970), Thermal Conductivity, Non Metallic Liquids and Gases, Thermophysical Properties of Matter (Touloukian et al. 1970a) and Viscosity, Thermophysical Properties of Matter (Touloukian et al. 1970b)

Existing mixing rule correlations for each of the thermophysical properties were reviewed from references provided in The Properties of Gases and Liquids (Reid et al. 1977) and Thermophysical Properties of Fluids: an Introduction to Their Prediction (Assael et al. 1996), along with the references in research papers.

Details of each reference are given in Table 2-1 including the range of experimental data available. A summary of the references that were used to collect experimental data and the references that were not used but which may be of interest, are given in Table 2-2. Where multiple sources covered the same range of data, preference was given to the latest data.

Table 2-1: Experimental data range in each reference

Reference	Organic Component	Temperature (C)	Concentration (Wt%)	No of Data Points	Property
ASHRAE (2001)	PG	T_{freeze}-125	0 - 90	271	ρ, μ, C_p, k
	EG	T_{freeze}-125	0 - 90	271	ρ, μ, C_p, k
Bates and Palmer (1938)	EtoH	10 - 60	0 - 100	105	K
	MeoH	10 - 60	0 - 100	105	K
Bearce et al. (2003)	EtoH	10 - 40	0 - 100	175	P
	MeoH	0 - 20	0 - 100	100	P
Bulone et al. (1991)	EtoH	-15 - 15	0 - 20	49	P
	MeoH	-15 - 15	0 - 10	49	P
Bulone et al. (1989)	EtoH	-15 - 20	0 - 20	64	M
	MeoH	-15 - 21	0 - 15	64	M
Dizechi and Marschall (1982)	EtoH	10 - 50	0 - 100	142	μ , ρ
	MeoH	10 - 50	0 - 100	252	μ , ρ
Dunstan and Thole (1909)	EtoH	20 - 30	0 - 99	21	M
Gillam and Lamm (1955)	EtoH	4	4 - 29	3	K
Halfpap (1981)	EtoH	-30 - 20	10 - 70	217	M
	MeoH	-20 - 20	5 - 20	137	M
Ivin and Sukhatme (1967)	MeoH	27 - 40	0 - 100	47	C_p
Kurata et al. (1971)	MeoH	-110 - 10	50 - 100	63	ρ , μ
Melinder (1997)	MeoH	-45 - 20	8 - 44	52	ρ, μ, C_p, k, T_{freeze}
	EtoH	-45 - 20	11 - 60	52	ρ, μ, C_p, k, T_{freeze}
Mikhail and Kimmel (1961)	MeoH	25 - 50	0 - 100	60	ρ , μ
Misra and Varshni (1961)	EtoH	0 - 80	40 - 100	25	M
Perry (1963)	EtoH	3 - 41	4 - 100	15	C_p
	MeoH	5 - 40	5 - 100	18	C_p
Reidel (1951)	EtoH	-40 - 80	0 - 100	71	K
	MeoH	-40 - 60	0 - 100	59	K
Commerical Solvent Corporation (1960)	MeoH	T_{freeze}- 0	20 - 50	144	P
	MeoH	25 - 40	0 - 100	63	P
Wagenbreth (1970)	EtoH	-20 - 20	30 - 100	68	P
Waterfurnace International Technical Bulletin (1985)	EtoH	-1.11, -9.44, -22.22, -34.33	15&20, 22&25, 35&36,45&52	4	ρ, μ, C_p, k
	MeoH	-1.11, -9.44, -22.22, -34.34	15&20,22&25, 35&36,45&53	4	ρ, μ, C_p, k
Westh and Hvidt (1993)	EtoH	-34 - 19	0 - 100	276	C_p
	MeoH	-34 - 20	0 - 100	284	C_p

* T_{freeze} = Freezing point of the mixture for a particular concentration.

Table 2-2: References used for experimental data collection

property	Aqueous Mixture of					
	Ethyl Alcohol		Methyl Alcohol		Ethylene Glycol	Propylene Glycol
	Ref. used	Ref. not used	Ref. used	Ref. not used	Ref. used	Ref. used
Density	**Melinder (1997), Wagenbreth (1970), Bulone et al. (1991), Waterfurnace International Technical Bulletin (1985), Sorensen (1983), Bearce et al. (2003)**	**Dizechi and Marschall (1982)**	**Bulone et al. (1991), Waterfurnace International Technical Bulletin (1985), Kurata et al. (1971), Melinder (1997), Mikhail and Kimmel (1961), Commerical Solvent Corporation (1960)**	**Dizechi and Marschall (1982)**	**ASHRAE (2001)**	**ASHRAE (2001)**
Viscosity	**Bulone et al. (1989), Dizechi and Marschall (1982), Halfpap (1981), Melinder (1997), Misra and Varshni (1961), Waterfurnace International Technical Bulletin (1985)**	**Dunstan and Thole (1909)**	**Bulone et al. (1989), Halfpap (1981), Waterfurnace International Technical Bulletin (1985), Kurata et al. (1971), Melinder (1997), Mikhail and Kimmel (1961)**		**ASHRAE (2001)**	**ASHRAE (2001)**
Thermal Conductivity	**Melinder (1997), Waterfurnace International Technical Bulletin (1985), Reidel (1951), Bates and Palmer (1938)**	**Gillam and Lamm (1955)**	**Melinder (1997), Waterfurnace International Technical Bulletin (1985), Reidel (1951), Bates and Palmer (1938)**		**ASHRAE (2001)**	**ASHRAE (2001)**
Specific Heat Capacity	**Westh and Hvidt (1993), Waterfurnace International Technical Bulletin (1985), Perry (1963)**	**Melinder (1997)**	**Westh and Hvidt (1993), Waterfurnace International Technical Bulletin (1985), Perry (1963), Ivin and Sukhatme (1967)**	**Melinder (1997)**	**ASHRAE (2001)**	**ASHRAE (2001)**

2.3 Melinder

The models given in Thermophysical Properties of Liquid Secondary Refrigerants (Melinder 1997) cover the same mixtures and much of the temperature range as models presented in this chapter. Thermophysical properties of eleven aqueous mixtures and six non-aqueous mixtures are presented. The thermophysical properties given are density, viscosity, specific heat, thermal conductivity, thermal volume expansion, freezing point,

boiling point, and surface tension. Correlations for the calculation of density, viscosity, specific heat, and thermal conductivity for the eleven aqueous mixtures as a function of freezing point temperature or concentration and temperature are also given. A comprehensive literature search was carried out and some laboratory measurements, primarily for unreliable or incomplete values of viscosity, were undertaken.

While Melinder's work is fairly comprehensive, it has two limitations with regards to GSHP system simulation applications. The first limitation is that data presented for methyl alcohol and ethyl alcohol only cover temperatures between the freezing point and 20^{o}C, whereas GSHP systems tend to operate at higher temperatures for part of the year. Secondly, the equation used to correlate the data is limited in terms of range of applicability and does not cover the operating range of a typical GSHP system in terms of both temperature and concentration. For example, the equation is applicable only for concentrations of 15% to 57% (by weight) for propylene glycol. In some GSHP applications, lower concentrations of propylene glycol might be sufficient to provide freeze protection. Also for optimization purposes, a constraint would have to be applied to prevent using less than 15% of propylene glycol. This is inconvenient and may result in the optimization results being wrong. Table 2-3 gives the range and accuracy of the equation.

Equation 2-1a gives the form of the equation used for specific heat, density, and thermal conductivity. Equation 2-1b gives the logarithmic form of the Equation 2-1a used for viscosity calculations. The equations give for the chosen freezing point or concentration and temperature the corresponding density, viscosity, specific heat or thermal conductivity.

$$f = \sum_{i=0}^{5}\sum_{j=0}^{3} Cij.(X - X_m)^i.(T - T_m)^j \quad (2\text{- }1a)$$

$$\log f = \sum_{i=0}^{5}\sum_{j=0}^{3} Cij.(X - X_m)^i.(T - T_m)^j \quad (2\text{- }1b)$$

Where, $i+j \leq 5$ and Cij is the coefficient for each term

X= mass fraction of the organic liquid or Freezing point temperature of the mixture (-)

T = Liquid temperature (^oC)

T_m = Mean value of the experimental range of temperature (^oC)

X_m = Mean value of the experimental range of concentration or freezing point temperature (-)

Table 2-3: Range of applicability and the maximum deviation for Equation 2-1

Aqueous mixture of	Applicable range (^{o}C or Wt%)	Density	Viscosity	Thermal Conductivity	Specific Heat Capacity
Propylene Glycol	$T_{freeze} \leq T \leq 40$ $15 \leq N \leq 57$ $-45 \leq T_{freeze} \leq -5$	0.08	2.74	0.29	0.17
Ethylene Glycol	$T_{freeze} \leq T \leq 40$ $0 \leq N \leq 56$ $-45 \leq T_{freeze} \leq 0$	0.1	2.29	0.34	0.39
Ethyl Alcohol	$T_{freeze} \leq T \leq 20$ $11 \leq N \leq 60$ $-45 \leq T_{freeze} \leq -5$	0.08	2.55	0.25	0.27
Methyl Alcohol	$T_{freeze} \leq T \leq 20$ $7.8 \leq N \leq 47.4$ $-50 \leq T_{freeze} \leq -5$	0.05	2.71	0.32	0.38

*T_{freeze} = Freezing point of the mixture for a particular concentration.

2.4 Literature Review of Mixing Rule Correlations

Mixing rule correlations use the properties of pure constituents in some algebraic combination to predict the mixture properties. Where an equation of state is not available,

a mixing rule correlation is considered as an alternate. Mixing rule correlations provide good accuracy and reasonable extrapolation as compared to equation fits but with fewer coefficients. Unlike equation fits, most mixing rules have some physical basis in the thermodynamic behavior of the mixture, making them less susceptible to error where interpolation or extrapolation is required.

2.4.1 Thermal Conductivity

Thermal conductivities of most mixtures of organic liquids tend to be less than would be predicted by a simple weight fraction average (Reid et al. 1977). Many mixing rules have been suggested. Reid et al. (1977) gives mixing rules suggested by Filippov (1956), Jamieson et al. (1973), and Li (1976). Another mixing rule is suggested by Rastorguev and Ganiev (1967).

Filippov (1956) gives Equation 2-2 for prediction of thermal conductivity of binary systems.

$$k = k_1 N_1 + k_2 N_2 - (A(k_2 - k_1) N_1 N_2) \qquad (2\text{-}2)$$

Where,

k= thermal conductivity of the mixture (W/m K)

k_1 & k_2= thermal conductivity of pure constituents (W/m K)

N= mass fraction (–)

A= coefficient (–)

Subscript: 1, 2= components of binary mixture

The equation was tested for ten systems with a single associated component, twelve systems of unassociated components, solutions of some salts and acids, and aqueous mixture of alcohols. The suggested equation is for a temperature range from the freezing point of the mixture to 80°C. The components are chosen such that $k_2 \geq k_1$. The coefficient A can be calculated using parameter estimation. If experimental data are not available, Filippov suggests that a value of 0.72 be used. A mean absolute deviation of 3.48% was observed for Equation 2-2 by Li (1976) for aqueous mixtures of organic liquids at 40°C.

Jamieson et al. (1973) tested Equation 2-3 on 60 binary systems. The nomenclature of Equation 2-2 applies to Equation 2-3.

$$k = k_1 N_1 + k_2 N_2 - [A(k_2 - k_1)(1 - (N_2)^{0.5}) N_2] \qquad (2\text{-}3)$$

As in Equation 2-2, the components are selected such that $k_2 \geq k_1$. The temperature range to which Equation 2-3 applies is not known but it seems to work well for data from freezing point to 125°C. The coefficient A can be determined using parameter estimation or taken as unity if experimental data are not available for regression purposes. A mean absolute deviation of 3.5% was observed by Li (1976) for aqueous mixtures of organic liquids at 40°C.

Li (1976) tested Equation 2-4 on a number of aqueous mixtures of organic liquid and aqueous mixtures of non-electrolytes at 0°C and 40°C.

$$k = k_1\varphi_1^2 + 2\varphi_1\varphi_2 k_{12} + k_2\varphi_2^2 \qquad (2\text{-}4)$$

Where,

φ = volume fraction (–)

k_{12}= harmonic mean approximation = $2(k_1^{-1} + k_2^{-1})^{-1}$

Subscript: 1, 2 = components of binary mixture

A similar form of the equation was also given for systems with more than two components. Li (1976) compared the results to Equation 2-2 and 2-3, and showed that the equation predicted thermal conductivity more accurately for the systems studied. He calculated a mean absolute deviation of 2.32% for aqueous mixtures of organic liquids at 40^{o}C, which represents a significant improvement over Equations 2-2 and 2-3.

Reid et al. (1977) give Equation 2-5.

$$k = \left(N_1 k_1^{\,A} + N_2 k_2^{\,A}\right)^{\left(\frac{1}{A}\right)} \qquad (2\text{-}5)$$

The range of applicability is not known. The coefficient A can be determined for each mixture using parameter estimation. The nomenclature is the same as for Equation 2-2.

Rastorguev and Ganiev (1967) give a mixing rule for aqueous mixtures of non-electrolytes and organic substances. Equation 2-6 is intended for thermal conductivity calculation within the temperature range of 0–100 ^{o}C.

$$k = \frac{k_2 N_2}{N_2 + (2\frac{V_1}{V_2} - 1)N_1} + \frac{k_1(2\frac{V_1}{V_2} - 1)N_1}{N_2 + (2\frac{V_1}{V_2} - 1)N_1} \quad (2\text{- }6)$$

Where,

V = molecular volume (grams/mole)

$\frac{V_1}{V_2}$ = molecular volume ratio of the two components of the mixture (–)

Molecular volume is the molecular weight divided by the specific gravity of the substance. The other nomenclature for Equation 2-6 is the same as Equation 2-2. It was noted in the study that the equation gives a mean absolute deviation of 2% for 0-100^{o}C temperature range for the aqueous mixtures compared, which included the four mixtures of interest in this study.

2.4.2 Viscosity

The earliest known of the mixing rules for viscosity is that proposed by Arrhenius (Grunberg and Nissan 1949). Arrhenius proposed a mixing rule correlation of the form given in Equation 2-7.

$$\ln \mu = N_1 \ln \mu_1 + N_2 \ln \mu_2 \quad (2\text{-}7)$$

Where,

μ = Dynamic viscosity of the mixture (mPa s)

μ_1 & μ_2 = Dynamic viscosity of pure constituents (mPa s)

N= mole fraction (–)

1, 2= components of binary mixture

It was noted by Grunberg and Nissan (1949) that the equation gives both positive and negative deviation.

Grunberg and Nissan (1949) proposed a characteristic constant of the system, which is a function of the activity coefficient and vapor pressure of the mixture. The activity coefficient is the ratio of the chemical activity of any substance to molar concentration. They compared the vapor pressure and viscosities of mixtures and deduced that Equation 2-8 yields closer agreement with experimental results.

$$\ln \mu = (N_1 \ln \mu_1 + N_2 \ln \mu_2) + N_1 N_2 D \tag{2-8}$$

Where,

D= characteristic constant of the system = $C \bullet b$ (–)

$C = \frac{\ln \mu}{\ln P_V}$ $\quad$ $b = \frac{\ln \gamma_1}{N_2^2}$

γ_1 = activity coefficient of the component 1 (–)

P_V = vapor pressure of the mixture (mPa)

The other nomenclature is the same as for Equation 2-7. The characteristic constant can be calculated using parameter estimation and determined for every mixture. While no quantitative comparison to Equation 2-7 was given, improved performance was shown in a graph.

Stephan and Heckenberger (1988) modified Equation 2-8 and came up with two forms of the equation, one suitable for one group of binary mixtures and the other form for aqueous mixtures of alcohols. Equation 2-9 was proposed for the binary fluid mixtures.

$$\ln \mu = (N_1 \ln \mu_1 + N_2 \ln \mu_2) + N_1 N_2 A \left| \ln \mu_1 - \ln \mu_2 \right| \tag{2-9}$$

Where, A is the coefficient that can be determined using parameter estimation.

For aqueous mixtures of alcohol Equation 2-10 was proposed to predict the viscosity of mixtures for temperature above 0^{o}C.

$$\ln \mu = (N_1 \ln \mu_1 + N_2 \ln \mu_2) + \ln(1 + \frac{N_1 N_2}{A_1 + A_2 N_2^{\ 2}}) \tag{2-10}$$

Where, A_1 and A_2 are the estimated coefficients.

The other nomenclature for Equation 2-9 and 2-10 is the same as Equation 2-7. Using Equation 2-10, the reported maximum error for aqueous mixture of methyl alcohol was 21.99% (mean absolute error of 5.69%) for a temperature range of 12^{o}C to 57^{o}C and 10-90% concentrations, whereas for the aqueous mixture of ethyl alcohol, maximum error was 84.58% (mean absolute error of 14.16%) for a temperature range of 12^{o}C to 77^{o}C. The maximum error was reduced to 3.38% for ethyl alcohol and 3.25% for methyl alcohol when the equation was used to correlate data at each available temperature point; that is the coefficients A_1 and A_2 were fitted for each temperature point. Equation 2-10 cannot be used as presented for system simulation purposes because of the large errors when it is fitted for the specified temperature range. Furthermore, the equation cannot be

used with data correlated at each temperature point because this will cause discontinuities in the answer.

2.4.3 Specific Heat Capacity

Dimoplon (1972) found that mass-weighted average specific heat is generally accurate within 10 to 15% for non-ideal mixtures. The weighted average mixing rule is given in Equation 2-11.

$$C_p = C_{p_1} N_1 + C_{p_2} N_2 \tag{2-11}$$

Where,

C_p= Specific heat of the mixture (kJ/kg K)

C_{p1} & C_{p2}= Specific heat of pure constituents (kJ/kg K)

N= mass fraction (–)

Subscript: 1, 2= components of binary mixture

The equation was tested on various binary aqueous mixtures. Aqueous mixtures of methyl alcohol were tested at 20^{o}C and three concentrations; a mean deviation of -4.5% was reported.

Jamieson and Cartwright (1978) tested Equation 2-11 on various binary mixtures and reported that maximum error was 16.9% for aqueous mixtures and 12.5% for non-aqueous mixtures. 95% of the values were within 14% for aqueous mixtures; for non-aqueous mixtures the maximum error was within 9% for 95% of the values. They also tried Equation 2-11 with mole fractions instead of mass fractions but did not find any

improvement. It was concluded that, for aqueous mixtures, the deviation was always positive. Where deviation from experimental results is unacceptable, Jamieson and Cartwright (1978) suggest adding a correction factor to Equation 2-11, shown in Equation 2-12:

$$C_p = (C_{p_1} N_1 + C_{p_2} N_2) * (1 + A N_1 N_2) \tag{2-12}$$

Where,

A = coefficient

$(1 + A N_1 N_2)$ = correction factor

The coefficient, A can be determined for each mixture using parameter estimation. If experimental data are not available for regression, it was suggested that a value of 0.2 should be taken for the coefficient. Jamieson and Cartwright (1978) tested Equation 2-12 for temperature above 0^{o}C and up to 72^{o}C on various binary mixtures. Results for the aqueous mixtures with coefficient value of 0.2 were reported to have a maximum error of 13.5% and 95% of the values were within ± 10 % of the experimental data. When coefficient values were calculated using parameter estimation and used in Equation 2-12, the maximum error reduced was to 10.2% and 95% of the values were within ± 7 % of the experimental data. The maximum deviation was observed at 50% weight concentration.

2.4.4 Density

Mandal et al. (2003) propose using the Redlich-Kister equation for density calculation of binary and ternary aqueous mixtures of organic substances. Equation 2-13 gives the form of the Redlich-Kister equation.

$$\rho = \sum_{i=1}^{n_c} \sum_{j=1}^{n_c} N_i N_j [(1 - A_{ij}) - (N_i - N_j) A_{ji}] (\rho_i \rho_j)^{0.5} \quad (2\text{-}13)$$

Where,

ρ = density of the mixture (kg/ litre)

ρ_{ij} = density of the pure constituents (kg/ litre)

n_c = Number of component of the mixture (-)

A_{ij} = coefficients (-)

N= mass fraction (–)

Densities of mixtures of six organic substances were correlated by the authors using Equation 2-13 for a temperature range of 20-50 ^{o}C. They report a mean absolute deviation within 0.04% for all the mixtures tested. Aqueous mixtures of interest in this study were not tested by Mandal et al. (2003).

2.5 Equations for Thermophysical Properties of Pure Liquids

The mixing rules discussed above require thermophysical properties of the pure liquid components. Various forms of equation fits are found in literature for the thermophysical properties of water, ethyl alcohol, methyl alcohol, ethylene glycol, and propylene glycol. In each case, the form reported to have the least error was chosen. In some cases, polynomial equation fits were developed from experimental data available in

literature where existing equations were not applicable to the desired temperature range. In the following text only the equations used are discussed.

2.5.1 Thermal Conductivity

The equation adopted for thermal conductivity of water, ethylene glycol, methyl alcohol, and ethyl alcohol is given in Thermal Conductivity, Non Metallic Liquids and Gases, Thermophysical Properties of Matter (Touloukian et al. 1970a). The equation has the maximum absolute deviation for ethylene glycol; a maximum deviation of 2.5% was reported from the experimental data. Equation 2-15 gives the form of the equation for thermal conductivity of pure liquids.

$$k = (a_0 + a_1 (T + T_{\text{ref}})) (0.004187) \quad (2\text{-}15)$$

Where,

k= thermal conductivity (W/m K)

T= temperature (^{o}C)

T_{ref}= reference temperature =273.15 (K)

$a_0 - a_2$ = coefficients

The value 0.004187 is a conversion factor to convert thermal conductivity from 10^{-6}cal/s cm ^{o}C to W/m K. The temperature range that Equation 2-15 is applicable to and the value of coefficients are given in Table 2-4.

Table 2-4: Temperature range for which the equations are applicable and coefficients of the equations of thermal conductivity of the pure components

Pure Liquid	Eq. No.	Temperature Range (^oC)	Coefficients			
			a_0	a_1	a_2	A_3
Water (1)	2-15	-43—127	273.778	3.9	N/A	N/A
Ethylene Glycol (1)	2-15	-23—127	519.442	0.32092	N/A	N/A
Methyl Alcohol (1)	2-15	-123—127	687.314	-0.68052	N/A	N/A
Ethyl Alcohol (1)	2-15	-123—127	609.512	-0.70924	N/A	N/A
Propylene Glycol (2)	2-16	-23—127	115.84	0.81874206	-0.00192452	0.000000653

(1) Touloukian et al. 1970a **(2)** Stephan and Hildwein 1987

The Equation for thermal conductivity of pure propylene glycol was taken from Recommended Data of Selected Compounds and Binary Mixtures (Stephan and Hildwein 1987). The equation is applicable for the temperature range of -23 ^{o}C —127 ^{o}C. The equation gives a mean absolute deviation of 3%. Equation 2-16 gives the form of the equation fit.

$$k = a_0 + a_1 T + a_2 T^{a3} \tag{2-16}$$

Where,

k= thermal conductivity (10^{-3} W/m K)

The other nomenclature for Equation 2-16 is the same as for Equation 2-15. The coefficients of the equation are given in Table 2-4.

2.5.2 Viscosity

The equation for viscosity of pure propylene glycol, ethylene glycol, ethyl alcohol, and methyl alcohol is taken from Recommended Data of Selected Compounds and Binary Mixtures (Stephan and Hildwein 1987). The equation (2-17) gives mean

absolute deviation of 1.9%, 0.8%, 1.9%, and 1.2% for propylene glycol, ethylene glycol, ethyl alcohol, and methyl alcohol respectively.

$$\mu = a_0 \bullet Exp\left(\frac{a_1}{T + T_{ref} + a_2} + a_3 \left[\frac{T + T_{ref}}{T_c} \right]^{a_4} \right) \qquad (2\text{-}17)$$

Where, μ = Dynamic viscosity of the mixture (10^{-3}mPa s)

T= temperature (^{o}C)

T_{ref}= reference temperature = 273.15 (K)

$a_0 - a_4$ = coefficients

T_c is the critical temperature (K) and is equal to 625, 645, 513.92, and 512.64 for propylene glycol, ethylene glycol, ethyl alcohol, and methyl alcohol respectively.

The temperature range to which Equation 2-17 is applicable and the coefficients of equation are given in Table 2-5.

Table 2-5: Temperature range for which the equations are applicable and coefficients of the equations of viscosity of the pure components

Pure Liquid	Eq. No.	T Range (^oC)	Coefficients				
			a_0	a_1	a_2	a_3	a_4
Propylene Glycol (1)	2-17	-30—127	626.021	1262.6	-151.492	-4.10426	-0.09794
Ethylene Glycol (1)	2-17	-13—127	520.24	1158.95	-132.353	-3.32075	-0.07027
Methyl Alcohol (1)	2-17	-73—127	473.977	284.111	-102.773	-3.00443	1.53842
Ethyl Alcohol (1)	2-17	-73—127	69.8963	877.267	-43.8958	- 2.13138	2.0094
Water (2)	2-18	-34—0	1.77_ 025356	-0.08_ 551866	-0.00_ 168979	-0.00_ 01927	N/A
	2-19	0—127	0.02414	247.8	140	N/A	N/A

(1) Stephan and Hildwein 1987

(2) Polynomial fit to data given by Halfpap 1981 (Temperature range -34—0 ^oC) / Touloukian et al. 1970b (temperature range 0—127 ^oC)

Experimental data for viscosity of pure water below 0^oC is given by Halfpap (1981). A third order equation fit was made. The equation fit has an RMSE of 0.5% and is applicable to the temperature range of -34^oC—0^oC. Equation 2-18 gives the third order polynomial.

$$\mu = \sum_{n=0}^{3} a_n T^n \tag{2-18}$$

Where,

μ = Dynamic viscosity of the mixture (mPa s)

T= temperature (^oC)

An equation for calculation of viscosity of pure water for the temperature range of $0^o C$—130^oC is given in Viscosity, Thermophysical Properties of Matter (Touloukian et

al. 1970b). The equation was reported to give a maximum deviation of ± 2.5%. The form of the equation is given in Equation 2-19.

$$\mu = a_0 \; 10^{\; a_1 / ((T+T_{ref}) - a_2)} \tag{2-19}$$

Where,

μ = Dynamic viscosity of the mixture (mPa s)

T= temperature (^{o}C)

T_{ref} = reference temperature = 273.15 (K)

The coefficients of Equation 2-18 and 2-19 are given in Table 2-5.

2.5.3 Specific Heat

The equations for specific heat of the pure water for temperature greater than 0^{o}C, and equations for specific heat of methyl alcohol, and ethylene glycol are given in Specific Heat, Non Metallic Liquids and Gases, Thermophysical Properties of Matter (Touloukian and Makita 1970). Methyl alcohol data below 20^{o}C is noted as not reliable by the citation, so the equation was used only for temperature above 20^{o}C. The Equation (2-20) gives mean absolute deviation of 0.14%, 0.4%, and 1% for pure water, methyl alcohol, and ethylene glycol respectively for all temperature range.

$$C_p = \left(\sum_{n=0}^{3} a_n (T + T_{ref})^n \right) * 4.184 \tag{2-20}$$

Where,

C_p= Specific heat of the mixture (kJ/kg K)

T= temperature (^{o}C)

T_{ref}= reference temperature = 273.15 (K)

$a_0 - a_2$ = coefficients

The value 4.184 is a conversion factor to convert calorie/gram °C to kJ/kg K. Experimental data for specific heat of water below 0^{o}C and specific heat of methyl alcohol below 20^{o}C was taken from Westh and Hvidt (1993). A third order polynomial equation was used to fit the data. The equation gives an RMSE of 0.6% for equation of specific heat of water and RMSE of 0.07% for equation of specific heat of methyl alcohol. Equation 2-21 gives the form of the polynomial for specific heat of water.

$$C_p = \sum_{n=0}^{3} a_n T^n \tag{2-21}$$

Where, C_p= Specific heat of the mixture (kJ/kg K)

Equation 2-22 gives the form of the equation for the specific heat of methyl alcohol.

$$C_p = \sum_{n=0}^{3} a_n (T + T_{ref})^n \tag{2-22}$$

The coefficients of the Equations 2-20, 2-21, and 2-22 are given in Table 2-6. The temperature range for which the equations are applicable is also reported in the Table 2-6.

Table 2-6: Temperature range for which the equations are applicable and coefficients of the equations of specific heat of the pure components

Pure Liquid	Eq. No.	T Range (^oC)	Coefficients				
			a_0	a_1	a_2	a_3	A_4
Water (1)	2-20	0—127	2.13974	- 0.00_ 968137	0.0000_ 268536	0.0000_ 00024214	N/A
	2-21	-37—0	4.2128_ 668864	- 0.0156_ 132429	- 0.0014_ 26597	-0.0000_ 554436	N/A
Methyl Alcohol (2)	2-22	20—127	- 9.2711_ 1942536	0.1308_ 06587813	- 0.0005_ 07395605	0.0000_ 00679332	N/A
	2-21	-34—20	0.582485	- 0.000_ 375646	- 0.0000_ 016784	0.0000_ 0001062	N/A
Ethylene Glycol (3)	2-20	-11—127	0.016884	0.0033_ 5083	- 0.0000_ 07224	0.0000_ 00007618	N/A
Propylene Glycol (4)	2-23	-60—127	58080	445.2	N/A	N/A	N/A
Ethyl Alcohol (5)	2-24	-32—127	8.3143	11.7928	- 6.49805	- 3.43888	33.9621

(1) Touloukian and Makita 1970 (Temperature range 0—127 ^oC) / polynomial fit to data given by Westh and Hvidt 1993 (Temperature range -37—0 ^oC)

(2) Touloukian and Makita 1970 (Temperature range 20—127 ^oC) / polynomial fit to data given by Westh and Hvidt 1993 (Temperature range -34—20 ^oC)

(3) Touloukian and Makita 1970 **(4)** Daubert and Danner 1989 **(5)** Stephan and Hildwein 1987

The equation for specific heat of propylene glycol was taken from Physical and Thermodynamic Properties of Pure Chemicals (Daubert and Danner 1989). The equation was reported to give less than 3% maximum error. The form of equation is given in Equation 2-23.

$$C_p = (a_0 + a_1 \ (T + T_{ref}))/M \qquad (2\text{-}23)$$

Where, C_p = specific heat of mixture (J/kg K)

M = molecular weight of propylene glycol = 76 (grams/mole)

The coefficients of the equation are given in Table 2-6 along with the temperature range.

The equation for specific heat of ethyl alcohol is taken from Recommended Data of Selected Compounds and Binary Mixtures (Stephan and Hildwein 1987). The equation was reported to give a maximum error of 0.7%. The form of equation is given in Equation 2-24

$$C_p = \frac{a_0\left[a_1 + a_2 \frac{T+T_{ref}}{T_c} - a_3\left(\frac{T+T_{ref}}{T_c}\right)^2 + a_4\left(\frac{T+T_{ref}}{T_c}\right)^3\right]}{M} \quad (2\text{-}24)$$

Where,

C_p= specific heat of the mixture (kJ/kg K)

T_c = critical temperature of ethyl alcohol = 513.92 (K)

T_{ref}= reference temperature = 273.15 (K)

M = molecular weight of ethyl alcohol = 46.069 (grams/mole)

As pressure is increased, the boiling point of the liquid is also increased, until the critical temperature is reached. The temperature where the gas cannot be condensed, regardless of the pressure applied is known as the critical temperature. The temperature range for which the Equation 2-24 is applicable and coefficients of the equation are given in Table 2-6.

2.5.4 Density

The equation for density of methyl alcohol, ethyl alcohol, ethylene glycol, and propylene glycol was taken from Physical and Thermodynamic Properties of Pure Chemicals (Daubert and Danner 1989). The equation predicts the pure density of the liquids with acceptable accuracy. An absolute maximum error of 2% was reported for

methyl and ethyl alcohol. The citation reports an absolute maximum error of less than 3% and 5% for propylene glycol and ethylene glycol respectively. Equation 2-25 shows the form of the equation.

$$\rho = \left[\frac{a_0}{a_1 \left(1 + \left(1 - \frac{T + T_{ref}}{T_{critical}} \right)^{a_2} \right)} \right] M \qquad (2\text{-}25)$$

Where,

ρ = density of the mixture (kg/ litre)

T_{ref} = reference temperature = 273.15 (K)

$T_{critical}$ = critical temperature (K)

M = molecular weight (grams/mole)

$a_0 - a_2$ = coefficients

The coefficients and other parameters necessary to use Equation 2-25 are given in Table 2-7. The temperature range for which the equation is applicable is also given in the table.

Table 2-7: Temperature range for which the equations are applicable and coefficients of the equations of density of the pure components

Pure Liquid	Eq. No.	T Range (^oC)	Coefficients					
			a_0	a_1	a_2	a_3	$T_{critical}$	M
Methyl Alcohol (1)	2-25	-60—127	2.308	0.27192	0.2331	N/A	512.58	32.042
Ethylene Glycol (1)	2-25	-73—127	1.2342	0.27029	0.21997	N/A	629	78.135
Propylene Glycol (1)	2-25	-98—127	1.0923	0.26106	0.20459	N/A	626	76.095
Ethyl Alcohol (1)	2-25	-114—127	1.5223	0.26395	0.2367	N/A	516.25	46.069

(1) Daubert and Danner 1989

Hare and Sorensen (1987) gave a sixth order polynomial for density of pure water applicable to the temperature range of -34^{o}C to 0^{o}C. They report a standard deviation between the data and the fit as about $\pm 10^{-4}$ g/ml. Equation 2-26 gives the sixth order polynomial; the coefficients are given in Table 2-8.

$$\rho = \sum_{n=0}^{6} a_n T^n \tag{2-26}$$

Where, ρ = density of water (g/ml)

A third order polynomial fit equation was used to fit density data for pure water taken from Density, Non Metallic Liquids and Gases, Thermophysical Properties of Matter (Touloukian and Makita 1970) for temperature above 0^{o}C. The equation gives a RMSE of 0.024% for the temperature range of 0^{o}C to 96^{o}C. Equation 2-27 gives the form of the equation; the coefficients are given in Table 2-8.

$$\rho = \sum_{n=0}^{3} a_n T^n \qquad (2\text{-}27)$$

Table 2-8: Coefficients of the equations for density of the pure water

Coefficients							
Eq. No.	**a_0**	**a_1**	**a_2**	**a_3**	**a_4**	**a_5**	**a_6**
2-26 **(1)**	0.99986	0.00006_69	- 0.0000_08486	0.0000_001518	- 0.00000_00069484	- 0.00000_000036449	- 0.000000_000007497
2-27 **(2)**	1.00009_41648	0.0000108821	0.0000000155	- 0.0000_058378	N/A	N/A	N/A

(1) Hare and Sorensen 1987 (Temperature range -34—0 ^{o}C)

(2) polynomial fit to data given by Touloukian and Makita 1970 (Temperature range 0—96 ^{o}C)

2.6 Results and Discussion of Mixing Rule Correlations

For each of the thermophysical properties the experimental data were correlated by the mixing rules presented above. Where necessary, parameter estimation was done to calculate the coefficients.

2.6.1 Thermal Conductivity

The results obtained by the mixing rules (Equations 2-2 to 2-6) taken from literature were comparable and within $\pm$ 5% maximum error of the experimental data for mixtures of ethyl and methyl alcohol and within $\pm$ 10% maximum error for the ethylene and propylene glycol. A quantitative comparison of the performance of the equations for aqueous mixtures of interest to this study is given in Table 2-9. The number of data points used for parameter estimation and the resulting coefficients are also given in the table.

Table 2-9: Comparison of the equations for thermal conductivity of mixtures

Aqueous Mixture of	No of Data Points	Range		Thermal Conductivity		
		T (^{o}C)	N (Wt%)	Eq. Number	Coefficient A	RMSE (%)
Ethyl Alcohol	120	-70 – 60	5 – 90	2-2	0.571066	1.6
				2-3	0.939604	1.9
				2-4	N/A	2.1
				2-5	0.051892	1.9
				2-6	N/A	2.3
Methyl Alcohol	116	-45 – 50	5 – 90	2-2	0.505995	1.0
				2-3	0.8501466	0.9
				2-4	N/A	1.8
				2-5	0.0201599	1.6
				2-6	N/A	1.6
Propylene Glycol	273	-35 – 125	10 – 90	2-2	0.4779272	3.0
				2-3	0.7550207	3.6
				2-4	N/A	3.2
				2-5	0.157237	2.0
				2-6	N/A	2.6
Ethylene Glycol	274	-35 – 125	10 – 90	2-2	0.6255879	2.9
				2-3	0.9999483	3.5
				2-4	N/A	2.7
				2-5	-0.4690312	2.0
				2-6	N/A	2.4

Figure 2-1 illustrates the performance of equation 2-5 for propylene glycol. The major deviation is seen at temperatures above 80^{o}C. Since temperature in GSHP systems seldom rise above 50^{o}C, the deviation above 80^{o}C is not very important in this application.

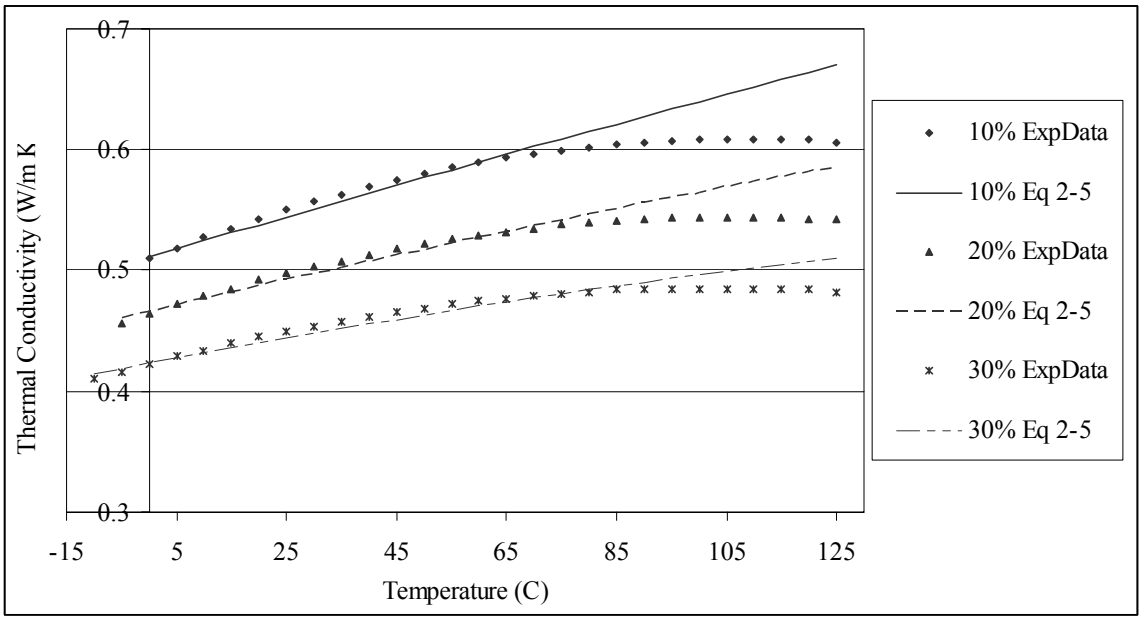

Figure 2-1. Performance of Equation 2-5 for thermal conductivity of aqueous mixtures of Propylene Glycol (Experimental data collected from ASHRAE (2001))

From Table 2-9 it can be concluded that Equation 2-5 performs better for the aqueous mixtures of propylene and ethylene glycols and is comparable to other equations studied for aqueous mixtures of methanol and ethanol. Equation 2-5 gives satisfactory results for all the mixtures studied for the operating range of a typical GSHP system in terms of both temperature and concentration. Therefore, Equation 2-5 is adopted for thermal conductivity calculations of aqueous mixtures of propylene and ethylene glycol, and methyl and ethyl alcohol.

2.6.2 Viscosity

Viscosity was correlated using Equations 2-7 through 2-10 found in the literature. As shown in Table 2-10 the results of the equations were unsatisfactory, especially for aqueous mixtures of ethyl and methyl alcohol. This may not be surprising, as the temperature range for which the equations are suggested is above 0^{o}C, but it is necessary

for GSHP applications to model the thermophysical properties at temperatures below 0^{o}C.

Table 2-10: Comparison of the equations for viscosity of mixtures

Aqueous Mixture of	No of Data Points	Range		Viscosity		
		T (C)	N (wt%)	Eq. Number	Coefficient A	RMSE (%)
Ethyl Alcohol	161	-35 – 50	1 – 96	2-7	N/A	56.2
				2-8	4.795200651	26.7
				2-9	9.062673408	44.1
				2-10	0.122037628, 0.0188077563	26.5
				2-28	0.29921813, 0.725703898, 0.0038682258, 1.61437032, 60.00840782	9.8
Methyl Alcohol	134	-45 – 50	2 – 95	2-7	N/A	49.1
				2-8	3.60195285	18.2
				2-9	4.97682824	22.8
				2-10	0.16776093, 0.115329355	18
				2-28	1.520446884, 14.70346315, 0.0456026517, 0.9753293756, 97.47210832	3.3
Propylene Glycol	273	-35 – 125	10 – 90	2-7	N/A	11
				2-8	-0.64984001194	18.5
				2-9	-0.1969604647	9.4
				2-10	53687091.3, 13352554.9	18.7
				2-29	-0.30998878, 4.876953323, 18.3337611545	8.5
Ethylene Glycol	274	-35 – 125	10 – 90	2-7	N/A	19.6
				2-8	-0.775007917	11.1
				2-9	-0.28721149899	9.3
				2-10	53687092.2,15250579.4	19.6
				2-29	-0.46265918457, 3.7063275478, 19.52078969	6.9

Figure 2-2 shows the performance of Equation 2-7 for viscosity of aqueous mixture of ethylene glycol for temperature ranges greater than 0°C.

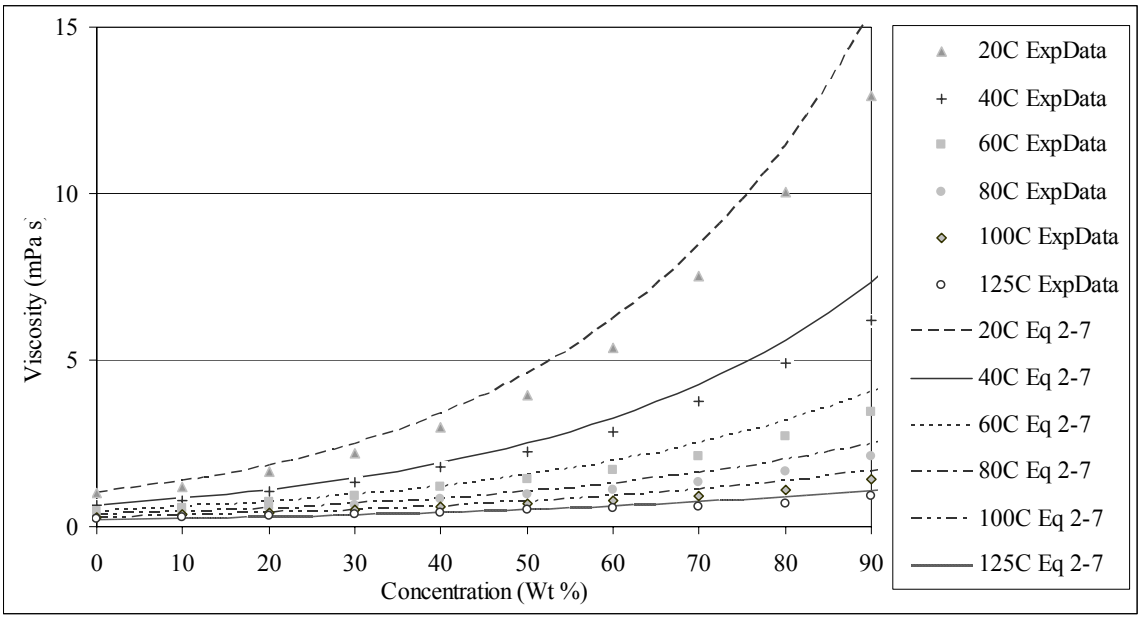

Figure 2-2. Performance of Equation 2-7 for viscosity of aqueous mixture of Ethylene Glycol at temperature above 0°C (Experimental data collected from ASHRAE (2001))

Equation 2-7 gives viscosity in reasonable agreement with experimental data above 0°C, but as shown in Figure 2-3, Equation 2-7 predicts the viscosity below 0°C poorly.

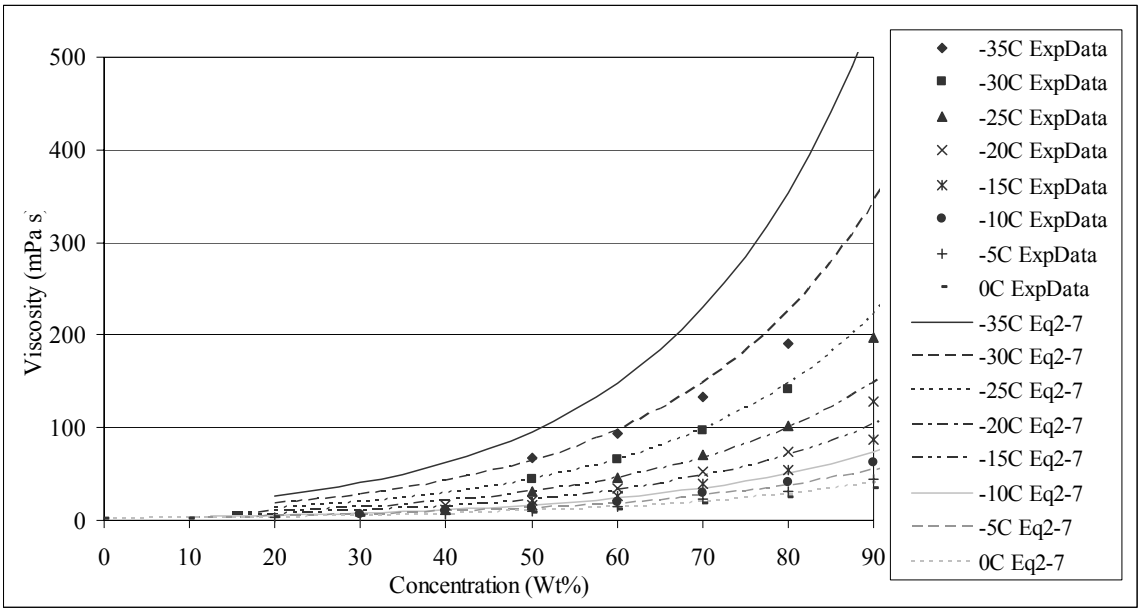

Figure 2-3. Performance of Equation 2-7 for viscosity of aqueous mixture of ethylene glycol at temperatures below 0^{o}C (Experimental data collected from ASHRAE (2001))

The equations taken from literature predict viscosity for aqueous methyl and ethyl alcohol mixtures poorly but give better fits for aqueous propylene and ethylene glycol mixtures. The aqueous methyl and ethyl alcohol mixture viscosities peaks at about 40% concentration unlike aqueous propylene and ethylene glycol mixtures for which the peak is observed at 100% concentration. The viscosity trend for aqueous mixtures of methyl alcohol is shown in Figure 2-4.

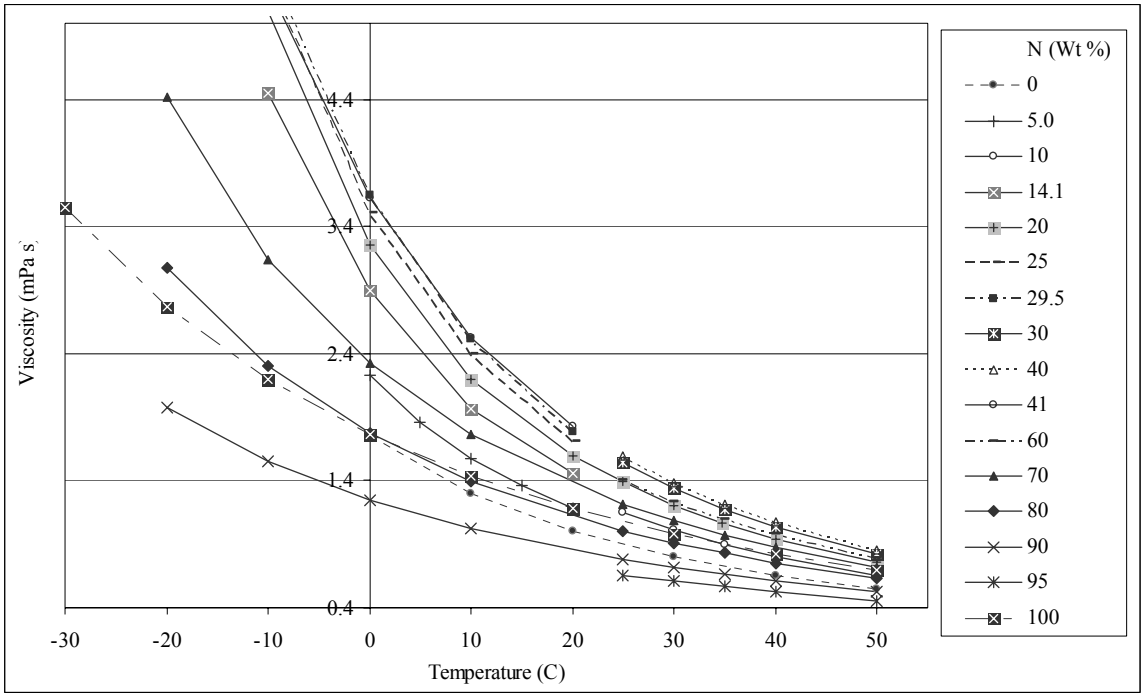

Figure 2-4. Viscosity of aqueous mixture of Methyl Alcohol (Experimental Data collected from Bulone et al. (1989), Halfpap (1981), Waterfurnace International Technical Bulletin (1985), Kurata et al (1971), Melinder (1997), Mikhail and Kimmel (1961))

The RMSE is unsatisfactory for all of the equations tested, especially for aqueous mixtures of methyl and ethyl alcohol. The aqueous mixtures of alcohols behave differently than glycol mixtures as explained above (the viscosity peaks at different concentrations) thus two different equations had to be devised for each set of mixtures. After some experimentation, Equation 2-28 was developed to predict the viscosity of aqueous mixtures of methyl and ethyl alcohols. A comparison of Equation 2-10 shows that Equation 2-28 was developed by adding more terms to the Stephan and Heckenberger (1988) equation.

$$\ln \mu = (N_1 \ln \mu_1 + N_2 \ln \mu_2) + \ln\left(1 + \frac{N_1 N_2}{A_1 N_1^{\,2} + A_2 N_2^{\,2}}\right) + A_3 (A_5 - T)^{A_4} N_1 N_2 \qquad (2\text{-}28)$$

Figure 2-5 and 2-6 show the performance of Equation 2-28 for aqueous mixture of methyl and ethyl alcohols respectively.

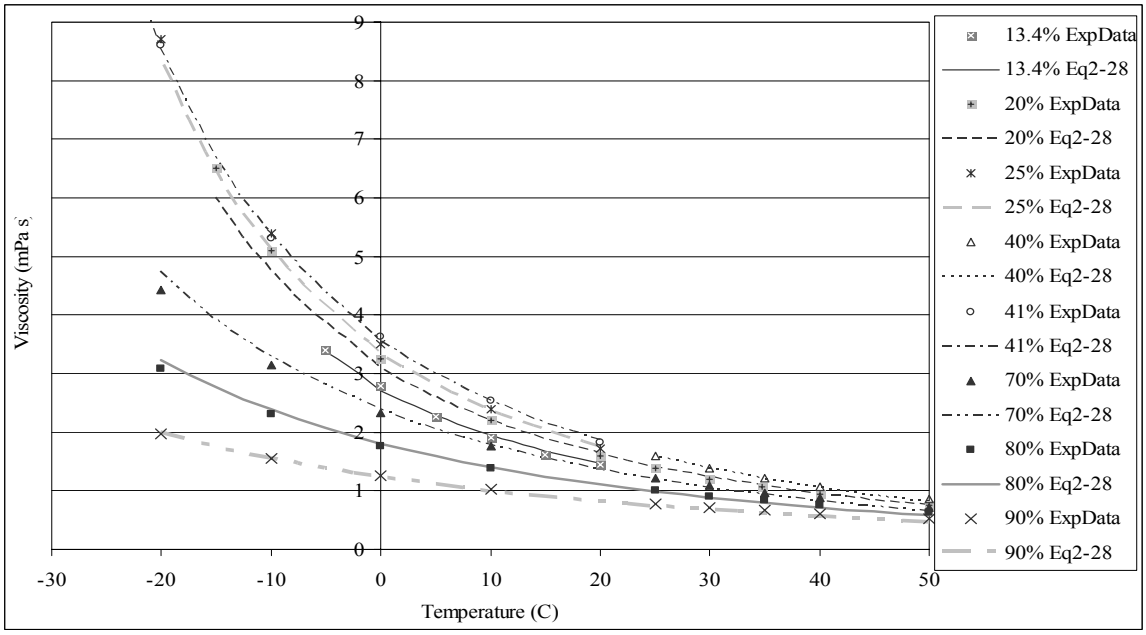

Figure 2-5. Performance of Equation 2-28 for viscosity of aqueous mixture of Methyl Alcohol at various concentrations (Experimental Data collected from Bulone et al. (1989), Halfpap (1981), Waterfurnace International Technical Bulletin (1985), Kurata et al (1971), Melinder (1997), Mikhail and Kimmel (1961))

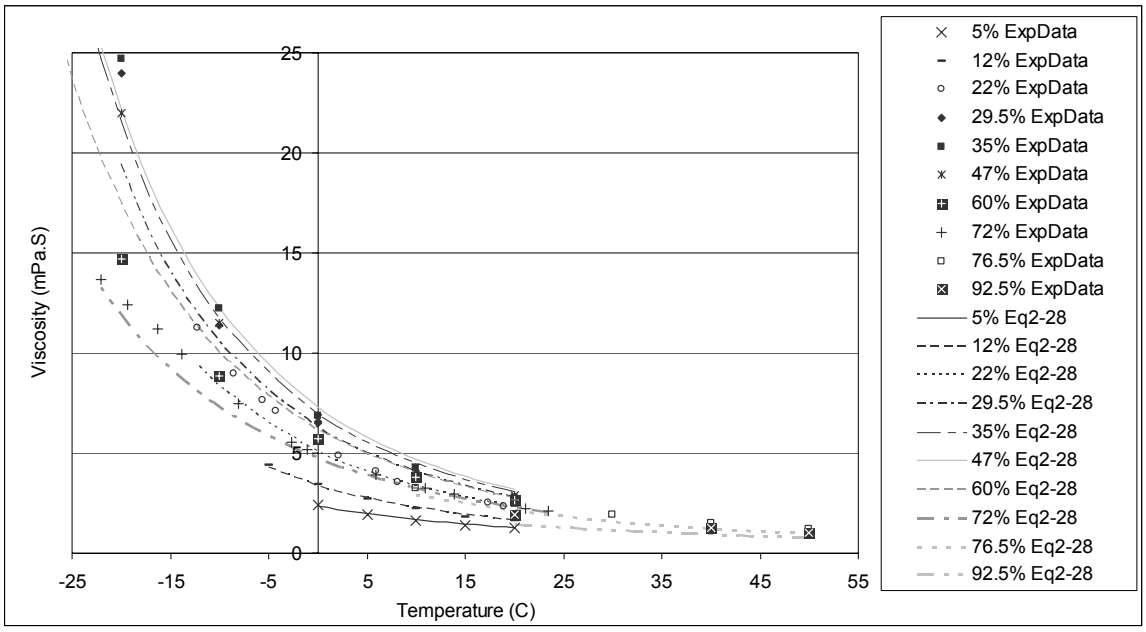

Figure 2-6. Performance of Equation 2-28 for viscosity of aqueous mixture of Ethyl Alcohol at various concentrations (Experimental data collected from Bulone et al. (1989), Dizechi and Marschall (1982), Halfpap (1981), Melinder (1997), Misra and Varshni (1961), Waterfurnace International Technical Bulletin (1985))

Most of the deviation shown by equation 2-28 for aqueous mixture of ethyl alcohol is at concentrations greater then 50% by weight of ethyl alcohol. For GSHP systems, concentrations greater then 50% are seldom required; the deviation above 50% is not very important in this application.

Equation 2-29 was developed to predict the viscosity of aqueous mixtures of ethylene and propylene glycol mixtures. A comparison of Equation 2-9 and 2-10 shows that Equation 2-29 was developed by combining the Stephan and Heckenberger (1988) equations.

$$\ln \mu = (N_1 \ln \mu_1 + N_2 \ln \mu_2) + N_1 N_2 A_1 \left| \ln \mu_1 - \ln \mu_2 \right| + \ln(1 + \frac{N_1 N_2}{A_2 {N_2}^4 + A_3 {N_2}^4}) \quad (2\text{-}29)$$

The coefficients of Equation 2-28 and 2-29 for each mixture are given in Table 2-10. Figure 2-7 show the performance of Equation 2-29 for all concentration and temperatures above 0^{o}C for aqueous mixture of ethylene glycol. While the equation gives better fits of data at lower concentrations than at higher concentrations, it gives reasonable results for the entire range of concentration.

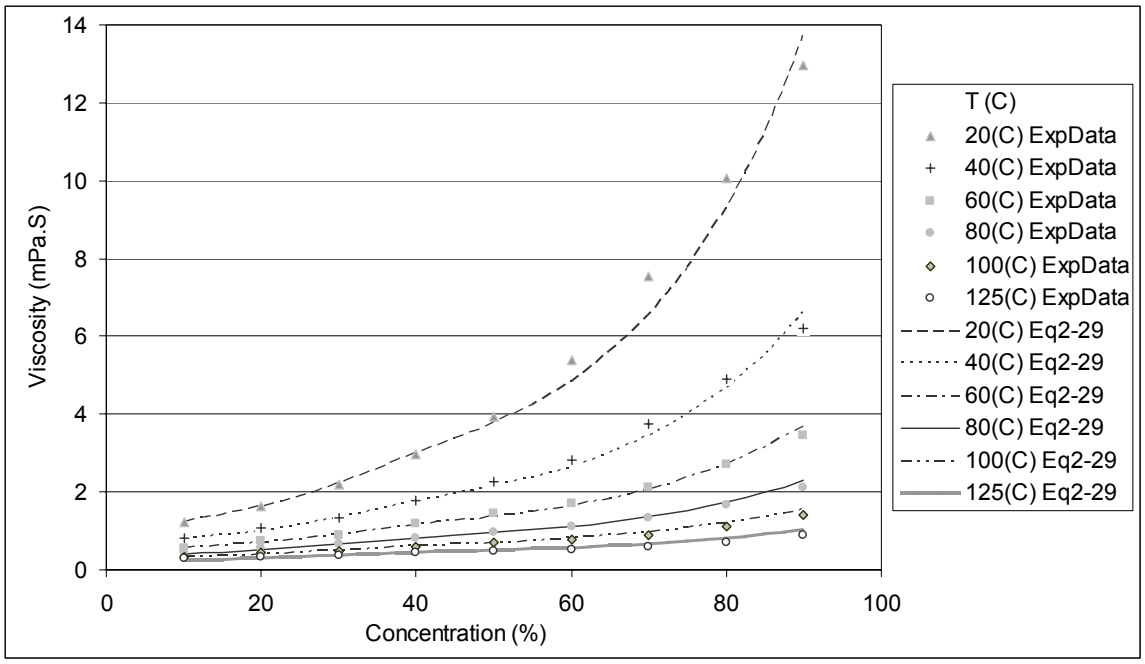

Figure 2-7. Performance of Equation 2-29 for viscosity of aqueous mixture of Ethylene Glycol at temperatures above 0^{o}C (Experimental data collected from ASHRAE (2001))

Figure 2-8 shows the performance of Equation 2-29 for all concentrations and temperatures below 0^{o}C for aqueous mixtures of ethylene glycol. Increasing deviation is seen in Figure 2-8 at lower temperatures and higher concentrations of ethylene glycol. As these concentrations seldom occur in GSHP systems, increased error in these regions may be tolerated.

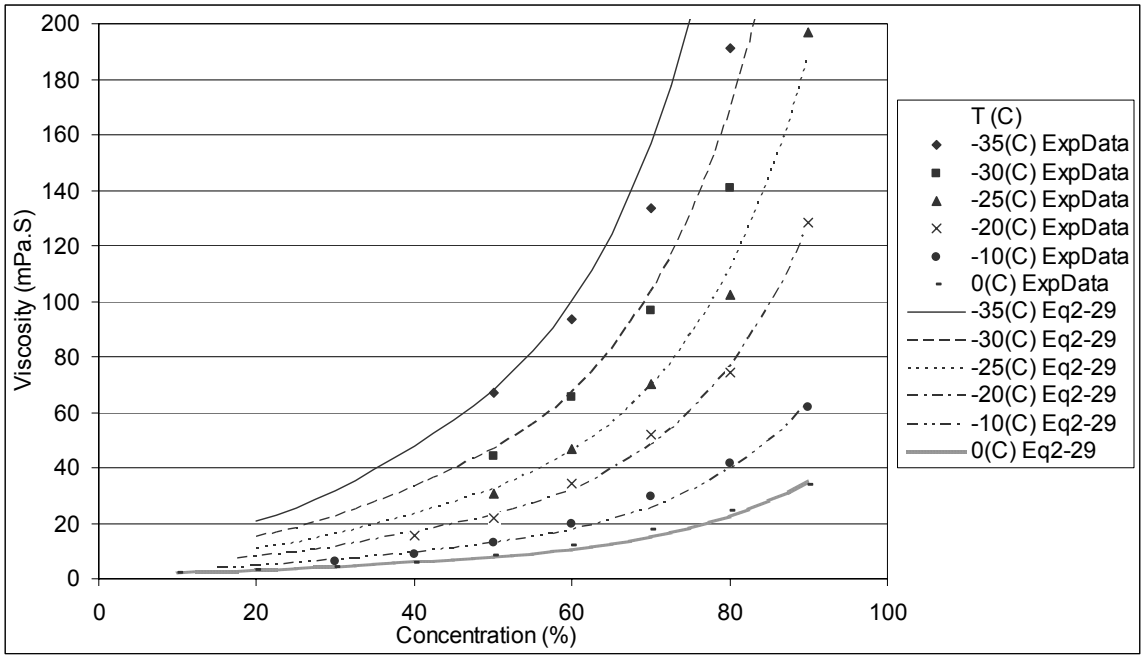

Figure 2-8. Performance of Equation 2-29 for viscosity of aqueous mixture of Ethylene Glycol at temperatures below 0°C (Experimental data collected from ASHRAE (2001))

Figure 2-9 shows the viscosity of aqueous mixture of propylene glycol as a function of temperature and concentration, for concentrations of propylene glycol typically used in GSHP system applications.

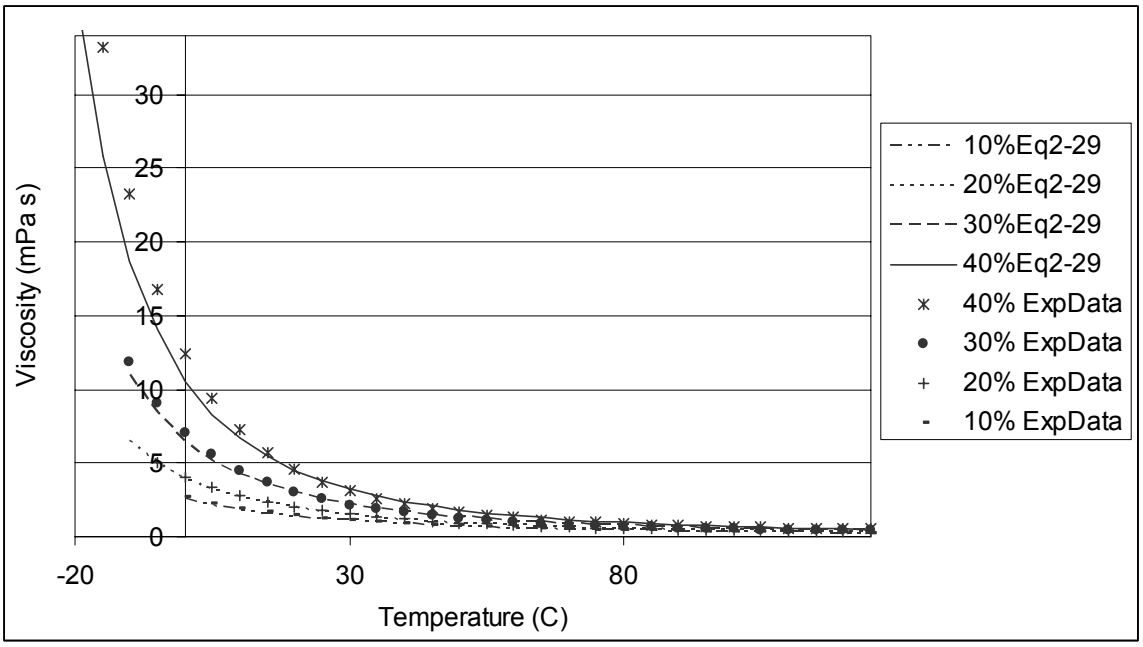

Figure 2-9. Performance of Equation 2-29 for viscosity of aqueous mixture of Propylene Glycol for concentration range applicable to typical GSHP system operation (Experimental data collected from ASHRAE (2001))

Figure 2-10 shows the viscosity of aqueous mixture of propylene glycol as a function of temperature and concentration. The figure illustrates the performance of Equation 2-29 at higher concentrations of propylene glycol.

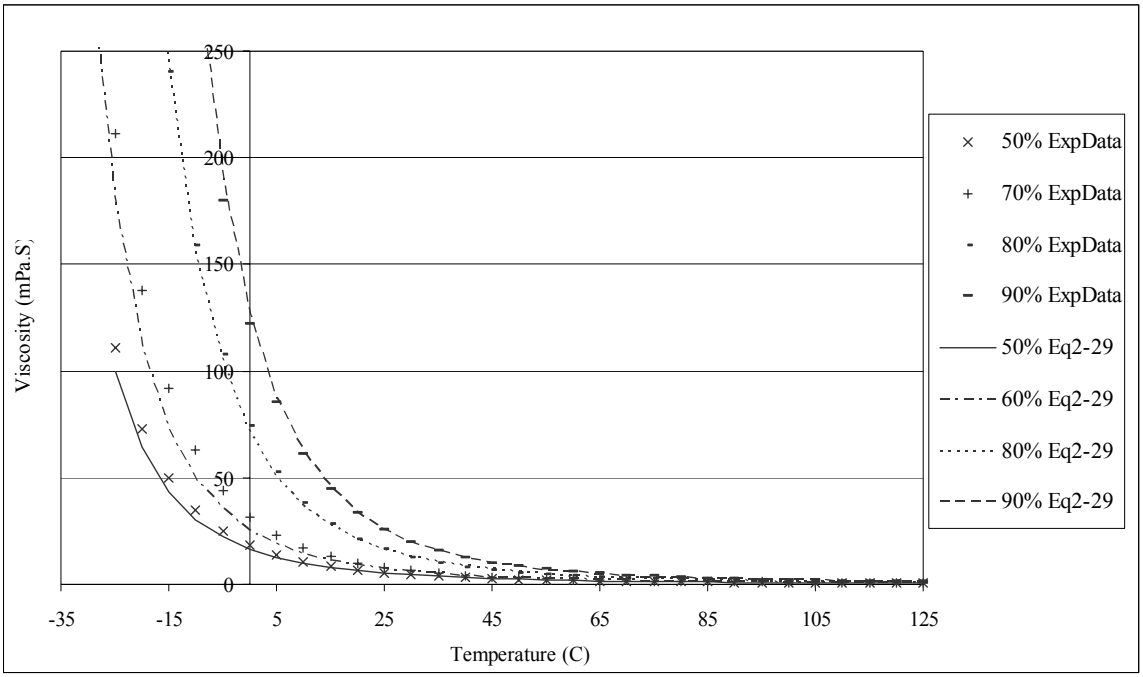

Figure 2-10. Performance of Equation 2-29 for viscosity of aqueous mixture of Propylene Glycol (Experimental data collected from ASHRAE (2001))

Figure 2-10 shows that Equation 2-29 gives some deviation from experimental data for higher concentrations of propylene glycol at temperatures below 0^{o}C. Equations 2-28 and 2-29 predict the mixture viscosities significantly better than the equations found in the literature. The equations can predict viscosity for all temperature ranges of available experimental data within 10% RMSE for the selected mixtures. Equations 2-28 and 2-29 are suggested for viscosity calculations of the selected aqueous mixtures for GSHP system simulation applications.

2.6.3 Specific Heat Capacity:

Specific heat capacity of the selected aqueous mixtures was calculated using the mixing rule correlations found in the literature, Equation 2-11 and 2-12 give a maximum error of about ± 5% for experimental data above 0^{o}C, but failed to predict within ± 10%

maximum error for the entire temperature range. The comparison of equations for the available data is given in Table 2-11.

Table 2-11: Comparison of the equations for specific heat capacity of mixtures

Aqueous Mixture of	No of Data Points	Range		Specific Heat Capacity		
		T (C)	N (wt%)	Eq. Number	Coefficient A	RMSE (%)
Ethyl Alcohol	228	-25 – 75	5 – 95	2-11	N/A	10.7
				2-12	0.158614745	8.6
				2-30	1.073308, -0.03601932, 74.3958442, 0.002081859	3.9
Methyl Alcohol	236	-35 – 40	5 – 90	2-11	N/A	6.7
				2-12	0.097391368	6. 8
				2-30	0.798624897, -0.06212194, 51.23724925, 0.00262289	3.3
Propylene Glycol	273	-35 – 125	10 – 90	2-11	N/A	4.6
				2-12	0.136759	3.0
				2-30	0.436989569, -0.00225207, 175.954738, -0.00077749	1.6
Ethylene Glycol	274	-35 – 125	10 – 90	2-11	N/A	4.0
				2-12	-0.00113	4.0
				2-30	0.223375729, -0.00503512, 122.398371, -0.00119436	2

For both equations from the literature and all four mixtures, Equation 2-11 gives maximum error for aqueous mixtures of ethyl alcohol. The specific heat capacity of the aqueous mixture of ethyl alcohol as a function of temperature and concentration is shown in Figure 2-11.

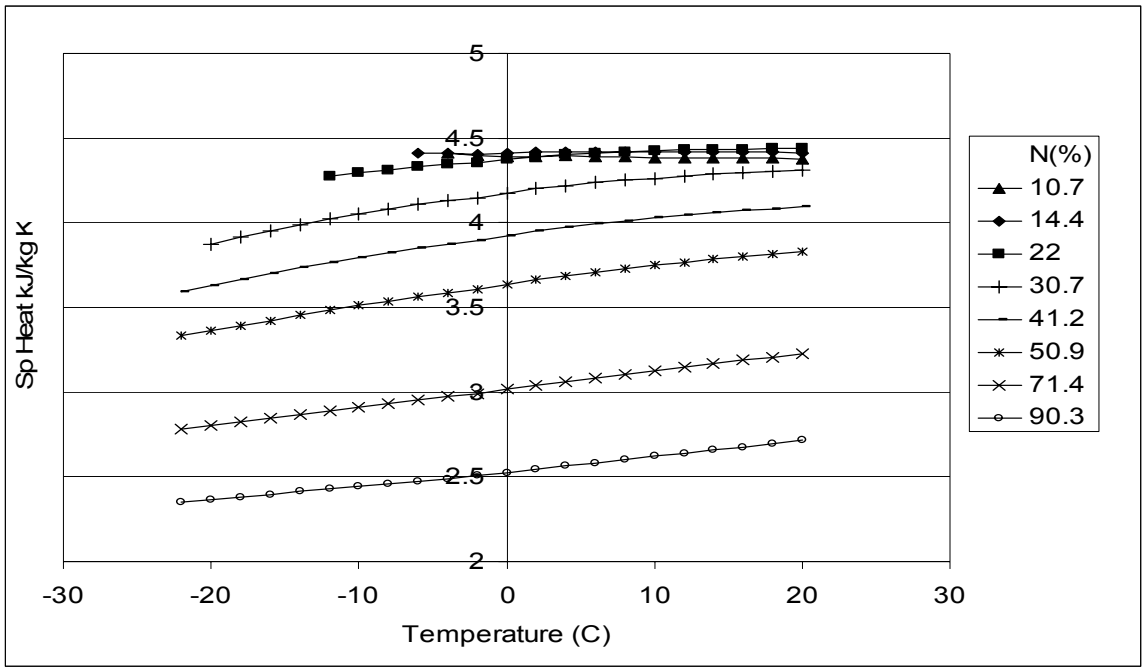

Figure 2-11. Specific heat of aqueous mixture of Ethyl Alcohol (Experimental data collected from Westh and Hvidt (1993), Waterfurnace International Technical Bulletin (1985), Perry (1963))

Equation 2-12 (Jamieson and Cartwright 1978) gives better performance than Equation 2-11, thus it was taken as the basis for improvement. Equation 2-12 was modified by introducing additional correction terms. Three coefficients and a temperature term were added to Equation 2-12. Equation 2-30 gives the form of the modified equation.

$$C_p = (C_{p1}N_1 + C_{p2}N_2) * (1 + A_1 N_1 N_2) + A_2 (A_3 - T) N_1 N_2 + A_4 (A_3 - T) \quad (2\text{-}30)$$

The nomenclature is the same as Equation 2-12. The coefficients of Equation 2-30 for each mixture are given in Table 2-11. Equation 2-30 predicts the specific heat of

selected aqueous mixture more accurately. The maximum error for all the selected mixtures for the temperature range of available data was within ± 10%.

2.6.4 Density

Equation 2-13 was tested for the selected aqueous mixtures. The RMSEs of the equation are given in Table 2-12.

Table 2-12: Comparison of the equations for density of mixtures

Aqueous Mixture of	No of Data Points	Range		Density		
		T (C)	N (Wt%)	Eq. Number	Coefficient A	RMSE (%)
Ethyl Alcohol	245	-45 – 40	2.5 – 95	2-13	-0.0658385, 0,0, -0.05073751	0.7
				2-31	N/A	2.1
				2-32	0.09279441	0.7
Methyl Alcohol	204	-50 – 50	1.4 – 95	2-13	-0.04770032, 0,0, -0.07894037	0.8
				2-31	N/A	2.2
				2-32	0.101864494	0.9
Propylene Glycol	273	-35 – 125	10 – 90	2-13	-0.01910107, 0,0, -0.080106158	0.4
				2-31	N/A	2.0
				2-32	0.0989810897	0.6
Ethylene Glycol	274	-35 – 125	10 – 90	2-13	-0.01321611, 0,0, -0.07017709	0.5
				2-31	N/A	1.7
				2-32	0.084211734	0.6

Equation 2-13 predicts density of the mixtures in very good agreement with the experimental data but the number of operations required by the equation is large. This can slow the system simulation. A simple weighted average was tried. Equation 2-31 gives the form of the equation.

$$\rho = \rho_1 N_1 + \rho_2 N_2 \tag{2-31}$$

Where, ρ = density of the fluid (kg/m^3)

By comparison to Equation 2-13, Equation 2-31 poorly predicts the density of the mixture below 0^{o}C. A correction factor was introduced in Equation 2-31. Equation 2-32 gives the form of the equation with correction factor.

$$\rho = (\rho_1 N_1 + \rho_2 N_2) * A N_1 N_2 \tag{2-32}$$

The coefficient 'A' in Equation 2-31 can be estimated using parameter estimation. The coefficient of Equation 2-32 for each mixture is given in Table 2-12. Equation 2-32 predicts aqueous mixture density with a maximum error of less than $\pm$ 6%. The maximum error was noticed at -50^{o}C and 50% concentration.

Figure 2-12 illustrates the performance of Equation 2-32 for aqueous mixture of methyl alcohol.

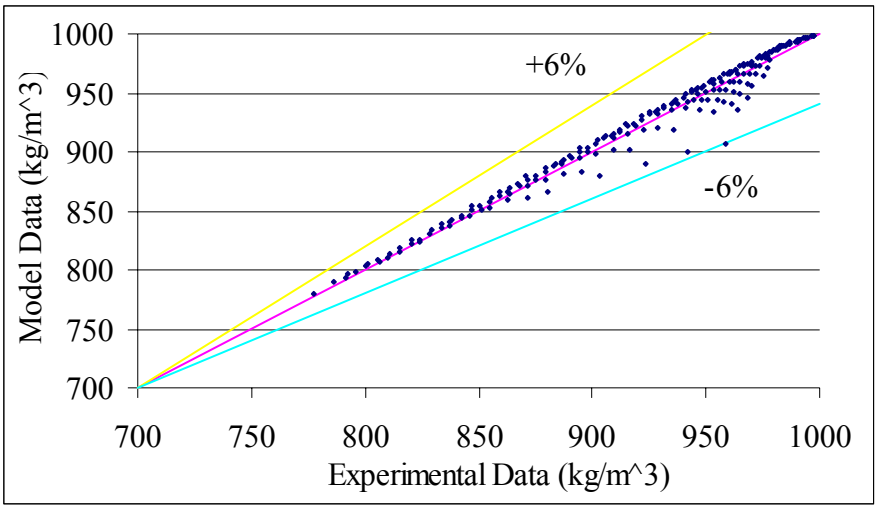

Figure 2-12. Performance of Equation 2-32 for density of aqueous mixture of Methyl Alcohol (Experimental data collected from Bulone et al. (1991), Waterfurnace International Technical Bulletin (1985), Kurata et al. (1971), Melinder (1997), Mikhail and Kimmel (1961), Commerical Solvent Corporation (1960))

For a typical GSHP system simulation it was determined that the density function is called about $13 \cdot 10^7$ times. Equation 2-32 requires 106 seconds for $13 \cdot 10^7$ iterations as compared to 130 seconds required by Equation 2-13. While significantly reducing the number of operations required with Equation 2-13, Equation 2-32 gives slightly higher errors. Equation 2-32 is suggested for density calculation of the selected aqueous mixtures because of speed and accuracy.

2.6.5 Freezing Point

Freezing point data for each of the fluids of interest for the concentration range given in Table 2-13 was taken from Melinder (1997). A third order polynomial was used to fit the data. The equation gives the freezing point temperature of the aqueous mixture as a function of concentration. Equation 2-33 gives the form of the equation

$$T_{freeze} = \sum_{n=0}^{3} A_n N^n \qquad (2\text{-}33)$$

Where, N = Concentration of the organic component (Wt %)

$A_0 - A_3$ = Coefficients

The range of concentration to which Equation 2-33 is applicable is given in Table 2-13 along with the coefficients.

Table 2-13: Range of applicability and coefficients for Equation 2-33

Aqueous Mixture of	Applicable Range N	Coefficient A	RMSE (^oC)
Ethyl Alcohol	0-60	0.00019919 -0.02051118 - 0.23235185 0.09685258	0.29
Methyl Alcohol	0-50	-0.00008979 -0.00496266 -0.62101652 0.074854652	0.06
Propylene Glycol	0-60	-0.00016667 0.00178571 -0.34404762 0.07142857	0.42
Ethylene Glycol	0-60	-0.00002778 -0.00869048 -0.212698413 4E-13	0.11

2.7 Summary of Suggested Equations

Table 2-14 gives the form of suggested equations for the thermophysical property calculation for the aqueous mixtures of ethyl and methyl alcohol, and ethylene and propylene glycol respectively.

Table 2-14: Form of the suggested equations

Property	Eq. No	Form of the Equation
Density	2-32	$\rho = (\rho_1 N_1 + \rho_2 N_2) * A N_1 N_2$
Viscosity	2-28	$\ln \mu = (N_1 \ln \mu_1 + N_2 \ln \mu_2) + \ln\left(1 + \frac{N_1 N_2}{A_1 N_1^{\,2} + A_2 N_2^{\,2}}\right) + A_3 (A_5 - T)^{A_4} N_1 N_2$
	2-29	$\ln\mu = (N_1 \ln\mu_1 + N_2 \ln\mu_2) + N_1 N_2 A_1 \lvert \ln\mu_1 - \ln\mu_2 \rvert + \ln\left(1 + \frac{N_1 N_2}{A_2 N_2^4 + A_3 N_2^4}\right)$
Thermal Conductivity	2-5	$k = \left(N_1 k_1^{\,A} + N_2 k_2^{\,A}\right)^{\left(\frac{1}{A}\right)}$
Specific Heat Capacity	2-30	$C_p = (C_{p_1} N_1 + C_{p_2} N_2) * (1 + A_1 N_1 N_2) + A_2 (A_3 - T) N_1 N_2 + A_4 (A_3 - T)$
Freeze point Temperature	2-33	$T_{freeze} = \sum_{n=0}^{3} A_n N^n$

Tables 2-15 and 2-16 give the estimated coefficients and the RMSE of each suggested equation.

Table 2-15: Coefficients of the suggested equations for aqueous mixture of ethyl and methyl alcohol

Property	Aqueous Mixture of									
	Ethyl Alcohol					Methyl Alcohol				
	Eq	Range		Coefficient A	RMSE	Eq	Range		Coefficient A	RMSE
		T (C)	N (Wt %)				T (C)	N (Wt %)		
Density	2-32	-45 – 40	2.5 – 95	0.09279441	0.7 %	2-32	-50 – 50	1.4 – 95	0.101864494	0.9 %
Viscosity	2-28	-35 – 50	1 – 96	0.29921813 0.725703898 0.003868226 1.61437032 60.00840782	9.8 %	2-28	-45 – 50	2 – 95	1.520446884 14.70346315 0.045602652 0.975329376 97.47210832	3.3 %
Thermal conductivity	2-5	-70 – 60	5 – 95	0.051892	1.9 %	2-5	-45 – 50	5 – 95	0.0201599	1.6 %
Specific Heat Capacity	2-30	-25 – 75	5 – 95	1.073308 -0.03601932 74.3958442 0.002081859	3.9 %	2-30	-35 – 40	5 – 95	0.798624897 -0.06212194 51.23724925 0.00262289	3.3 %
Freeze point temperature	2-33	N/A	0 – 60	0.00019919 -0.02051118 -0.23235185 0.09685258	0.3 ^{o}C	2-33	N/A	0 – 50	-0.00008979 -0.00496266 -0.62101652 0.074854652	0.06 ^{o}C

Table 2-16: Coefficients of the suggested equations for aqueous mixture of ethylene and propylene glycol

Property	Aqueous Mixture of									
	Ethylene Glycol					Propylene Glycol				
	Eq	Range		Coefficient A	RMSE	Eq	Range		Coefficient A	RMSE
		T (C)	N (Wt %)				T (C)	N (Wt %)		
Density	2-32	-35 – 125	10 – 90	0.084211734	0.6 %	2-32	-35 – 125	10 – 90	0.098981089	0.6 %
Viscosity	2-28	-35 – 125	10 – 90	-0.462659185 3.7063275478 19.52078969	6.9 %	2-28	-35 – 125	10 – 90	-0.30998878 4.876953323 18.333761154	8.5 %
Thermal conductivity	2-5	-35 – 125	10 – 90	-0.4690312	2%	2-5	-35 – 125	10 – 90	0.157237	2%
Specific Heat Capacity	2-30	-35 – 125	10 – 90	0.223375729 -0.00503512 122.398371 -0.00119436	2%	2-30	-35 – 125	10 – 90	0.436989569 -0.00225207 175.954738 -0.00077749	1.6 %
Freeze point temperature	2-33	N/A	0 – 60	-0.00002778 -0.00869048 -0.212698413 4E-13	0.1 °C	2-33	N/A	0 – 60	-0.00016667 0.00178571 -0.34404762 0.07142857	0.42 °C

For GSHP applications the concentration of antifreeze needed is not above 50% for any of the mixtures studied and the loop temperature does not go above 80°C. Using data for concentration no higher than 50% and temperatures no higher than 80°C allow more accurate equation fits, within this range. Tables 2-17 and 2-18 give the coefficients of the suggested equations fitted to data in this range, applicable to GSHP applications. For most predictions, the RMSE is significantly reduced by limiting the range in this manner.

Table 2-17: Coefficients of the suggested equations for aqueous mixture of ethyl and methyl alcohol for data fitted to typical GSHP application range

Property	Aqueous Mixture of									
	Ethyl Alcohol					Methyl Alcohol				
	Eq	Range		Coefficient A	RMSE	Eq	Range		Coefficient A	RMSE
		T (C)	N (Wt %)				T (C)	N (Wt %)		
Density	2-32	-45 – 40	2.5 – 50	0.0976903485	0.7 %	2-32	-50 – 50	1.4 – 50	0.0991198263	0.9 %
Viscosity	2-28	-35 – 50	1 – 50	0.301859728 1.049620852 0.0022566826 1.77176716 60.0020972	4.5 %	2-28	-45 – 50	2 – 50	1.340454355 14.9965323 0.0116235 1.229762188 113.94885845	2.9 %
Thermal conductivity	2-5	-70 – 60	5 – 50	0.0943208975	1.9 %	2-5	-45 – 50	5 – 50	0.0626245655	1.1 %
Specific Heat Capacity	2-30	-25 – 75	5 – 50	1.073308 -0.03601932 74.3958442 0.002081859	3.9 %	2-30	-35 – 40	5 – 50	0.798624897 -0.06212194 51.23724925 0.00262289	3.3 %
Freeze point temperature	2-33	N/A	0 – 60	0.00019919 -0.02051118 -0.23235185 0.09685258	0.3 ^{o}C	2-33	N/A	0 – 50	-0.00008979 -0.00496266 -0.62101652 0.074854652	0.06 ^{o}C

Table 2-18: Coefficients of the suggested equations for aqueous mixture of ethylene and propylene glycol for data fitted to typical GSHP application range

Property	Aqueous Mixture of									
	Ethylene Glycol					Propylene Glycol				
	Eq	Range		Coefficient A	RMSE	Eq	Range		Coefficient A	RMSE
		T (C)	N (Wt %)				T (C)	N (Wt %)		
Density	2-32	-35 – 80	10 – 50	0.066069075	0.2 %	2-32	-35 – 80	10 – 50	0.09225881	0.3 %
Viscosity	2-28	-35 – 80	10 – 50	-0.515524366 3.242611466 14.67586599	3.7 %	2-28	-35 – 80	10 – 50	-0.111207612 84649.5237 424963.466	4.1 %
Thermal conductivity	2-5	-35 – 80	10 – 50	-0.326368886	1.4 %	2-5	-35 – 80	10 – 50	0.208807513	0.9 %
Specific Heat Capacity	2-30	-35 – 80	10 – 50	-1.003330988 -0.012570721 -209.3375852 -0.000423319	1.8 %	2-30	-35 – 80	10 – 50	0.47787832 -0.004759962 175.9460211 -0.000289212	0.7 %
Freeze point temperature	2-33	N/A	0 – 60	-0.00002778 -0.00869048 -0.212698413 4E-13	0.1 ^{o}C	2-33	N/A	0 – 60	-0.00016667 0.00178571 -0.34404762 0.07142857	0.42 ^{o}C

2.8 Computational Speed

The original intention of the study was to get better results in terms of reliability, speed, and accuracy as compared to Melinder's models. As mixing rules in general have some basis in the thermodynamic characteristics of the mixture, they can be deemed reliable even with some interpolation or extrapolation. Some work needs to be done to improve the accuracy of the models especially for the case of viscosity. The equations were tested for computational speed and compared to Melinder's models. The number of times a property subroutine would be called in a typical GSHP system simulation with two heat pumps and one GLHE, solving for mass flow rate, was determined. Each property subroutine was tested by calling it the number of times determined for the

typical simulation and keeping track of the required time with a stopwatch. The results are shown in Table 2-19. Models given by Melinder (1997) execute faster in all the cases tested.

Table 2-19: Computational speed test results

	Number of calls given to the models	Time Taken by Melinder Models (seconds)	Time Taken by Models developed in this study (seconds)
Specific Heat	8,610,801	105	125
Density	13,201,470	87	105
Thermal Conductivity	4,202,489	32	45
Viscosity	4,402,906	45	75

The simulation took 15 minutes to complete of which about 5 minutes were used to compute the thermophysical properties, making it a significant factor in time taken for the simulation to complete. Improvement in the computation time is important and should be the focus of future study. The mixing rules subroutines computation time can be reduced by developing models for pure properties that work for the entire range, as now some of the pure properties require two equations to cover the entire temperature range. Another way to reduce the computation time would be to initialize a lookup table at the first time step of the simulation. As the concentration for GSHP system simulation does not change during the simulation, a lookup table can be initialized which contains properties for a fixed concentration and a specified temperature range. During the simulation instead of calling the subroutines, the values in the lookup table could be interpolated to get the thermophysical property at the required temperature.

Even though the Melinder's models execute faster and can result in time saving, the equation fit formulation is strictly limited to the range of data for which it was fit. As the available data in literature is limited, both interpolation and extrapolation are required to cover the entire range. This may cause accuracy problems and result in the simulation results being wrong.

2.9 Concluding Remarks and Recommendations for Future Work

Thermophysical properties of aqueous mixtures of Methyl alcohol, Ethyl alcohol, Propylene glycol, and Ethylene glycol were found in literature. The properties were correlated using the mixing rule correlations found in the literature. In some cases, the mixing rules had to be modified to fit data below 0^{o}C. The root mean square error was calculated for all the properties and was below 4%, except for viscosity for which it was below 10% for all temperature and concentration range used for fitting data.

For typical GSHP applications, a different set of coefficients for each of the models were calculated for typical concentration and temperature range. For most predictions, the RMSE is significantly reduced by limiting the range.

The mixing rule correlations developed are applicable to a broader range than equation fit models given by Melinder (1997). Further work needs to be done to increase the computational speed of the models.

CHAPTER 3

Ground Source Heat Pump System Modeling and Simulation

3.1 Introduction

Building energy efficiency is increasingly becoming a focus of attention as energy costs rise. There are around 81 million buildings in the U.S.; these buildings consume more energy than any other sector of the U.S economy (DOE 2004). Engineers have increasingly begun to focus on the relationship between design variables and building energy efficiency. With the increase in available desktop computing power, there has been an increased interest in simulation of building heating and cooling systems used as a tool in designing energy efficient buildings. The impact of changing a design variable can be evaluated with ease using computer simulations. Computer simulation can also be used to evaluate different designs for selection of an acceptable design, study system behavior under off-design conditions, improve or modify existing systems and optimize design. Computer simulation is not the same as physically running a system but it is the most powerful tool available in predicting how a complex system will behave.

One computer simulation package designed to simulate HVAC systems is HVACSIM+ (Clark 1985). HVACSIM+ is a non-proprietary simulation package developed at the National Institute of Standards and Technology (NIST), Gaithersburg, Maryland, U.S.A. HVACSIM+ stands for 'HVAC SIMulation PLUS other systems'. It is capable of modeling HVAC (heating, ventilating, and air-conditioning) systems, HVAC controls, the building shell, and other energy management systems. HVACSIM+ represents HVAC elements as individual components, which are connected to form a

complete system. The program uses a hierarchical, modular approach and advanced equation-solving techniques to perform simulations of building/HVAC/control systems.

The kernel of HVACSIM+ is called MODSIM, which stands for 'modular simulation'. The modularity of the package is attained by component models represented as TYPE subroutines. Each TYPE subroutine is linked by manipulating a unique index number assigned to each input and output. To the user, each component model is presented as a black box, which takes in a set of inputs and gives outputs. MODSIM uses a hierarchical approach to handle large simulations; a number of functionally related component models can form a BLOCK. A number of BLOCKS make up a SUPERBLOCK(S) that comprises the simulation. MODSIM assumes a weak coupling between SUPERBLOCKS and solves each SUPERBLOCK as an independent subsystem.

The HVACSIM+ simulation package came with a menu-driven user interface, HVACGEN. The problem with the original user interface as pointed out by Clark (1985) is that, during the simulation setup, if the user makes a mistake, either the process has to be aborted or arbitrary values must be supplied to get to the next menu.

A graphical user interface was developed in order to overcome the shortcoming of the menu-driven user interface, along with a means to define the system in terms of boundary values, simulate the system and plot the simulation output (Varanasi 2002). The main features of the tool are as follows:

- The tool uses icons to represent units, boundary variables and connections between them.

- The tool imitates the functionality of HVACGEN using an event-driven approach but also goes a step forward and makes calls to SLIMCON and MODSIM programs in the background. The need for the user to use three different programs to build and run a simulation is thus eliminated.

- The tool features ease of inputting the parameters through a grid component or a model parameter file.

- The user is not required to keep track of variable indices.

- The tool provides facilities to plot or write the results in CSV file format.

- An online help system supports the tool.

System simulation is an essential design tool for GSHP systems, particularly hybrid ground source heat pump (HGSHP) systems (Spitler 2001). In the following text, setting up GSHP, HGSHP, and direct cooling system simulation using the Visual Tool in HVACSIM+ is explained along with the description of models of individual components. The flow network analysis methodology developed is described and a tool developed for running multiyear simulations is explained.

3.2 Model Descriptions

The models developed or translated from various sources for use in HVACSIM+ are described in this section. The mathematical descriptions, inputs, outputs, and parameters of each model are given in Appendix A.

3.2.1 Water-to-Air Heat Pump Models

The heat pump is a reversible air-conditioner; it can operate to provide both heating and cooling. The GSHP systems installed in residential buildings usually use a water-to-air heat pump, the name "water-to-air" indicating the heat is extracted /rejected from water, and air is used as the medium to transport heat to the conditioned space. Two approaches can be taken for mathematical modeling of the heat pump as explained below.

3.2.1.1 Equation Fit Model

Equation fit models, often referred to as "curve fit" models, treat the system as a black box and fit the system performance to one or a few equations. A simple equation fit model was developed that simulates the performance of water-to-air heat pump with an assumption that load-side entering conditions are constant and the equations are fit for these conditions. The model also assumes there are no losses from the heat pump; that is in cooling mode, the heat rejection is always equal to the cooling plus the power input.

Entering fluid temperature, the space heating/cooling loads, and fluid mass flow rate are inputs to the model. By convention, the space heating loads are positive and the space cooling loads are negative. The exiting fluid temperature, power consumption, runtime fraction and unmet loads are outputs of the model. Two sets of coefficients are parameters of the model, one for heating mode and the other for cooling mode. The coefficients of the equation are used to determine the coefficient of performance (COP), minimum and maximum entering fluid temperatures for which the equation is valid, and the capacity of the heat pump.

The COP is computed using an equation fit to the manufacturer's catalog data. The equation is a function of both mass flow rate and entering water temperature:

$$COP(T,\dot{m}) = C_1 + C_2 * T + C_3 * T^2 + C_4 * \dot{m} + C_5 * \dot{m}^2 + C_6 * \dot{m} * T \quad (3\text{-}1)$$

Where, C_i= coefficients

T= entering fluid temperature (^oC)

$\dot{m}$ = mass flow rate (kg/s)

Subscript i= 1 to 6

Power consumption is calculated using the COP. As the model is an equation fit to catalog data, no extrapolation is allowed. To prevent extrapolation, maximum and minimum entering fluid temperatures are given as parameters. If the EFT goes out of range of the catalog data, minimum/maximum temperatures are used to calculate COP.

Assuming no losses, the ratio of heat of extraction to heating provided (heating) and heat of rejection to cooling provided (cooling) is determined using Equations 3-2a and 3-2b.

$$Ratio_{(HE/Heating)} = 1 - 1/COP \quad (3\text{-}2a)$$

$$Ratio_{(HR/Cooling)} = 1 + 1/COP \quad (3\text{-}2b)$$

Real heat pumps are thermostatically controlled in an on-off manner, which results in the cycling of the heat pump. Circulating pumps are often slaved to the heat pump. As GSHP simulations are often run with one-hour time steps, it is necessary to consider this cycling effect of the heat pump on the circulating pump power consumption. This is done by calculating the runtime of the heat pump and providing it as an output,

which is then used by the circulating pump model to calculate the part load power consumption. The heat pump capacity is required to calculate the runtime of the heat pump. Heat pump capacity is computed as the function of entering fluid temperature (EFT) using a linear-fit equation to the manufacturer's catalog data. Runtime is calculated as the ratio of the space heating load to the heat pump heating capacity or the ratio of space cooling load to the heat pump cooling capacity.

The unmet loads are reported for optimization purposes and quality assurance. For hours where the space heating or cooling load exceeds the heat pump capacity, unmet loads are calculated as space heating/cooling loads minus heating/cooling provided by heat pump.

The model cannot directly handle the effect of antifreeze mixture, though performance degradation can be modeled by correction factor given in the catalog data. The correction factors should be applied to catalog data before calculating coefficients of the model for the intended antifreeze mixtures.

If mass flow rate or space heating/cooling load inputs become zero, the model mimics shut off by setting the exiting fluid temperature to entering fluid temperature, setting unmet loads to space heating/cooling loads and setting power consumption and runtime fraction to zero.

3.2.1.2 Parameter Estimation Model

This heat pump model is a parameter estimation-based steady state simulation model (Jin 2002), built up from models of individual components i.e. compressor, heat exchangers, etc. Various unspecified parameters for individual components are estimated

simultaneously from the heat pump manufacturer's catalog data using a multivariable optimization procedure. Several additional features have been added as a part of this work, which includes some consideration of cycling effects, reporting of unmet loads, and better exception handling.

The entering air wet-bulb temperature, entering air dry-bulb temperature, entering water temperature, air and water mass flow rates and space heating/cooling loads are inputs to the model. The space heating/cooling loads are used to calculate the unmet loads and estimate runtime of the heat pump. The sensible and total load-side heat transfer rates, source-side heat transfer rate, power consumption, leaving air dry-bulb temperature, leaving source-side temperature, runtime fraction, and unmet loads are outputs of the model. Various parameters required by the models of individual components of the heat pump and antifreeze mixture type and concentration are parameters of the model.

This model can predict the performance variation when an antifreeze mixture is used as circulating fluid (Jin and Spitler 2003). A degradation factor (Equation 3-3) is calculated which is multiplied by the fluid-side heat transfer coefficient (originally estimated for water.) In turn, the heat pump performance with antifreeze can be modeled.

$$DF = \frac{h_{antifreeze}}{h_{water}} = \left(\frac{\mu_{antifreeze}}{\mu_{water}}\right)^{-0.47} \left(\frac{\rho_{antifreeze}}{\rho_{water}}\right)^{0.8} \left(\frac{C_{p\,antifreeze}}{C_{p\,water}}\right)^{0.33} \left(\frac{k_{antifreeze}}{k_{water}}\right)^{0.67} \tag{3-3}$$

Where, h = convection coefficient (W/m^2 K)

μ = viscosity (mPa s)

ρ = density (kg/m^3)

C_p = specific heat (kJ/kg K)

k = thermal conductivity (W/m K)

The overall heat transfer coefficient with antifreeze mixture is calculated as equation 3-4.

$$UA_{total\_antifreeze} = \frac{1}{C_3 \dot{V}^{-0.8} / DF + C_2} \tag{3-4}$$

Where, $C_3 \dot{V}^{-0.8}$ = estimated coolant side resistance (-)

C_2 = estimated resistance due to refrigerant to tube wall convection, tube wall conduction and fouling. (K/W)

C_2 and C_3 can be estimated from the catalog data given for use with pure water.

A number of issues arise when an attempt was made to translate this model to use it within HVACSIM+. The following text explains the issue and the solution to address each of the issues.

The first issue was that no consideration of the cycling effect of the heat pump was made in the original model. Space heating/cooling loads were made an input to the model, and the runtime fraction is calculated as the ratio of space heating/cooling loads to calculated heat pump capacity. The heat pump runtime fraction is multiplied by the power consumption and heat transfer rates to calculate the hourly power consumption and hourly heat transfer rates accordingly.

The second issue was that the original model does not report if the heat pump was unable to meet the space heating/cooling loads. This is required for quality assurance and

optimization purposes. The unmet loads are now calculated as the space heating/ cooling loads minus heat pump capacity and reported as an output of the model.

The third issue arises because of the refrigerant property subroutines. The subroutines use curve fit equations (adapted from Downing 1974). Extrapolation can lead to failure, as the subroutines do not feature exception handling. Unrealistic inputs (a likely scenario in system simulation packages when the program is automatically adjusting variables to find a solution) to the curve fit equations used in the model are the likely cause of the program to crash. The source side heat exchanger in both heating and cooling mode, and the load side heat exchanger in the heating mode are treated as a sensible heat exchangers with phase change on one side. Equation 3-5 gives the thermal effectiveness of the sensible heat exchanger.

$$\varepsilon = 1 - e^{\left(\frac{-UA_s}{\dot{m}_F C_{pF}}\right)} \tag{3-5}$$

Where, ε = heat transfer effectiveness (-)

UA= heat transfer coefficient (kW/K)

$\dot{m}_F$ = water mass flow rate or air mass flow rate in case of heating operation (kg/s)

C_{pF} = specific heat of water or air (kJ/kgK)

The evaporating and condensing temperatures in heat pump are computed using the effectiveness calculated with Equation 3-5; the evaporating and condensing temperatures for heating modes for both source and load side and the cooling mode for the source side are calculated using Equation 3-6.

$$T = T_i - \frac{Q_{guess}}{\varepsilon \dot{m} C_p} \tag{3-6}$$

Where, T= condensing or evaporating temperature (^oC)

T_i= source or load side entering fluid temperatures (^oC)

Q_{guess}= initial values of the heat transfer rates (W)

The heat transfer rates are updated every iteration until the convergence criterion is met. Very small flow rate on the evaporator or condenser side cause very high temperatures, which in turn crash the refrigerant property subroutines due to negative square root or negative logarithmic errors. This exception is now handled by checking the mass flow rate on the evaporator and condenser side and if the mass flow rate is very small (less than 0.01 kg/sec) the iteration is started again with a new guess of heat transfer rates.

The other issue related to refrigerant properties subroutines is related to suction and discharge pressures. The suction pressure and the discharge pressure are calculated using equations 3-7 and 3-8.

$$P_{suction} = P_e + \Delta P_1 \tag{3-7}$$

$$P_{discharge} = P_c + \Delta P_2 \tag{3-8}$$

Where, ΔP_1 = pressure drop across the suction valve (kPa)

ΔP_2 = pressure drop across the discharge valve (kPa)

Very low evaporating temperatures result in low evaporating pressure and can result in negative suction pressures, which crashes the property subroutines. This exception is handled by starting the iterations for heat transfer calculations again with a new guess if

the calculated suction or discharge pressure becomes equal or greater to maximum and minimum suction and discharge pressures set by the user.

Finally, another issue that made the program crash is related to mass flow rates. Mass flow rate appears in the denominator of number of equations. Thus, zero flow rates on the evaporator or condenser sides cause the program to crash due to a division by zero error. This exception is comparatively easy to handle; if the mass flow rate input is zero, computation of equations is skipped, exiting fluid temperature is set equal to entering fluid temperature; power consumption and the heat transfer rates are set to zero.

3.2.2 Counter Flow Single Pass Single Phase Heat Exchanger Model

The model computes heat transfer rate and exiting fluid temperatures given mass flow rates and entering temperatures of the two fluids. The overall heat transfer coefficient and the fluid types (antifreeze mixture or pure water, used for specific heat calculation) are the parameters for the model. A typical application of the model would be in hybrid ground source heat pump (HGSHP) system where the ground loop and supplemental heat rejecter loop are configured separately and the heat is transferred through a heat exchanger between the two loops. The model can compute the heat transfer between the ground loop and supplemental heat rejecter loop in HGSHP system application.

The model uses the Number of Transfer Units (NTU) method. The NTU method is derived around the concept of a formal definition of effectiveness (Hodge and Taylor 1998). The effectiveness of the heat exchanger is defined as the ratio of actual rate of heat transfer to the maximum thermodynamically possible rate of heat exchange. Equation 3-9

gives the effectiveness of a counter flow single pass heat exchanger (Hodge and Taylor 1998).

$$\varepsilon = \frac{1 - \exp[-\mathrm{NTU}(1-\mathrm{C})]}{1 - \mathrm{C}\exp[-\mathrm{NTU}(1-\mathrm{C})]} \tag{3-9}$$

Where, C = C_{min}/C_{max} (-)

C_{min} = the smaller of the C_h and C_c (kW K)

C_{max} = the greater of the C_h and C_c (kW K)

$C_c = \dot{m}_c C_{pc}$ (kW K)

$C_h = \dot{m}_h C_{ph}$ (kW K)

$\dot{m}$ = the mass flow rate of the fluid (kg/s)

C_p = the specific heat of fluid (kJ/kg.K)

Subscript: h = hot fluid

c= cold fluid

Equation 3-10 gives the NTU.

$$\mathrm{NTU} = \frac{UA}{C_{\min}} \tag{3-10}$$

UA is the overall heat transfer coefficient (kW/K); it can be estimated from catalog data or laboratory experiments.

The total heat transfer rate is calculated using Equation 3-11 and exiting fluid temperature is calculated using the heat transfer rate.

$$Q = \varepsilon C_{\min}(T_{h,in} - T_{c,in}) \tag{3-11}$$

Where, Q = heat transfer rate (kW)

$T_{h,in}$ = entering fluid temperature on hot side (^{o}C)

$T_{c,,in}$ = entering fluid temperature on cold side (^{o}C)

ε = Effectiveness of the heat exchanger given in Equation 3-9. (-)

The exceptions of either of the input mass flow rates being zero or capacitance 'C' equal to one is handled by setting equal the exiting fluid temperatures to entering fluid temperatures and setting heat transfer rate to zero.

3.2.3 Cooling Tower Model

The cooling tower model was translated from the HVAC1Toolkit (LeBrun et al. 1999) for use in HVACSIM+. Mass flow rates of water and air, entering water temperature, and entering air wet-bulb temperature are inputs to the model. The exiting air wet-bulb and water temperature are outputs of the model. The overall heat transfer coefficient is the parameter of the model.

The model is based on Merkel's theory. The sensible plus latent heat transfer for a differential element under steady state conditions may be defined by Merkel's theory:

$$d\dot{Q}_{w-air} = \frac{UdA}{C_p}(h_s - h_a) \tag{3-12}$$

Where, $d\dot{Q}_{w-air}$ = total heat transfer between air and water for a differential area (W)

h_s = enthalpy of saturated air at wetted-surface temperature (J/kg)

h_a = enthalpy of air in free stream (J/kg)

U = overall heat transfer coefficient (W/m^2 K)

C_p = specific heat of moist air (J/kg.K)

dA = differential area (m^2)

The model does not take into account the effect of water loss by evaporation and assumes no heat is added by the fan. The cooling tower, in effect, is modeled as a classical counter flow heat exchanger with water as one of the fluids and moist air treated as an equivalent ideal gas as the second fluid. Equation 3-13 gives the total (sensible + latent) heat transfer based on these assumptions.

$$d\dot{Q}_{w-air} = U_e dA(T_w - T_{wb}) \tag{3-13}$$

Where, $U_e = \dfrac{UC_{pe}}{C_p}$ = effective overall heat transfer coefficient (W/m^2 K)

T_w = entering water temperature (^oC)

T_{wb} = entering air wet bulb temperature (^oC)

The equivalent fluid specific heat is given by Equation 3-14.

$$C_{pe} = \Delta h / \Delta T_{wb} \tag{3-14}$$

Where, C_{pe} = mean specific heat (J/kg K)

Δh = difference of entering and exiting moist air enthalpy (J/kg)

ΔT_{wb} = difference of entering and exiting moist air temperature (^oC)

An energy balance on the water and air sides gives Equation 3-15a and 3-15b.

$$d\dot{Q}_{w-air} = \dot{m}_w C_{pw} \Delta T_w \tag{3-15a}$$

$$d\dot{Q}_{w-air} = \dot{m}_a C_{pe} \Delta T_{wb} \tag{3-15b}$$

Where, $\dot{m}_w$ = mass flow rate of water (kg/s)

$\dot{m}_a$ = mass flow rate of air (kg/s)

C_{pw} = specific heat of water (J/kg K)

ΔT_w = difference of entering and exiting water temperature (^oC).

Equation 3-13, 3-15a and 3-15b are integrated and combined with the effectiveness expression given in Equation 3-16

$$\varepsilon = \frac{T_{win} - T_{wout}}{T_{win} - T_{wbin}} \tag{3-16}$$

Where, T_{win} = inlet water temperature (^oC)

T_{wout} = outlet water temperature (^oC)

T_{wbin} = inlet air wet bulb temperature (^oC)

Equation 3-17 results from integrating Equations 3-13, 3-15a and 3-15b and combining them with Equation 3-16.

$$\varepsilon = \frac{1 - \exp[-NTU(1-C)]}{1 - C\exp[-NTU(1-C)]} \tag{3-17}$$

Where, ε = effectiveness (-)

$C = C_w/C_e$ (-)

$C_w = \dot{m}_w C_{pw}$ (kJ/s K)

$C_e = \dot{m}_a C_{pe}$ (kJ/s K)

$\dot{m}$ = the mass flow rate of the fluid (kg/s)

C_p = the specific heat of fluid (kJ/kg.K)

Subscript: e = equivalent ideal fluid

w= water

Equation 3-18 gives the NTU.

$$\text{NTU} = \frac{UA_e}{C_w} \tag{3-18}$$

Equation 3-17 is the same expression used for effectiveness of counter flow heat exchanger, thus the cooling tower can be modeled under steady state conditions as an equivalent counter flow heat exchanger.

The model requires heat transfer coefficient as a parameter, this can be estimated using catalog data or laboratory tests and is assumed a function of air mass flow rate only (A utility was developed in Java for the estimation of the heat transfer coefficient; a brief description and step by step installation procedure is given in Appendix B).

The exception of either of the input mass flow rates being zero is handled by setting equal the exiting fluid temperatures to entering fluid temperatures.

The cooling tower power consumption is not modeled. Future work should be aimed at incorporating the power consumption of the cooling tower.

3.2.4 Circulating Pump Model

Circulating pumps are used in GSHP systems to circulate the fluid in the system. Two approaches can be taken for modeling of circulating pump as explained below. For the ideal model, the user supplies the pump pressure rise, the fluid flow rate and the efficiency, which is used to determine the pumping power. The detailed model gives the fluid mass flow rate output for a pressure drop input and determines the pumping power

but require a large number of parameter inputs. In practice, this is used with models of pipes, fittings, etc., which gives pressure loss as a function of mass flow rate. By solving all component models simultaneously, the detailed model allows the user to solve for the fluid flow rate, rather than set it.

3.2.4.1 Ideal Pump Model

This model is "ideal"- the user supplies the fluid flow rate and pump pressure rise. It is primarily used to calculate pumping power. Fluid flow rate, fluid temperature, and runtime fraction are inputs to the model. Pump power consumption and outlet fluid temperature are outputs of the model. The fluid type (antifreeze mixture type) and nominal values of flow rate, pump pressure rise, and efficiency are parameters of the model.

Equation 3-19 is used to calculate power consumption of the circulating pump

$$P = \frac{\Delta P \dot{m}}{\rho \cdot \eta} \tag{3-19}$$

Where, P = Power consumption of the pump (W)

$\dot{m}$ = mass flow rate of the fluid (kg/s)

ΔP = pressure rise across the pump (kPa)

η = efficiency of the pump (-)

ρ = density of fluid (kg/m^3)

In the system, all energy input to the pump is eventually dissipated. The motor and pump losses increase the temperature of the fluid at the pump exit:

$$T_{out} = T_{in} + \Delta P \left[\frac{\frac{1}{\eta} - 1}{\rho . C_p} \right] \quad (3\text{-}20)$$

Where, T_{in} = inlet fluid temperature (^{o}C)

C_p = specific heat (kJ/kg K)

The ideal pumping power is dissipated as frictional losses in the rest of the system. Currently, the temperature rise due to the frictional losses is not taken into account in the pipe and fitting models. In the future, this should be corrected by modifying the pipe and fitting models.

The runtime fraction input to the model is used for modeling the cycling effect of the heat pumps used in residential GSHP or commercial GSHP system with secondary pumping. In these systems, the circulating pump is controlled to run only when the heat pump is running. The runtime fraction is multiplied by the power consumption of the circulating pump calculated with Equation 3-19 to determine the power consumption when the system is not on for the whole hour.

3.2.4.2 Detailed Circulating Pump Model

The detailed model determines the fluid flow rate for a pressure drop input. Entering fluid temperature, pressure drop and runtime fraction are inputs to the model. Mass flow rate corresponding to the input pressure drop and the power consumption are outputs to the model. Rotational speed, impeller diameter, maximum and minimum pressure rise for which the equations were fit and the fluid type are parameters to the models.

Circulating pumps have different characteristics depending on their design, size, and speed. This complicates the modeling of the circulating pumps, as some means of obtaining physically realistic behavior is required to model the circulating pump when running under speed not specified in manufacturers catalog and using a fluid other than water. Similarity laws governing the relationship between variables within geometrically similar machines can be derived using dimensional analysis. In application, the similarity laws hold for geometrically similar machines and dynamically similar operating conditions (Miller 1995) though this is not the case in practice, as Reynolds number does not remain constant over the year especially when an antifreeze mixture is used. Dynamically similar conditions may exist for water as circulating fluid and fully turbulent flow. Hodge and Taylor (1998) give a method based on dimensional analysis and similitude that allow extrapolation of manufacturers' data within a small variation in speed. Equations 3-21 and 3-22 give the dimensionless parameters.

$$\varphi = \frac{\dot{m}}{\rho N D^3} \tag{3-21}$$

$$\psi = \frac{\Delta P}{\rho N^2 D^2} \tag{3-22}$$

Where, φ = dimensionless mass flow rate (-)

ψ = dimensionless pressure rise (-)

N= rotational speed (revolutions/sec)

D= impeller diameter (m)

Manufacturers catalog data are used to get dimensionless flow rate and pressure rise. Then, forth-order polynomial equation fits are used to get dimensionless flow rate and efficiency as a function of dimensionless pressure rise:

$$f(\varphi) = \sum_{i=0}^{4} C_i \psi^i \tag{3-23}$$

Maximum and minimum pressure rise are specified as parameters and then used to prevent exceptions caused by extrapolation.

The runtime fraction input to the model is used for modeling the cycling effect of the circulating pump, if slaved to a heat pump. The runtime fraction is multiplied by the power consumption of the circulating pump to determine the power consumption when the system is not on for the whole hour.

3.2.5 Fluid Mass Flow Rate Divider Model

This model is needed when the fluid flow network is modeled separately to get the mass flow rate at operating conditions (Fluid flow networks are explained in detail in Section 3.4). In this case, it is convenient to model some flow network elements in parallel as if they are identical and the total flow will be divided uniformly. This is a reasonable approximation when the pressure drop-mass flow rate relationship of the parallel elements is approximately the same. An example of this is a GSHP system with multiple boreholes. Even though the header piping lengths are different for different boreholes the pressure drop-mass flow rate relationship is dominated by the identical U-tube in each borehole. In this case, the fluid mass flow rate divider would be used to divide the total flow by the number of boreholes, and then the pressure drop will be

calculated for a single U- tube. This pressure drop will be added to other pressure drops that are in series. The total pressure drop is input to the detailed circulating pump model; the circulating pump model gives the power consumption and the mass flow rate at the operating conditions.

The fluid mass flow rate to be divided is input to the model. The divided fluid mass flow rates are outputs. (The model in HVACSIM+ has six fluid flow rates as outputs, though only one is needed in most cases). The fractions used to divide the input flow are parameters of the model.

3.2.6 Pressure Drop Adder Model

The total pressure drop is an input to the detailed circulating pump model. The pressure drops from individual elements of the fluid flow network in series are summed with this model to get the total pressure drop. The pressure drops of individual elements of the flow network are input to the model (the model in HVACSIM+ has six pressure drops as inputs) and a single pressure drop is an output.

Six pressure drop inputs are required by the model. If fewer pressure drops are needed, the remaining pressure drop inputs should be assigned to constant boundary conditions and set equal to zero.

3.2.7 Pipe Pressure Drop Model

This model computes pressure drop through a pipe with a given mass flow rate and temperature input. The pipe length, diameter, roughness ratio, and the type of circulating fluid (antifreeze mixture type) are parameters of the model.

Equation 3-24 is used for pressure drop in straight pipe.

$$\Delta P_{pipe} = \frac{f\dot{m}^2 L}{2A^2 D\rho g_c} \tag{3-24}$$

Where, ΔP_{pipe} = pressure drop through a straight pipe (Pa)

f = friction factor (-)

g_c = constant of proportionality = 1 (kg m/ N s^2)

A = Area (m^2)

L = Length of pipe (m)

ρ= Density of the fluid (kg/m^3)

$\dot{m}$ = mass flow rate (kg/sec)

The friction factor can be calculated by a number of correlations given in literature. The friction factor given by Churchill (Churchill 1977) is applicable to all flow regimes. Equation 3-25 gives the Churchill correlation.

$$f = 8\left[\left(\frac{8}{\mathrm{Re}}\right)^{12} + (a+b)^{-15}\right]^{\frac{1}{12}} \tag{3-25}$$

Where, Re= Reynolds number (-)

$$a = \left(2.457 \ln\left[\frac{1}{\left(\frac{7}{\mathrm{Re}}\right)^{0.9} + 0.27rr}\right]\right)^{16}$$

$$b = \left[\frac{37530}{\mathrm{Re}}\right]^{16}$$

rr = roughness ratio (-)

The Reynolds number is calculated using Equation 3-26.

$$\mathrm{Re} = VD/\nu \tag{3-26}$$

Where, V= velocity (m/s)

ν =kinematic viscosity (m^2/s)

D= diameter of the pipe (m)

Kinematic viscosity is calculated using the thermophysical models explained in Chapter 2 based on the entering fluid temperature.

3.2.8 Fitting Pressure Drop Model

This model computes pressure drop in fittings. Fluid mass flow rate and entering fluid temperature are inputs to the model. The model parameters are diameter, fluid type, and loss coefficient (K).

The 'K' value can be obtained from various handbooks. A list of commonly used fittings and their 'K' values are given in Hodge and Taylor (1998). The pressure drop is calculated using Equation 3-27.

$$\Delta P_{fit} = K \frac{V^2}{2g_c} \tag{3-27}$$

Where, ΔP_{fit} = pressure drop through a fitting (Pa)

V= velocity (m/s)

g_c = constant of proportionality = 1 (kg m/ N s^2)

3.2.9 Vertical GLHE Model

The GLHE model is an updated version of that described by Yavuzturk and Spitler (1999), which is an extension of the long-time step temperature response factor model of Eskilson (1987). Yavuzturk and Spitler (1999) extended Eskilson's (1987) model to shorter time scales of less than an hour. Liu (2004) revised the solution solving method to incorporate variable time steps and a hierarchical load aggregation algorithm to increase the computational efficiency of the model. The model is based on dimensionless, time-dependent temperature response factors known as "g-functions", which are unique for various borehole field geometries. The g-function for the geometry specified can be calculated using GLHEPRO software (Spitler 2000). The latest version of GLHEPRO (Version 3.1) writes the g-functions and the parameters defining the borehole configuration to the HVACSIM+ required parameter file format.

The vertical ground loop heat exchanger (GLHE) model computes the exiting fluid temperature, the average fluid temperature and the normalized heat extracted/rejected. The fluid mass flow rate and entering fluid temperature are inputs to the model. The g-functions and geometric configuration of the borehole and U-tube are parameters of the model.

3.2.10 Hydronic-Heated Pavement Model

The model can be used for as a supplemental heat rejecter in HGSHP systems or as a bridge deck with a hydronic snow-melting system. The hydronic-heated pavement system consists of hydronic tubing embedded in the concrete. The heat transfer, snow free area ratio, exiting fluid and surface temperatures are computed by the model. The

weather boundary conditions and the inlet temperature and fluid mass flow rate are inputs to the model. The geometric configurations of the pavement system are required as parameters to the model.

The hydronic-heated pavement system model was developed by Chiasson (1999) and modified by Liu (2004). The different modes of heat transfer considered at the top surface are the effects of solar radiation heat gain, convection heat transfer to the atmosphere, thermal or long-wave radiation heat transfer, sensible heat transfer to snow, heat of fusion required to melt snow, and heat of evaporation lost to evaporating rain or melted snow. The heat transfer modes considered for the bottom surface include convection heat transfer to the atmosphere and heat transfer due to radiation to the ground. Heat transfer mechanisms within the pavement include conduction through the pavement material and convection due to flow of the heat transfer fluid through the embedded pipes. The finite-difference equation for all nodes is obtained by the energy balance method for a control volume about the nodal region (i.e. using a "node-centered" approach) assuming all heat flow is into the node. Weather data are supplied by the user at a desired time interval and read from the boundary file.

3.2.11 Set Point Controller

The model was primarily developed for use in hybrid ground source heat pump (HGSHP) system simulation but its usefulness is not limited to this application. The model can be used in other applications where a switching signal is required based on a single input. In an HGSHP system, the set point controller is used to give signal to a three-way valve to direct flow to the supplemental heat rejecter when the loop temperature rises above a user specified set point temperature. The model has a

temperature as an input and gives a binary signal as output. The user specified set point temperature is a parameter of the model.

The model gives a binary switching signal as an output. The binary signal is set to 'on' (1) when temperature input equals or is greater than a user specified set point and the signal is set to 'off' (0) when the input temperature falls below the user specified set point temperature.

3.2.12 Differential Set Point Controller

This model as the set point controller model was primarily developed for use in HGSHP system simulation to give signal to a three-way valve to direct flow to a supplemental heat rejecter based on the difference of the loop temperature and ambient temperature. Typically, this is done if there is potential to reject heat from the loop to the atmosphere. The model has two temperature inputs and a single binary signal output. The upper and lower set point temperatures are parameters of the model.

Unlike the set point controller, the switching signal is based on the difference of the two temperature inputs and the user specified upper and lower set points. If the difference of the two temperature inputs is equal or greater than the user specified upper set point, an 'on' signal is given and if the difference falls below the user specified lower set point an 'off' signal is given as output. If the difference in the temperatures is in between the two set point temperature differences ('dead band'), the signal is not changed and remains at the last state set by the controller.

3.3 Modifications to the Visual Tool

The graphical user interface for HVACSIM + called Visual Modeling Tool (Varanasi 2002) was modified to fix bugs and to ease setting up a simulation and processing of output. Major modifications done to the tool are as follows

- Developed an editable grid form to enter parameters and initial guesses.
- From the editable grid form, files containing parameters can be read and written.
- Removed the GLHE parameters being read from a special file.
- Developed a subroutine that generates a comma delimited file (CSV) for export of results to spreadsheet.

The editable grid form features reading and writing of parameters to a text file, copying and pasting of parameters from the clipboard and manual editing of parameters by clicking the desired cell. These features are especially helpful when a model with large number of parameters is used; for example, the GLHE model has 210 parameters. This feature eliminated the need for a separate file containing the g-function values previously required by the GLHE model. Figure 3.1 shows the editable grid.

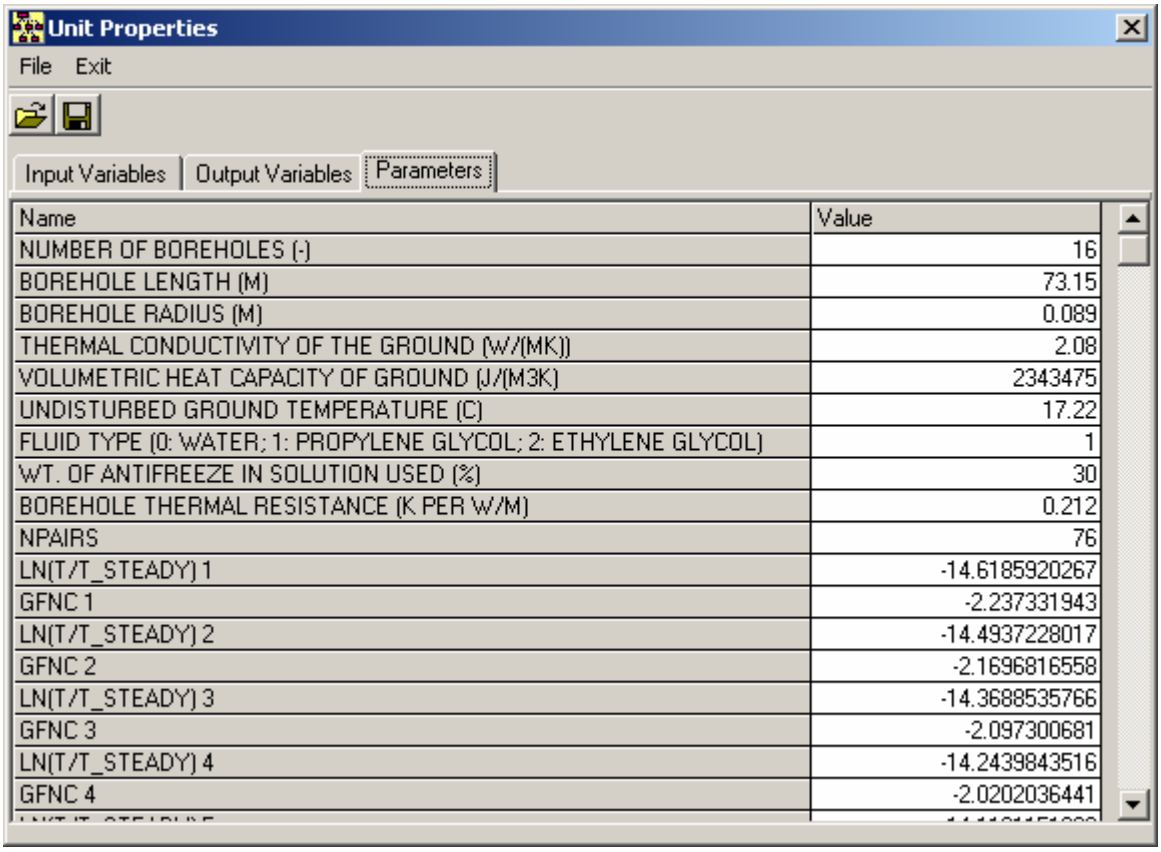

Figure 3-1. Editable grid for ease of parameter entry

The editable grid was made by designing a new form with the Microsoft grid component. When the icon representing the model is double clicked in the Visual Modeling Tool, the editable grid form opens with parameter names and parameter values set to zero if the model is newly created. For models loaded from a file, the form loads the parameter names and values associated with the model (from a global data-structure). The parameter names cannot be changed using the editable grid and only the values of the parameters can be changed. The changes made to the values are stored once the form is closed.

The values of the parameters can be stored using the 'write parameter file' option in the editable grid form. The files are written with a ".par" extension and in ASCII

format. The file can be opened with any text editor and editing manually if desired. The 'read parameter file' option in the editable grid form can be used to read the parameter values stored in the parameter file. The form can handle exceptions for example, if a parameter file is opened with more parameters than the component is expecting, a message is displayed indicating the file opened is not the correct parameter file for the component.

To extend plotting capabilities beyond the plotting tool of the graphical user interface the output file can be converted to a comma-delimited format so that more powerful commercially available plotting tools can be used to analyze results.

The output file generated by HVACSIM+ is in tab-delimited format and if the simulation contains more than one SUPERBLOCK the output format writes each of the reported variables in one SUPERBLOCK for each time step and than writes the next SUPERBLOCK reported variables. This format can be read by Microsoft Excel but plotting the results of interest would require some post processing if more than one SUPERBLOCK is used to setup the simulation. Figure 3-2 shows the format of the output file with more than one SUPERBLOCK used.

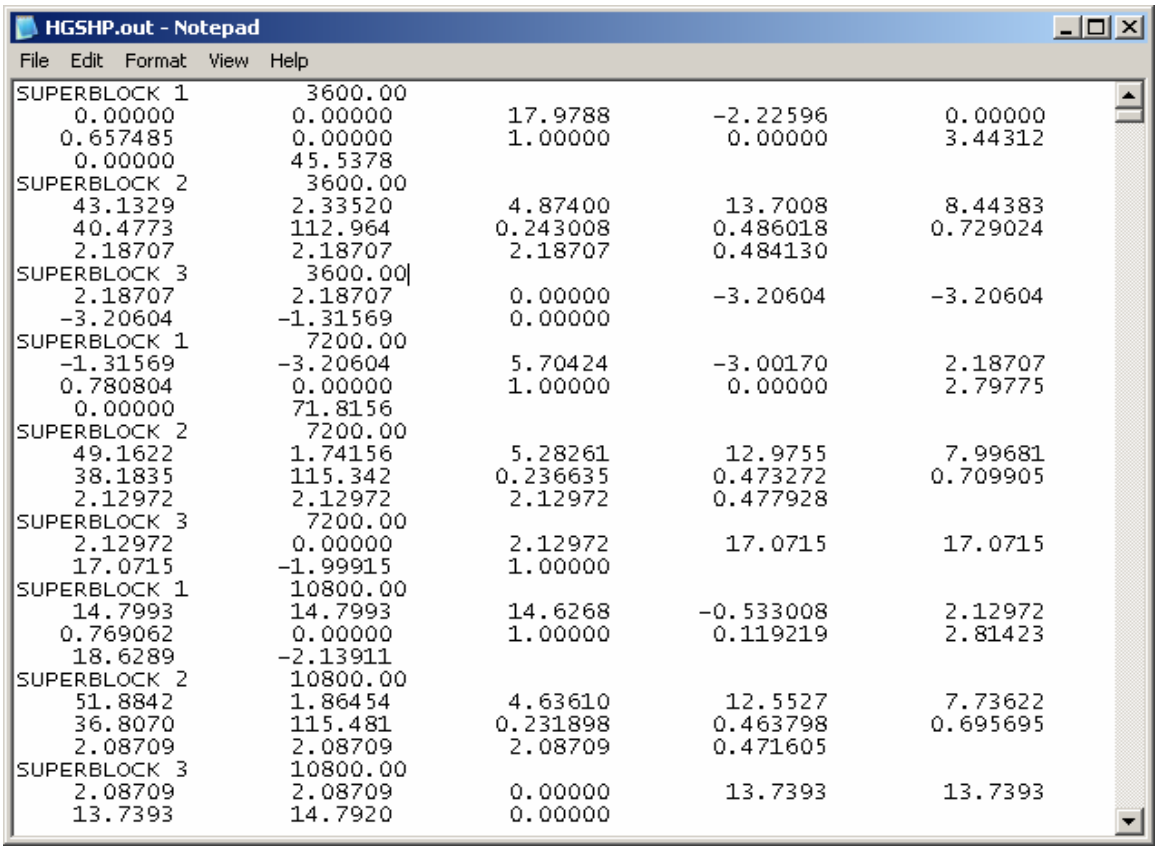

Figure 3-2. HVACSIM+ output file format

The new feature in the visual modeling tool reads the reported variables for each SUPERBLOCK into a data-structure, and then writes them to another file in a comma-delimited format with a 'CSV' extension. Every variable, regardless of the SUPERBLOCK, is written into its own column.

3.4 Fluid Flow Network System Simulation

An important aspect of GSHP system simulation is choosing the method for determining fluid mass flow rate. The simplest approach would be to simply set flow rate, and assume a fixed value. However, the flow rate will vary over the year as fluid

temperatures, densities and viscosities change. This may be relatively unimportant with pure water, but it may be significant when an antifreeze mixture is used.

Issues related to solving mass flow rates and pressure differences simultaneously with temperatures and energy flows in duct/pipe networks in HVACSIM+ have been discussed at some length by Chen et al. (1999). They developed a separate flow rate and pressure calculation module with its own solution procedure.

A simpler, but less powerful procedure (compared to Chen et al. 1999) was developed where the fluid flow and the temperatures for a single component are resolved in two separate components; one for the fluid flow and the other for temperatures. Every component ends up being represented twice, for example, the GLHE is represented by two components with one component used to get the heat extraction/rejection and temperatures and the other used for the pressure drop through the length of the GLHE. The advantage of representing the system in this way is that it does not require a solver inside the component subroutines.

First, component models for pipes and fittings (models explained in the preceding text) were developed that took mass flow rates as input variables and gave pressure drops as output variables. Second, a dimensionless model of a centrifugal circulation pump was developed that gives mass flow rate as an output with pressure rise as an input. Using a simple pressure drop summing component and a mass flow dividing component, the flow network is configured.

In the Visual Tool, the entire system is configured as shown in Figure 3-3.

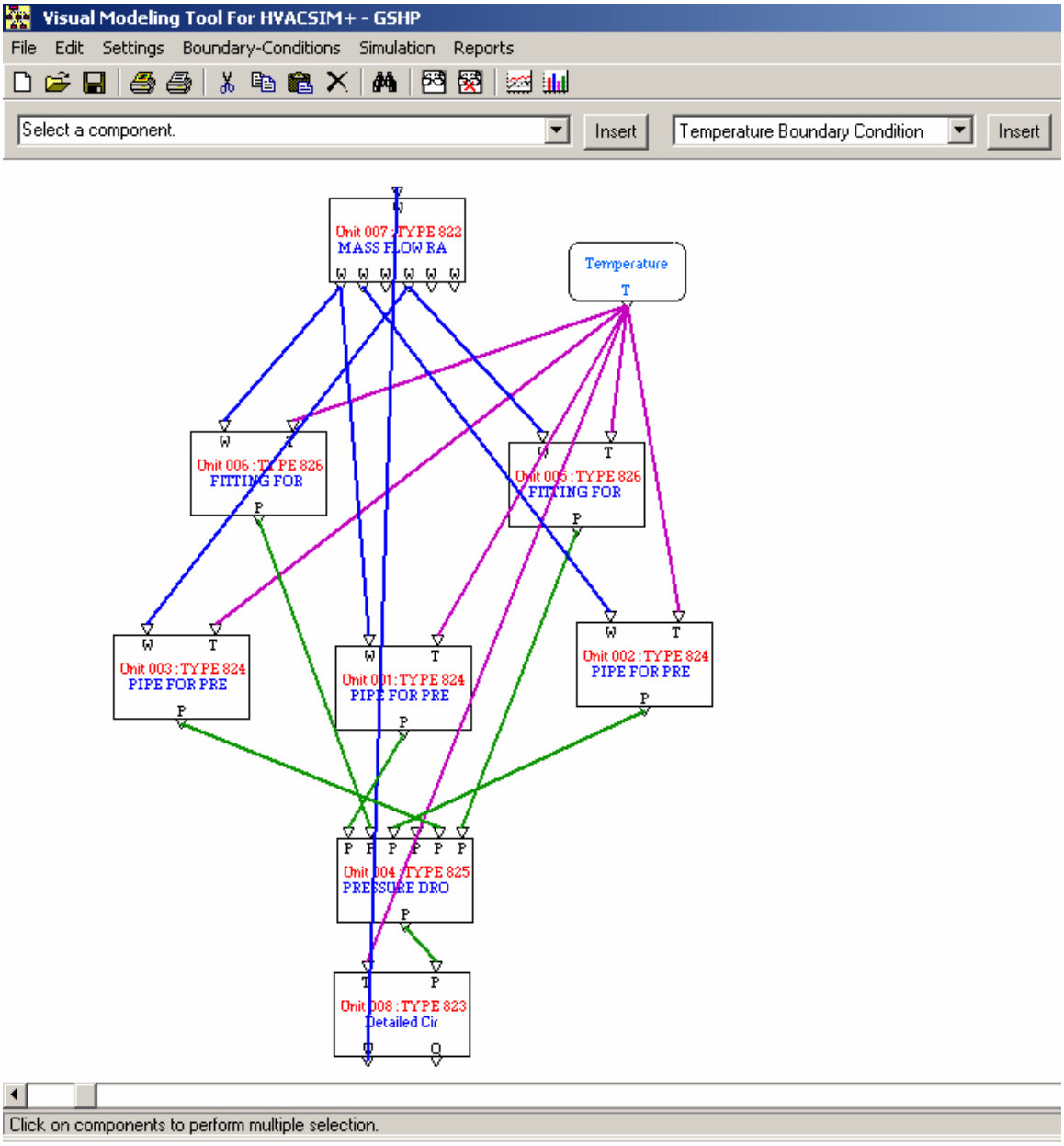

Figure 3-3. System simulation setup of a fluid flow network in Visual Tool

The flow network represents some balance between lumping everything together and showing every component. The heat pump and fittings are represented as two different fittings (TYPE 826). The U-tubes are represented by a single pipe component (with the total mass flow rate divided by the number of boreholes); the supply, return and connecting pipes are each represented separately (TYPE824).

Depending on the complexity of system, the difficulty in solving of fluid flow network in HVACSIM+ can be significant. The number of algebraic equations that result due to the large system takes considerable time and effort by the routines that implement the numerical methods to solve them. The HVACSIM+ hierarchical approach provides a solution to this problem. As explained, the structure of MODSIM is such that the simulation can be broken down into BLOCKs and SUPERBLOCKs, with equations within one SUPERBLOCK solved simultaneously. In most systems with solution of fluid flow network, the simulation must be broken down into a number of SUPERBLOCKS. Care must be taken in selecting which component should go in which SUPERBLOCK as an imbalance in heat is caused if components that solve the temperatures of an interconnected system are put in different SUPERBLOCKS. A heat balance should always be checked on simulation results that have more than one SUPERBLOCK.

The Visual Modeling Tool provides the user a facility to create a BLOCK and/or SUPERBLOCK easily. Figure 3-4 shows the form that is used to configure the models into various BLOCKs / SUPERBLOCKs. This form is opened by right clicking any of the icons representing the desired models to be configured, in the main workspace form and choosing “Superblock/Block numbers” option from the menu.

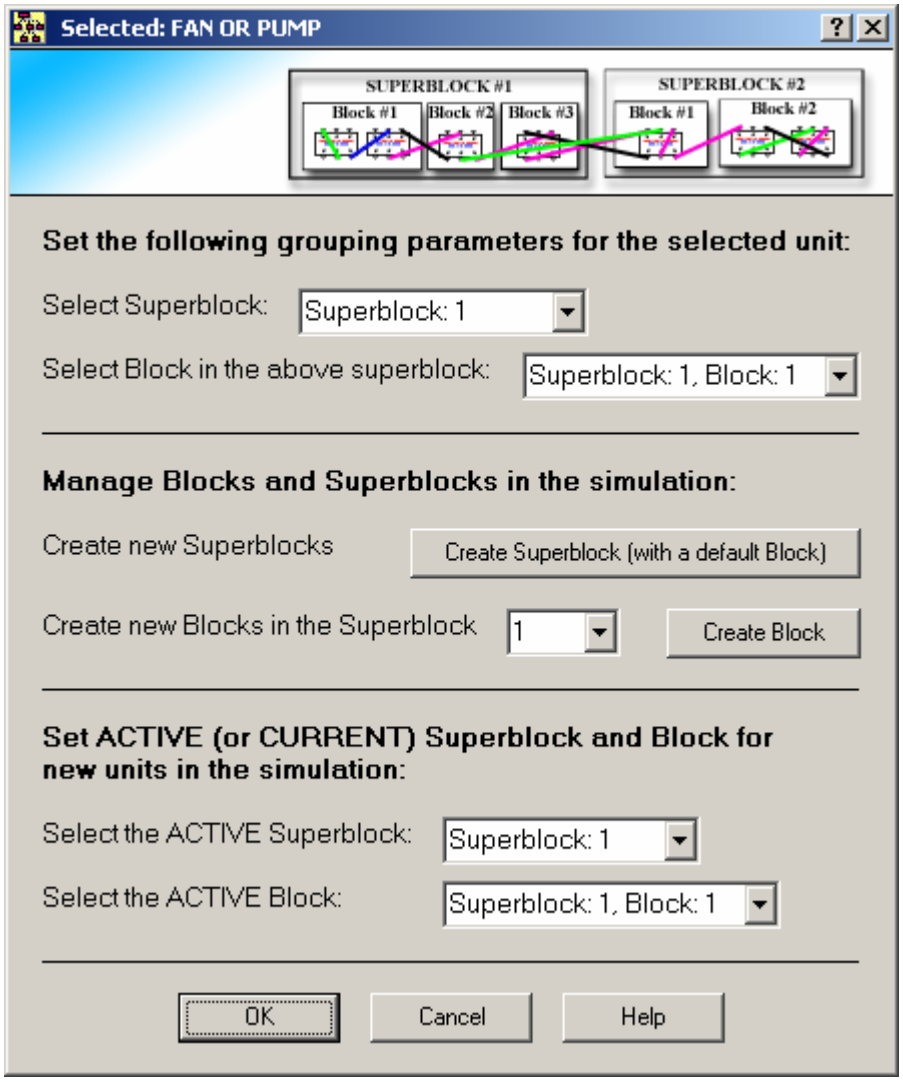

Figure 3-4. BLOCK / SUPERBLOCK configuration form

Each model can be configured to be in a specific SUPERBLOCK and BLOCK from the drop down menu "select Superblock" and "select block in above "superblock".

Initial guesses must be specified, if the initial guesses in the flow related components are set to zero, the solver could give negative mass flow rate values to the pipe and fitting models, which would result in crashing of the MODSIM. One approach to avoid this problem is to give good initial guesses as outputs to every model; this helps prevent the solver from taking negative guesses. Future work should be aimed at finding

a better scheme for handling bad initial guesses. This could take the form of an algorithm for modifying the initial guesses or otherwise coming up with a consistent set of initial guesses.

3.5 GSHP System Simulation

Setting up a GSHP system simulation in the Visual Tool requires some preprocessing to get the required parameters for the models that make up the system. A typical residential GSHP system comprises a GLHE, heat pump and the circulating pump.

The decision to use either the equation fit model or parameter estimation model can be made by simulating the GSHP system first in GLHEPRO and analyzing the range of heat pump entering fluid temperature (EFT), if the temperature falls above or below the rating of the heat pump, the equation fit model shouldn't be used. If the heat pump EFT is in the range specified in the catalog and no antifreeze is used, the equation fit model should be used as this reduces the simulation run-time. Spreadsheets to calculate the coefficients of the equation fit heat pump model and the parameters for the parameter estimation model using manufacturers' catalog data were developed and are available for use in the HVACSIM+ package CD.

The ideal circulating pump model can be used if the fluid flow rate is set by the user rather than being calculated. The dimensionless circulating pump models gives an accurate prediction of the power consumption and gives the mass flow rate variation over the year as compared to the ideal pump model but the setup is slightly complicated as explained in Section 3.4. A spreadsheet that computes the coefficients of the

dimensionless pump model using manufacturers' catalog data is available in the HVACSIM+ package CD. The parameters required for the ideal pump need some engineering judgment and experience.

Figure 3-5 shows a typical GSHP system with constant fluid flow rates set by the user.

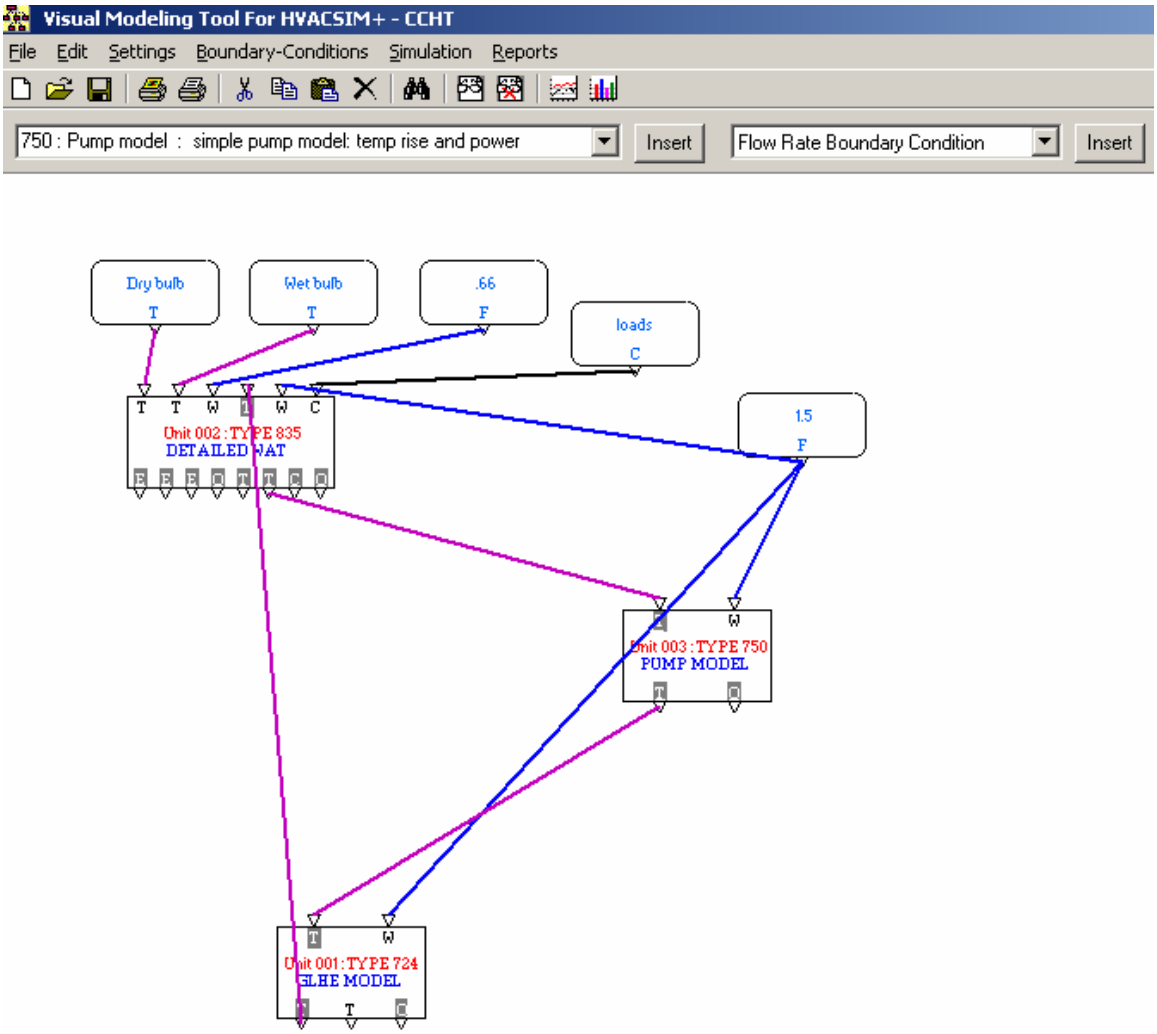

Figure 3-5. System simulation setup of a typical GSHP system with constant mass flow rate in Visual Tool

Figure 3-6 shows the same GSHP system, but with fluid flow rates calculated by the simulation.

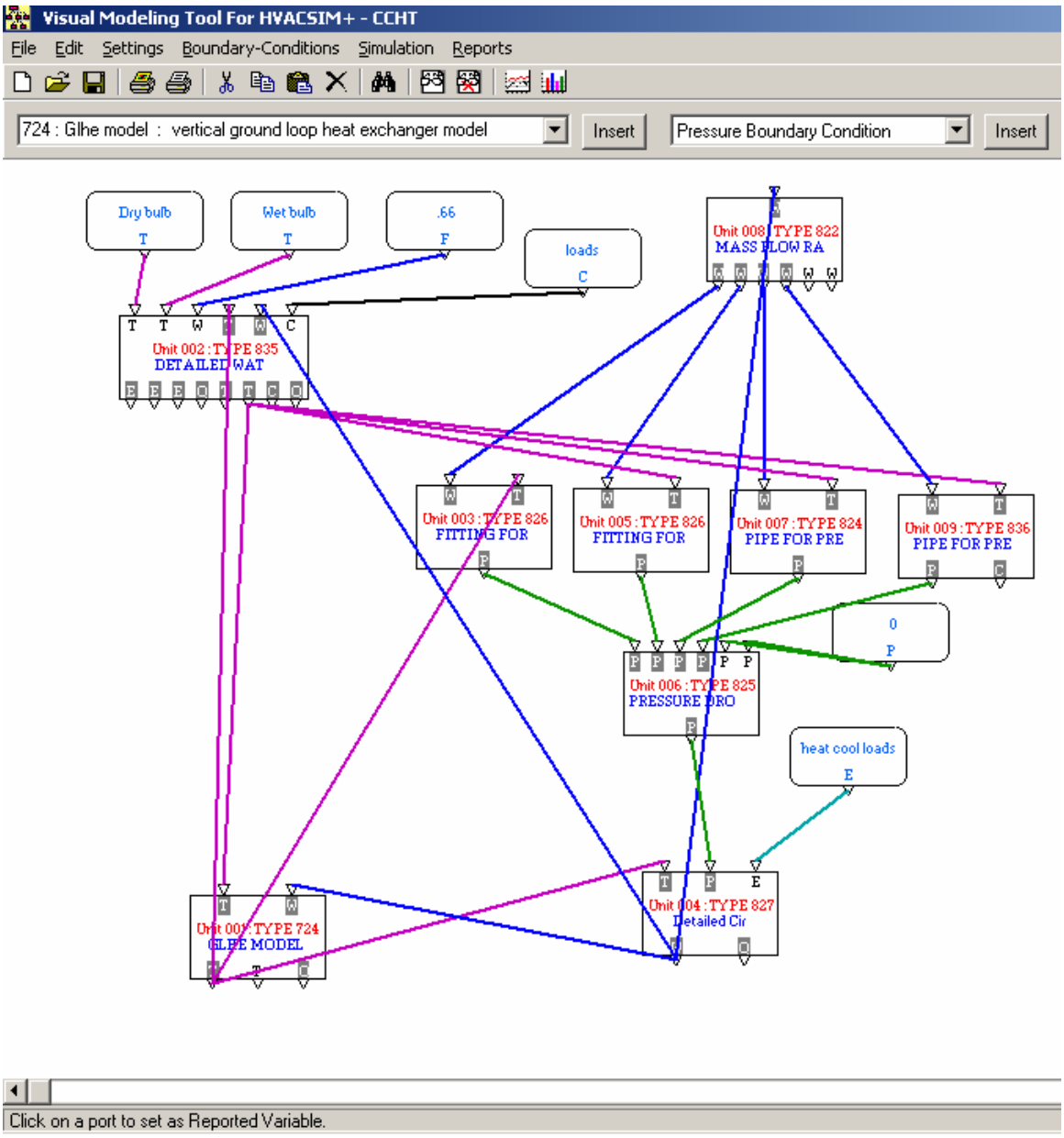

Figure 3-6. System simulation setup of a typical GSHP system in Visual Tool

The GSHP system was setup using the parameter estimation heat pump model (TYPE835) and the dimensionless circulating pump model (TYPE827). The space heating/cooling loads, the load side entering conditions to the heat pump are specified as boundary conditions. The space heating/ cooling loads are calculated using an external building simulation package, for example BLAST (1986). The flow network is simplified

by only considering the components with major pressure drop. The flow network comprises of two pipe models representing the U-tube and the manifold pipe (TYPE824), and two fitting models representing the heat pump and elbow joints (TYPE826). The exiting fluid temperature from the GLHE model (TYPE724) is input to the heat pump, circulating pump, and heat pump pressure drop calculation model. The heat pump exiting fluid temperature is input to the GLHE model, manifold pipe model, GLHE pressure drop calculation model and fitting model. MODSIM is able to run the simulation even if all the component models are in one SUPERBLOCK, as the GSHP system does not become extremely complex because of simplification in the flow network.

3.6 HGSHP System Simulation

The HGSHP system, as explained in Chapter 1, is used to balance the annual heat rejection to the ground with the annual heat extraction from the ground. This is done by adding a supplemental heat rejecter to the typical GSHP configuration along with a flow controller, diverter, mixing T-piece and a secondary circulating pump. Various control strategies can be used as explained by Yavuzturk and Spitler (2000) and a cooling tower, fluid cooler, cooling pond or pavement heating system can be chosen as supplemental heat rejecter. The system operates much like a typical GSHP system except when there is a potential to cool the ground or reduce the loop temperature (weather is favorable) the controller switches flow to pass through pavement heating system allowing the circulating fluid to reject heat to the atmosphere, thus cooling the ground.

Mass flow rate can be set by the user or a detailed flow network analysis can be done as explained in Section 3.4 in order to obtain the actual time-varying flow rate. The simulation becomes complex if the mass flow rate is solved, and the system has to be

broken up into number of SUPERBLOCKs using the hierarchical approach of HVACSIM+ as explained in preceding text. The finding of an earlier study (Khan et al. 2003) suggests it might be unnecessary to calculate the mass flow rate at operating point in HGSHP systems.

If the mass flow rate calculations are desired, the simulations can be setup in the Visual Tool as shown in Figure 3-7. Figure 3-7 represents a HGSHP system with a pavement heating system as a supplemental heat rejecter. The simulation must be broken into 3 SUPERBLOCKS with the flow related models including the primary circulating pump model in one SUPERBLOCK, the GLHE, mixing T-piece, secondary circulating pump, heat pump and hydronic-heated pavement model in another SUPERBLOCK, the flow controller and diverter in the third SUPERBLOCK. The mass flow rate in the secondary loop (supplemental heat rejecter) is fixed and an ideal circulating pump model is used to avoid further complication.

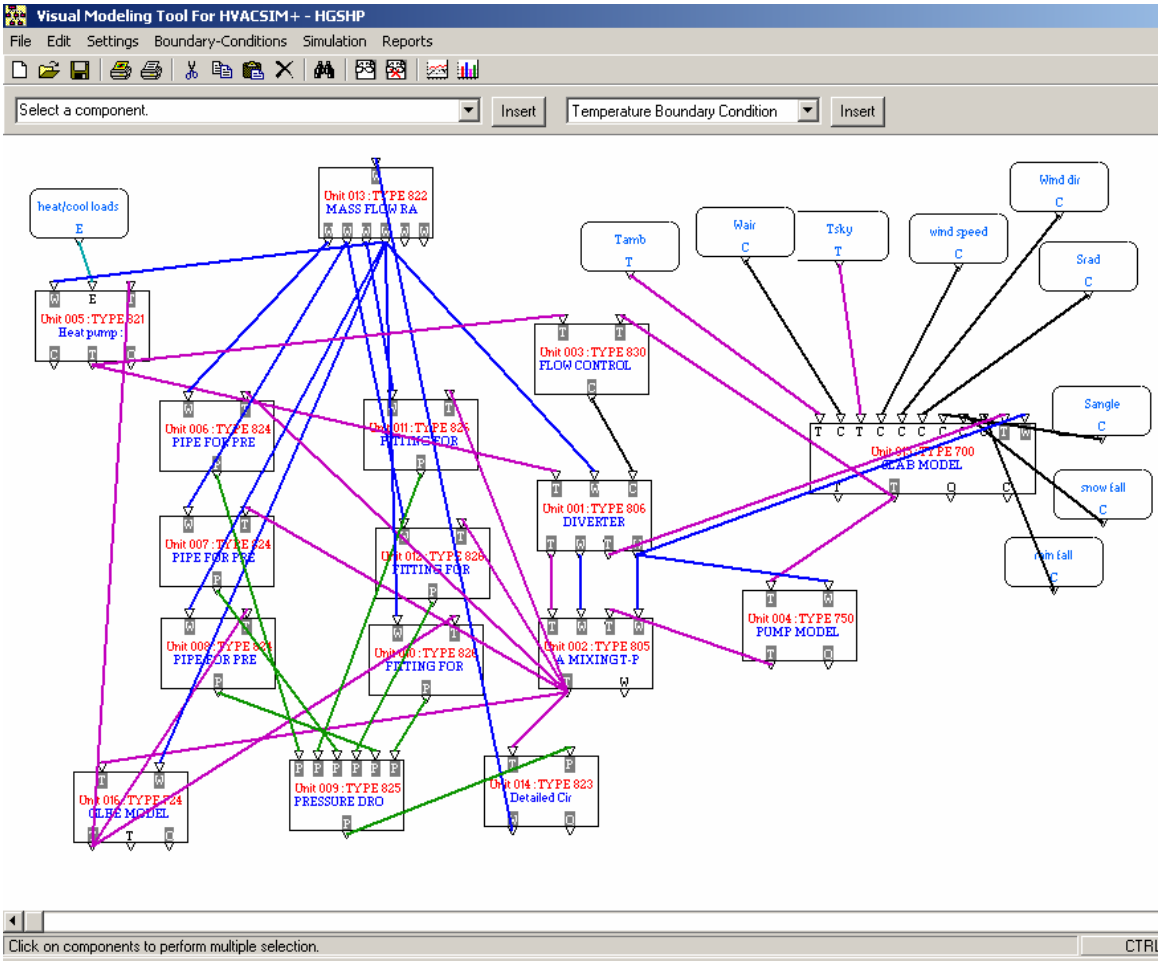

Figure 3-7. System simulation setup of a HGSHP in Visual Tool

The temperature differential set point controller was used to switch flow. The space heating/cooling loads calculated using an external simulation package along with weather data are boundary conditions to the simulation.

3.7 Multi Year System Simulation

One of the shortcomings of the Visual Modeling Tool is that it cannot be used to run multi-year simulations. This problem is inherent to the design of Visual Modeling Tool because it was developed in Microsoft Visual Basic 6 and the grid component used for the boundary file editor in Visual Modeling Tool has a limitation of the number of rows it can support (limit of integer data type i.e. 32,767). The number of data points

involved in running multiyear simulation is very large. If 10 years simulation is desired and hourly boundary data are given, it requires 87,600 rows to represent the data.

A tool was developed in the Java programming language to facilitate multiyear simulation setup, including pre and post processing of data.

The pre-processing feature can extend the boundary file to the user specified number of years. The 1-year boundary file is copied and written to a file for number of times equal to the number of years the simulation is run. It is assumed the boundary conditions repeat from one year to the next.

The tool automatically edits the input file to MODSIM to include the names of the extended boundary file and change the ending time of the simulation. The program also has the capability of calling MODSIM to run the simulation.

The post-processing feature lets the user choose from a variety of functions that can be performed to a specific variable or complete output. Examples include

- Sum first and last year – might be useful to find the total power consumption of a piece of equipment, e.g. heat pump, for the first and last year of operation.
- Daily min and max – for plotting temperatures or other variables over multiyear periods, hourly data are denser than needed, and merely retaining the daily minimum and maximum will speed plotting.
- Annual hourly data – used to extract the hourly data for all the variables in the selected SUPERBLOCK for the desired simulation year.

Figure 3-8 shows the user interface for the program, with the main, pre and post processing forms.

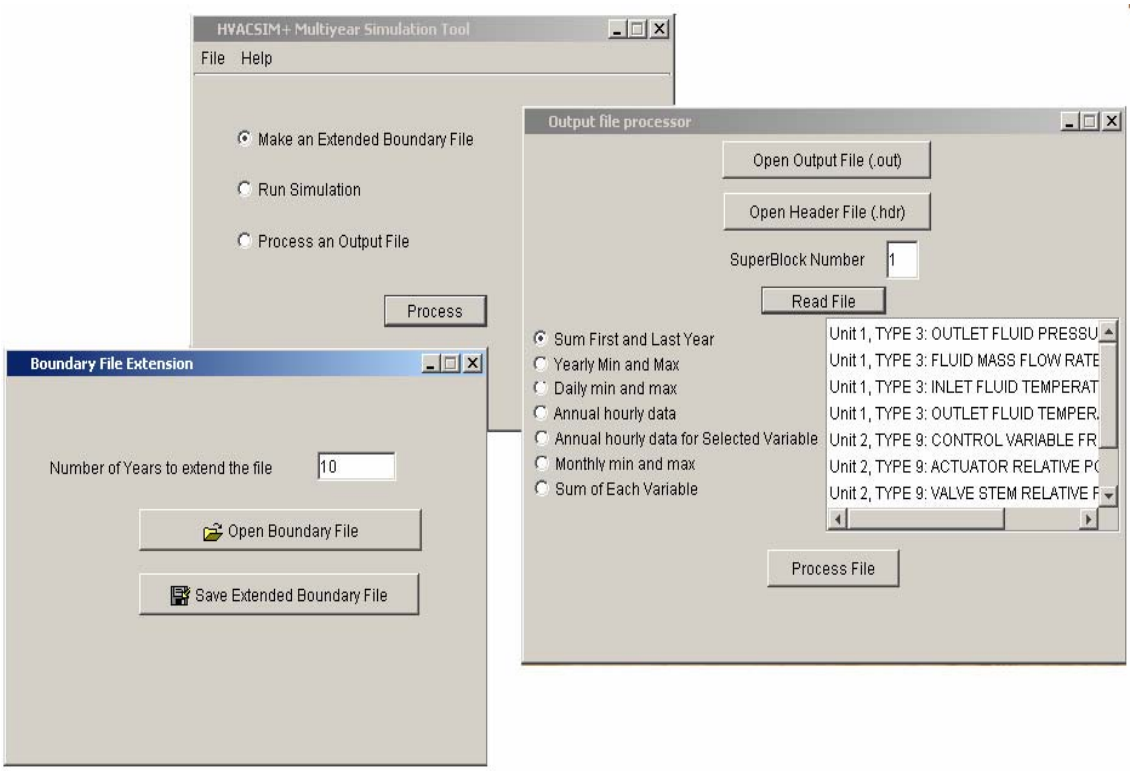

Figure 3-8. Multi-year simulation tool

Systematic instructions on how to use Multi-year simulation tool are given in Appendix C.

3.8 Conclusions and Recommendations

Models developed or translated from various sources for use in HVACSIM+ are explained. The methodology developed to solve for the fluid flow rate is discussed and setup of two configurations of GSHP system in Visual Tool is discussed. The tool developed to run multi year simulation is also briefly discussed.

It is recommended that care must be taken in setting up simulation in Visual Tool with more than one SUPERBLOCK as, if the components that solve temperature are put in different SUPERBLOCKS a heat imbalance is created. A check of the heat balance should always be made on simulation results that have more than one SUPERBLOCK. Good initial guesses should always be given for systems where fluid flow rate at operating point calculations are desired.

CHAPTER 4

Significant Factors in Residential Ground Source Heat Pump System Design

4.1 Introduction

The design problem of the GSHP system with vertical GLHE might be summarized as finding a combination of GLHE length, heat pump capacity, circulating pump, working fluid, borehole diameter, grout conductivity and U-tube diameter that allows the heating and cooling loads to be met for many years, avoids freezing of the working fluid, and minimizes life cycle cost. A typical design procedure would involve first selecting equipment and then choosing minimum and maximum heat pump entering fluid temperatures (EFT) which allow the loads to be met. In parallel, the antifreeze concentration would be chosen. The GLHE would then be sized (and other parameters – U-tube size, grout type and borehole diameters chosen) to meet the minimum and maximum heat pump EFT. (Note that, for most systems, either the minimum or the maximum heat pump EFT will be the limiting constraint.) Finally, a circulating pump would be chosen. All of these parameters, to some degree, trade off against each other. For example, increasing the antifreeze concentration allows lower entering fluid temperatures, which in turn allow shorter and less expensive GLHE. However, operating costs for heating will increase as entering fluid temperatures decrease. Increasing the antifreeze concentration also decreases the heat pump capacity, so a unit with larger nominal capacity might be required.

Generally, the typical sequential design procedure leads to economical working designs if due care is given to pump and piping design. However, whether or not significantly more optimal designs might be found is unknown.

The focus of this chapter is the development of a computer simulation aimed at residential GSHP systems, which can account for all of the interacting design parameters and determine the relative importance of the design parameters. The study describes the simulation methodology and a demonstration for a typical North American house. Several design alternatives are evaluated and discussed.

4.2 Simulation Methodology

The GSHP system simulation was done using HVACSIM+. The Visual Modeling Tool was used to create and run the simulation as explained in the previous chapter.

The component models used to simulate the system are described in the model description section in Chapter 3. In terms of overall organization, it is of interest in this problem to simultaneously model the thermal performance and fluid flow, partly because temperature-induced changes in viscosity have the possibility of resulting in moderate changes in flow rate, depending on which antifreeze is used.

The mass flow rate at the operating point was calculated by methodology explained in previous chapter. The system is not extremely complex so all models are solved simultaneously within one SUPERBLOCK.

4.3 Building Description

The heating/cooling loads were calculated (Purdy 2004) using the ESP-r program (ESRU 2000) for a typical Canadian residential building. The example residential building is one of the two similar test houses at the Canadian Center for Housing Technology (CCHT) in Ottawa, Ontario, which was built to the R-2000 energy efficiency standard for research purposes. The CCHT house is composed of two above-grade floors and a fully conditioned basement. Its wood-framed construction is built upon a cast-in-place concrete foundation. It has 2583 ft² (240 m^2) of conditioned floor area including the basement, which is typical of a modern Canadian suburban house. The nominal U-value of the above-grade walls is 0.042 Btu/h-ft^2.F (0.24 W/m^2K), ceiling 0.06 Btu/h-ft^2.F (0.34 W/m^2K) and the windows have a U-value of 0.335 Btu/h-ft^2.F (1.9 W/m²K). The basement walls are covered with RSI 2.72 rigid insulation board. The air-tightness rating of the house is 1.5 ach at 50 Pa depressurization. The house was modeled so that the living space and basement zones were conditioned by the house's HVAC system while the attic and garage were "free floating". The basement, attic space, stairwell, attached garage, and two stories of living space were represented as thermal zones.

For this house, a GSHP system was designed such that one heat pump meets the living area heating/cooling loads and the basement loads were met by a second heat pump. The hourly loads for the top two floors are shown in Figure 4-1, with the convention that heating loads are positive and cooling loads are negative. There are no cooling loads in the basement as shown in Figure 4-2.

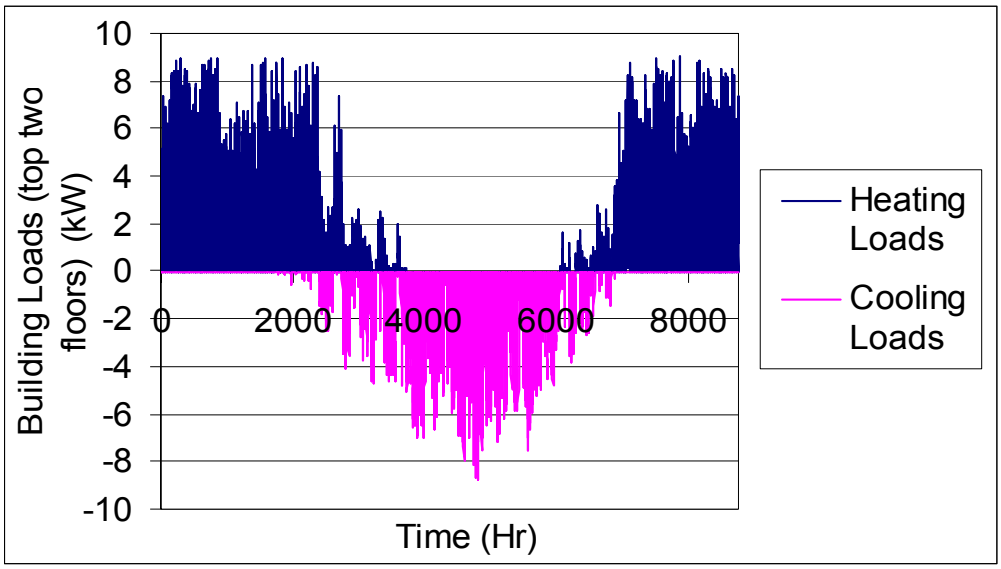

Figure 4-1. Annual hourly building loads for top two floors

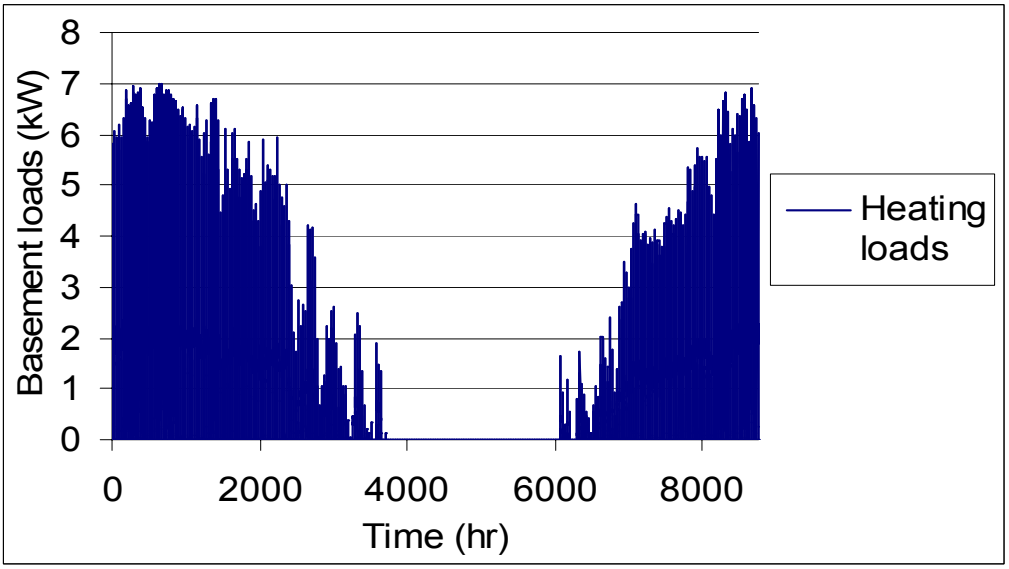

Figure 4-2. Annual hourly basement loads

4.4 Life Cycle Cost Analysis Methodology

Life cycle cost analysis of the system was done on a present value basis with an assumed life of 20 years and an annual interest rate of 6 %. First costs and operating costs were determined based on the unit costs shown in Table 4.1. Annual electricity

consumption for the heat pump and circulating pump were used to determine the annual operating cost. Operating cost for the first year was multiplied with the net present value factor (Equation 4-1), to get the present value of 20 years of operation. (The operating cost does change slightly with time, but this was neglected).

$$NPV = \frac{(1+IR)^{years} - 1}{IR*(1+IR)^{years}} \quad (4\text{-}1)$$

Where, *IR*= interest rate (%)

Table 4-1: Cost Of components of residential GSHP system

Component	Cost (US $)
Pipe / Ft (m)	
Sdr 11 ¾ " (22 Mm Internal Diameter)	0.2 (0.66)
Sdr 11 1" (27 Mm Internal Diameter)	0.28 (0.92)
Antifreeze / Gallon (Liter)	
Propylene Glycol	4.01 (1.06)
Ethylene Glycol	2.69 (0.71)
Methanol	0.68 (0.18)
Ethanol	1.44 (0.38)
Grout / Gallon (Liter)	
Bentonite Grout	0.23 (0.06)
Thermally Enhanced Grout	1.44 (0.38)
Heat Pump (Unit Cost)	
Florida Heat Pump Model (Gt042)	2000
Circulating Pump (Unit Cost)	120
Drilling / Ft (m)	
0.057 M Borehole Diameter	2.99 (9.8)
0.076 M Borehole Diameter	3.11 (10.2)
Electrical Energy / kWh	0.0725

4.5 Results

4.5.1 Base Case

For the base case, the following GSHP system configuration was assumed:

- Two nominal 3.5 ton water-to-air heat pumps (Florida Heat Pump Model GT 042)
- 1" nominal diameter SDR-11 HDPE pipe forming a single U-tube in the 4.5" (114 mm) diameter boreholes.
- Three boreholes spaced 15.1ft (4.6 m) apart.
- Standard bentonite grout with a thermal conductivity of 0.5 Btu.ft/h-ft^2.F (0.8 W/mK)
- An aqueous mixture of propylene glycol was used as the antifreeze.

To determine the optimal antifreeze concentration and GLHE length with the above parameters held constant, the pattern search Hooke-Jeeves algorithm in GenOpt (Wetter 2000) was used to find the combination that gave the minimum life cycle cost. In GenOpt, the Hooke and Jeeves (1961) algorithm is implemented, with modifications of Smith (1969), Bell and Pike (1966), and De Vogelaere (1968). This direct search algorithm is a coordinate based (derivative free) algorithm and is useful for minimization problem with continuous variables. The number of function evaluations increases only linearly with the number of design parameters, thus reducing the number of iterations required.

The algorithm takes a step in various directions from the initial starting point. If the "likelihood score" of the exploration is better than the old result, then the algorithm uses the new point as starting point for its next iteration, and if it is worse then the old result is retained. The search proceeds in series of these steps, each step slightly smaller

than the previous one. The algorithm stops when an improvement cannot be made with a small step in any direction and accepts the last point as the optimal result.

A general point to be noted about Hooke-Jeeves algorithm is that it is vulnerable to produce local minima, so it is advisable to run the optimization more than once, using the result of the first run as the initial guess for the second run and so forth.

The following parameter values were used for the Hooke-Jeeves algorithm in GenOpt:

MeshSizeDivider = 2, InitialMeshSizeExponent = 0,

MeshSizeExponentIncrement = 1, and NumberOfStepReduction = 4.

Penalty function constraints were applied to prevent both freezing of the circulating fluid and unmet loads (Unmet loads result when the capacity of the equipment, which changes with the flow rate and entering fluid temperature, falls below the hourly building heating or cooling load). The penalty function forces the optimization to find a solution in which neither the circulating fluid freezes nor does the system have unmet loads. The penalty function is determined mainly by trial and error; it works by forming a 'barrier' for the search algorithm to prevent it from going out of the design domain.

The penalty function chosen after trial and error for penalizing unmet loads is given in Equation 4-2. The penalty function for preventing fluid freezing is given in Equation 4-3.

$$f_p = 40 \bullet unMet_{tot} + 4600 \qquad (4\text{-}2)$$

$$f_p = 120 \bullet \Delta T + 4600 \quad (4\text{-}3)$$

Where,

$unMet_{tot}$ = sum of annual unmet load (kW h)

ΔT= Difference of the freezing point of the fluid plus a 3 ^oC margin of safety (^oC) and minimum heat pump entering fluid temperature

The sum of annual unmet load is determined from the simulation result. If the value is greater than zero the sum of unmet loads is used to calculate the value of the penalty using Equation 4-2. The penalty is then added to the objective function value. This results in a large value of the objective function, which forces the optimization algorithm to ignore the design parameters resulting in unmet loads.

The minimum loop temperature over the year is determined from the simulation result. If the minimum temperature is lower than fluid freezing point temperature plus 3^oC (margin of safety), the penalty is calculated using Equation 4-3. The penalty is then added to the objective function value.

It was observed that if the slope of the penalty function was high the search algorithm had difficulty in finding the minimum. This is because the coordinate based search algorithm proceeds in the direction where the function is decreasing. The minimum lies at the deepest point of a valley, which is adjacent to a point where penalty is applied, the algorithm can change direction if high values of objective function are encountered. The valley where the optimum lies is as shown in Figures 4-3, 4-4 and 4-5.

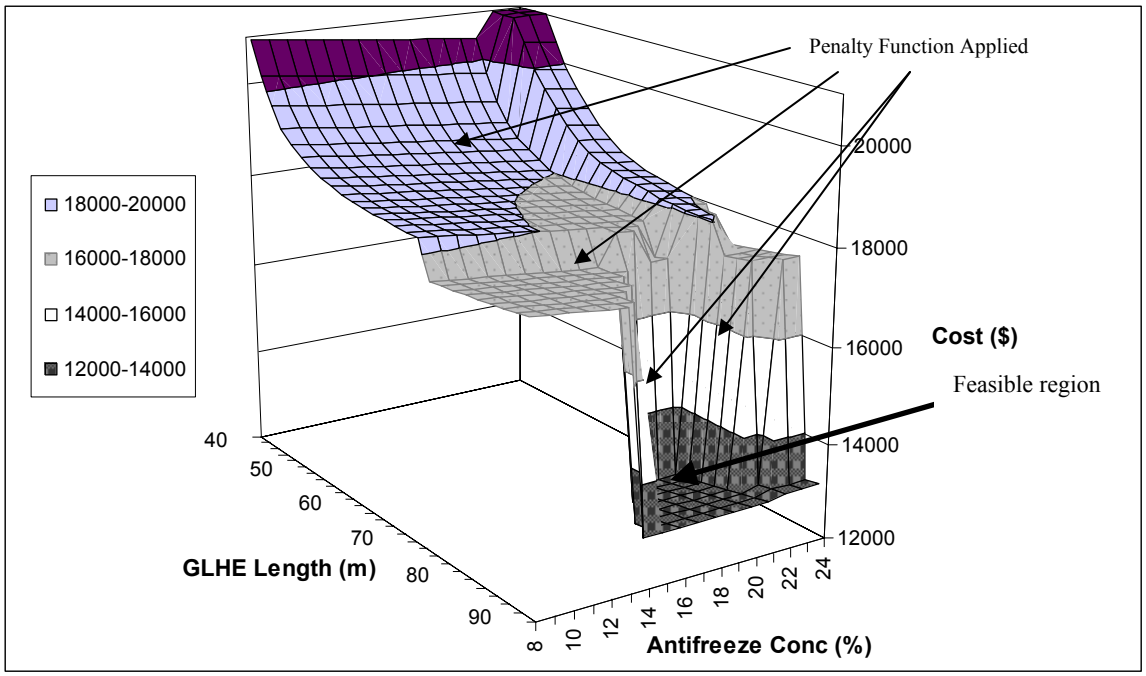

Figure 4-3. Graphical representation of objective function with GLHE length and antifreeze concentration.

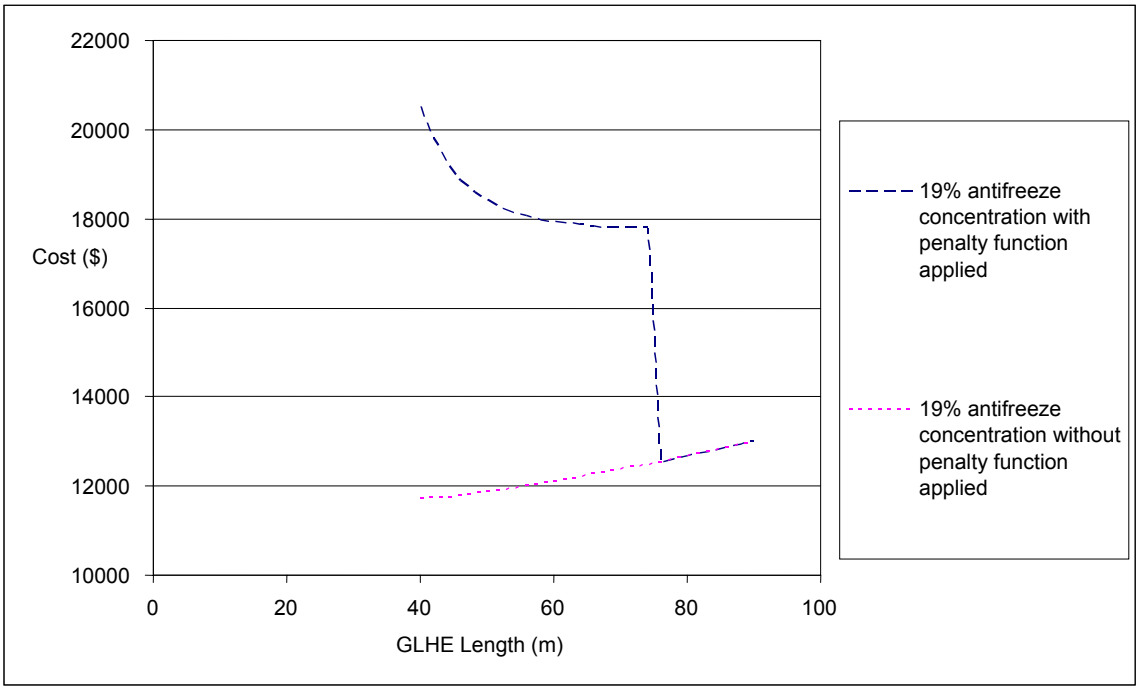

Figure 4-4. Graphical representation of objective function with variable GLHE length

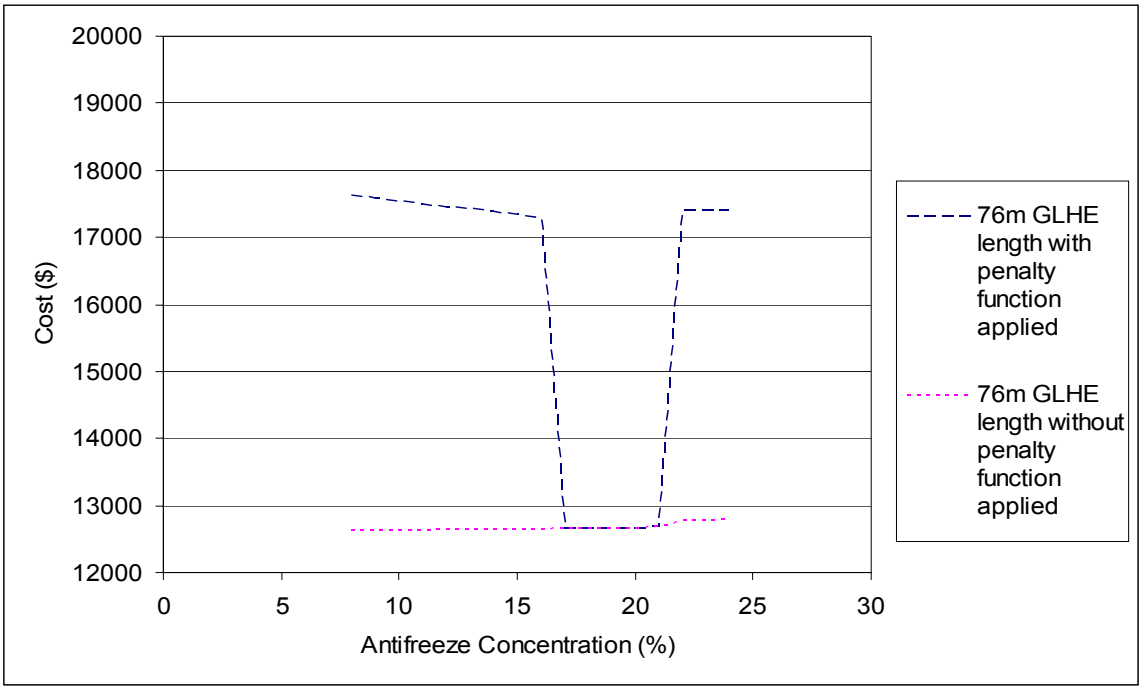

Figure 4-5. Graphical representation of objective function with variable antifreeze concentration and fixed GLHE length

One other observation that was made is that the algorithm should be started with a feasible starting point (the first calculation of the objective function made by the algorithm should be in the workable design domain) or the algorithm will have difficulty in finding the minimum; this is explained in more detail in Rao (1996).

The optimization results in a borehole depth of 249 ft (76 m) or a total borehole length, for all three boreholes, of 748 ft (228 m) and an antifreeze concentration of 19 % propylene glycol by weight.

To put this in perspective, Figure 4.6 shows a plot of the amount of antifreeze mixture required to prevent freezing as a function of total GLHE length. As expected, longer total GLHE lengths allow higher minimum fluid temperatures and hence permit lower concentrations of antifreeze. It is important to note that total GLHE lengths below

748 ft (228 m) cause unmet loads. This is because the lower entering fluid temperatures to the heat pump result in lower heat pump capacities.

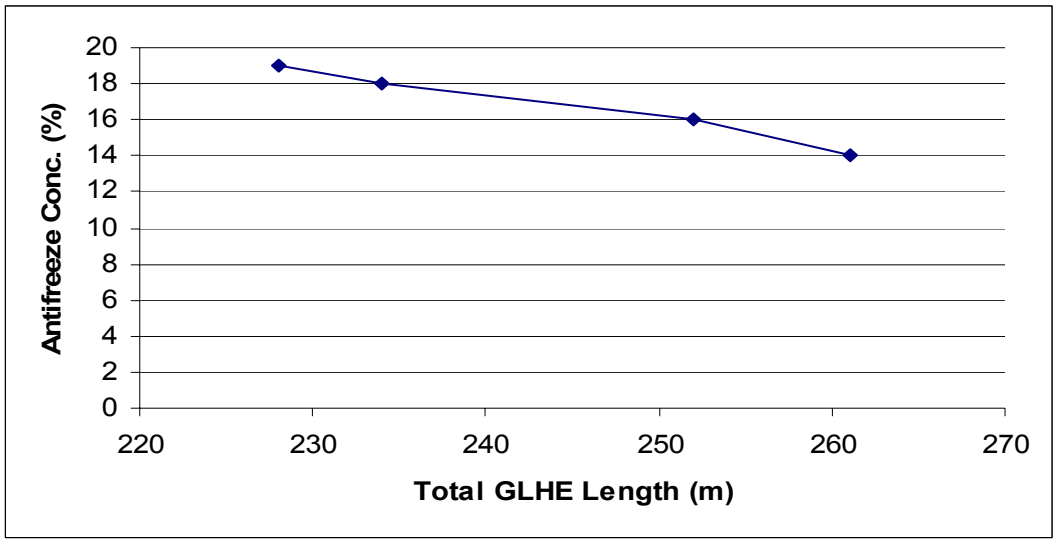

Figure 4-6. Amount of antifreeze mixture required to prevent freezing for a GLHE length.

Figure 4.7 shows life cycle costs for a range of systems with different combinations of antifreeze and GLHE length. For antifreeze concentrations below 19 %, with corresponding GLHE lengths above 748 ft (228 m), these combinations represent the minimum GLHE length required to prevent freezing at a given concentration. At concentrations above 19 %, the GLHE length remains at 748 ft (228 m) to prevent unmet loads.

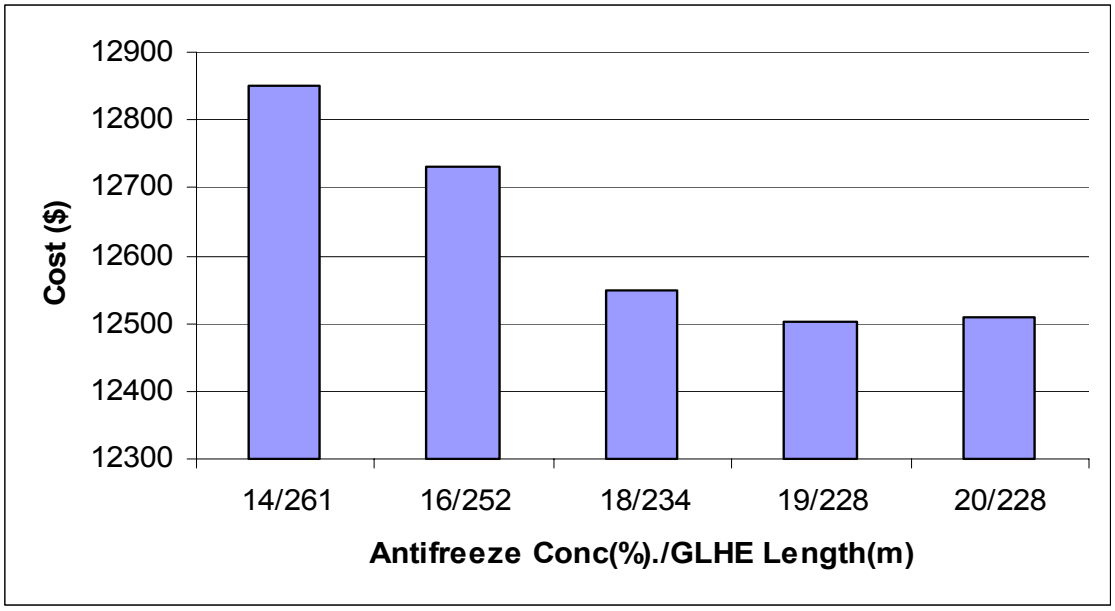

Figure 4-7. Life cycle cost as a function of propylene glycol concentration and GLHE length.

The average annual electrical energy consumption for the two heat pumps and the circulating pump was calculated as 6551 kWh and 124 kWh respectively. The heat pump power includes the fan power consumed. A breakdown of life cycle costs for the system is shown in Figure 4.8. The energy costs for the heat pump and the circulating pump shown are based on the present value approach and economic assumptions described above. The net present value of the system is equal to $12,503.

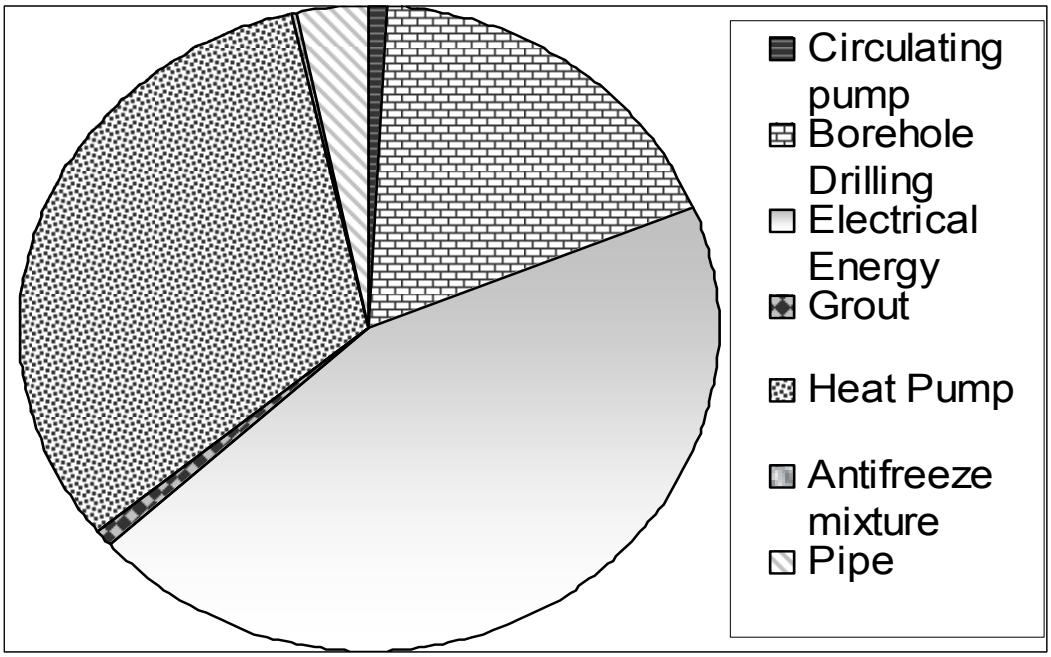

Figure 4-8. Base case life cycle cost breakup of the GSHP system

4.5.2 Grout Conductivity

Having determined a partly-optimal base case, it may be interesting to look at variations in a few other parameters. Thermally-enhanced grout contains additives (often quartz sand) that increase the thermal conductivity of standard bentonite grout. The increased conductivity results in lower borehole resistance (the thermal resistance between the fluid and the borehole wall.) This in turn allows shorter GLHE with lower drilling costs. If the GLHE is not shortened, slightly lower heat pump operating costs might be expected due to more favorable operating temperatures. However, the unit grout cost and grout installation costs are higher for thermally-enhanced grout.

To look at this, the grout conductivity was increased from 0.5 Btu.ft/h-ft^2.F (0.8 W/mK) (bentonite grout) in the base case to 1.4 Btu.ft/h-ft^2.F (2.4 W/mK) (thermally enhanced grout). From Table 4.1, the unit cost of the grout increases by a factor of 6.

For the first alternative, shown in the column "Thermally Enhanced Grout" in Table 4.2, only the grout conductivity is changed from the base case. In this case, there is approximately a 3 % reduction in the average annual heat pump energy consumption due to more favorable operating temperatures. However, the life cycle cost is increased because of the extra first cost of the thermally-enhanced grout.

Table 4-2: Life cycle cost and energy consumption of system with grout conductivity and U-tube diameter varied

	Base Case	Thermally Enhanced Grout	Thermally Enhanced Grout With Decreased GLHE Length	Optimized Grout Conductivity and Decreased GLHE Length	Decreased U-Tube Diameter
U-Tube Diameter - ft (m)	0.09 (0.027)	0.09 (0.027)	0.09 (0.027)	0.09 (0.027)	0.07 (0.022)
Grout Conductivity - Btu.ft/h-ft^2.F (W/mK)	0.5 (0.8)	1.4 (2.4)	1.4 (2.4)	0.8 (1.4)	0.5 (0.8)
Borehole Radius – ft (m)	0.19 (0.057)	0.19 (0.057)	0.19 (0.057)	0.19 (0.057)	0.19 (0.057)
Total GLHE Length - ft (m)	748 (228)	748 (228)	567 (173)	636 (194)	748 (228)
Heat Pumps Annual Energy Consumption (kWh)	6551	6381	6530	6534	6782
Circulating Pump Annual Energy Consumption (kWh)	124	124	127	126	114
Total Annual Operating Cost ($)	484	472	482	483	500
20 Years Net Present Value Of Operating ($)	5,551	5,410	5,536	5,539	5,734
First Cost Of The System ($)	6,953	7,746	6,875	6,792	6,825
Total Net Present Value Of The System ($)	12,503	13,155	12,411	12,330	12,559

A more likely scenario is that the thermally-enhanced grout is used to reduce the GLHE length. As shown in the next column in Table 4.2, "Thermally Enhanced Grout with decreased GLHE length", it is possible to reduce the GLHE length from 748 ft (228 m) to 568 ft (173 m) by using thermally-enhanced grout. At the same time, heat pump power is slightly reduced. Life cycle cost is about $100 lower than the base case.

Another option is that some blend of grouting materials can be used that gives a grout with an intermediate thermal conductivity. If we assume that the cost of the grout and its thermal conductivity can be approximated with linear interpolation between the pure bentonite grout and the thermally-enhanced grout, it is possible to find an optimal combination of the grout mix and GLHE length. Again, the Hooke-Jeeves algorithm in GenOpt was used to find an optimum combination. The resulting mixture has a thermal conductivity of 0.8 Btu.ft/h-ft^2.F (1.4 W/mK) and a cost of 0.53 $/Gallon (0.14 $/Liter). The corresponding GLHE length is 637 ft (194 m) and the total life cycle cost is about $170 less than the base case.

4.5.3 U-tube Diameter

Another parameter of interest is the U-tube diameter. In practice, the U-tube diameter can be traded off against pump size, mass flow rates, pumping power, etc. In order to look at the sensitivity, the U-tube diameter was changed to the next smaller size (nominal ¾") and no other changes were made to the system. In practice, a smaller U-tube diameter might have also allowed a smaller borehole diameter with additional savings in grout costs and drilling costs. Reducing the U-tube diameter while changing no other parameters resulted in lower mass flow rates, which in turn increased the heat pump power consumption. A negligible reduction in pumping power also occurred,

though this depends on the pump curve and change in the operating point. The overall life cycle cost increased from the base case because the savings in U-tube cost and antifreeze cost outweighed the increases in grout cost and heat pump power. This is shown in Table 4.2, in the column labeled "Decreased U-tube Diameter."

4.5.4 Antifreeze Mixture

The antifreeze mixture used in the system has a number of effects on the economics. These include the cost of the antifreeze, the change in the borehole resistance and heat pump performance, and the change in pumping requirements and pumping power. A few previous studies related to the use of antifreeze mixtures with GSHP systems are briefly described below.

Stewart and Stolfus (1993) made an analysis for a single operating point, for several antifreeze types. They concluded that methanol provided the best combination of good heat transfer properties with low pressure losses. Ethanol was recommended as a viable alternative to methanol solutions because of only slightly lower performance than methanol, in conjunction with lower toxicity and perceived risk.

Heinonen et al. (1997) modeled a residential GSHP system with six different antifreeze solutions in order to estimate relative energy use and the life-cycle cost. The six different antifreeze solutions studied were methanol, ethanol, propylene glycol, potassium acetate, calcium magnesium acetate (CMA) and urea. A series of risk analyses (fire, corrosion, leakage, health, environmental impact) were also described. Regarding operating costs, ethanol had the lowest and propylene glycol the highest. For total life cycle cost, ethanol was the lowest and potassium acetate was the highest. The antifreeze

mixtures were modeled only for specific concentrations and no attempt at optimization of the concentration or other parameters was made.

In this study, life cycle costs for several antifreeze mixtures are compared. The pattern search Hooke-Jeeves algorithm in GenOpt was used to find the optimal combination of GLHE length and antifreeze concentration for each of the antifreeze mixtures studied. These include ethylene glycol, methanol, and ethanol. The resulting combinations are antifreeze concentration (by weight) of 19.9% for ethylene glycol and total GLHE length of 752 ft (229.2 m), 11.6% for methanol with 730 ft (222.6 m) GLHE length and 15.8% for ethanol with 737 ft (224.7 m) GLHE length. In addition, a system with pure water is compared. The circulating pump was the same for all cases; with different viscosities, flow rates varied slightly between the cases.

For the pure water system, it was necessary to increase the GLHE size significantly. A five-borehole system with boreholes 275 ft (84 m) deep, spaced 15 ft (4.6 m) apart was sufficient to prevent freezing of the water. The same circulating pump used as in cases with antifreeze mixture resulted in lower flow rate.

The life cycle cost analysis is shown in Table 4.3 for the base case and each of the alternatives. Methanol gives the best performance, and a saving of $125 is shown over the base case. Ethanol also gives a savings of about $100. Ethylene glycol performs almost identically to the propylene glycol base case.

Table 4-3 Life cycle cost and energy consumption of system with different circulating fluids

	Base Case (Propylene Glycol)	Ethylene Glycol	Methyl Alcohol	Ethyl Alcohol	Water
Antifreeze Concentration (Wt %)	19	19.9	11.6	15.8	N/A
Total Borehole Depth – ft (m)	748 (228)	752 (229.2)	730 (222.6)	737 (224.7)	1384 (422)
Heat Pump Annual Energy Consumption (Kwh)	6,551	6,559	6,538	6,549	6,093
Circulating Pump Annual Energy Consumption (Kwh)	124	126	121	119	193
Total Annual Operating Cost ($)	484	485	483	483	455
20 Years Net Present Value Of Operating ($)	5,551	5559	5,538	5,545	5,223
First Cost Of The System ($)	6,953	6948	6,840	6,873	11,332
Total Net Present Value Of The System ($)	12,503	12,508	12,379	12,419	16,555

As expected, with much higher flow rate, more favorable operating temperature, and the "best" heat transfer fluid, the water system shows significantly lower heat pump energy consumption, but somewhat higher circulating pump energy consumption. However, the increased GLHE size dominates the life cycle cost, which is significantly higher than any of the antifreeze systems.

4.6 Conclusions and Recommendations

A system simulation of residential GSHP systems has been presented. This simulation is capable of predicting the interactions between a number of parameters, including antifreeze type, antifreeze concentration, heat pump capacity, circulating pump size, GLHE depth, U-tube diameter, and grout type. In this study, sensitivity analyses were presented for several different variables.

For this specific case, a sensitivity analysis of the grout thermal conductivity showed savings in the life cycle cost if thermally-enhanced grout (k= 1.4 Btu.ft/h-ft^2.F (2.4 W/mK)) was used to reduce the GLHE length. A further savings in life cycle cost

was shown when using slightly enhanced grout (k = 0.8 Btu.ft/h-ft^2.F (1.4 W/mK)) to reduce the GLHE length.

With different antifreeze types optimized with GLHE length and antifreeze concentration, with all other parameters held the same, the life cycle cost decreased for methanol and ethanol significantly more than ethylene glycol.

The ultimate goal of this work is to be able to determine an optimal design of the GSHP system that minimizes life cycle cost with all design parameters being treated as independent variables. The next chapter of the thesis deals with optimal design, with special emphasis on the variables found to have the most sensitivity in this study.

Also, to date, the convective resistance between the U-tube and the fluid has been assumed constant over the simulation period. In the case with methanol as circulating fluid, the flow is always turbulent, and the minor changes in convective resistance will have little effect on the results. However, in other cases, the flow rate falls into the laminar region, a fixed borehole resistance calculated assuming the flow only in the laminar region might not give accurate results (as the flow shift to turbulent regime in the summer when the temperature of the loop is higher). It would be interesting to be able to at least roughly model the effects of this phenomena (Given the uncertainties in transition, “roughly” may be the best that can be done).

It is advisable to run the Hooke-Jeeves algorithm more than once, using the result of the first run as the initial guess for the second run and so forth, because of the vulnerability of the algorithm to produce local solutions as it is limited to in the sense that it cannot look beyond a local ‘hill’.

CHAPTER 5

Optimization of Residential Ground Source Heat Pump System Design

5.1 Introduction

A workable GSHP system design can be obtained as explained in Chapter 4 by first selecting equipment and then choosing minimum and maximum heat pump entering fluid temperatures (EFT) which allow the loads to be met. In parallel, the antifreeze concentration would be chosen. The GLHE would then be sized (and other parameters – U-tube size, grout type and borehole diameters chosen) to meet the minimum and maximum heat pump EFT. Finally, a circulating pump would be chosen. All the parameters can be varied within geometric and operational constraints such that a workable solution is obtained.

The focus of this chapter is to find the best or optimal GSHP system design within the workable design domain, which gives the lowest life cycle cost while meeting the space heating/cooling loads and preventing the circulating fluid from freezing. A methodology for optimizing the life cycle cost of residential GSHP systems using detailed hourly simulation of the GSHP system, implemented in HVACSIM+, is used as the basis for the performance analysis. The residential GSHP system explained in Chapter 4 is optimized using GenOpt (Wetter 2000). The program that mediates between GenOpt and HVACSIM+, and calculates life cycle cost is also described.

Because of time constraints, the operating cost is calculated with a one-year simulation. Accordingly, long-term effects of the ground-temperature drifting upwards or

downwards are not modeled. Hence, the optimization in this chapter might be considered to be a preliminary investigation.

5.2 Optimization Problem Statement

The goal of optimal GSHP system design can be defined as minimizing the life cycle cost of the system with the independent variables being borehole depth, pipe diameter, heat pump capacity, number of boreholes, borehole diameter, antifreeze concentration, antifreeze type and grout thermal conductivity, subject to constraints described below. All variables are discrete except borehole depth and antifreeze concentration which are continuous.

Minimize:

$$LCC = OC \bullet NPV + IC \tag{5-1}$$

Subject to:

$$EFT_{min} > T_{freeze,}$$

$$Q_{heatPump} \geq Q_{heating/cooling}, \textit{for all hours}$$

$$Lower \leq (DesignParameters) \leq Upper$$

$$\forall\ (DesignParameters) \in (L_{GLHE}, D_{U\text{-}tube}, D_{borehole}\ \ k_{grout}, No_{Boreholes}, Q_{cap}, Fluid_{type}, N)$$

Where,

LCC = system life cycle cost ($)

OC = first year energy cost ($)

IC = initial cost ($)

NPV = Net present value factor (-)

EFT = heat pump entering fluid temperature (^{o}C)

T_{freeze} = Freezing point (^{o}C)

$Q_{heatPump}$ = heating / cooling from the heat pump (kW)

$Q_{heating/cooling}$ = heating/cooling loads on the heat pump (kW)

L = length (m)

D = diameter (m)

k_{grout}= grout conductivity (W/mK)

$No_{Boreholes}$ = number of boreholes (-)

Q_{cap} = nominal heat pump heating/cooling capacity (W)

$Fluid_{type}$ = antifreeze mixture type (-)

N = antifreeze mixture concentration (Weight %)

Lower and Upper= the lower and upper bound due to geometric or physical constraints (-)

5.2.1 Constraints

The design specifications are introduced as constraints in the optimization problem and the constraints define the viability of the design solution.

Penalty function constraints:

1. Unmet loads: space heating/cooling loads should be met. This is enforced by a penalty function given in Equation 5-2

$$f_p = 40 \bullet unMet_{tot} + 4600 \quad (5\text{-}2)$$

Where,

$unMet_{tot}$ = sum of annual unmet load (kW)

If the sum of annual unmet load is greater than zero, it is used to calculate the value of the penalty, which is then added to the objective function value to give the penalized value of the objective function.

2. Circulating fluid temperature: the circulating fluid must be kept above the freezing point. This is enforced by a penalty function given in Equation 5-3

$$f_p = 120 \bullet \Delta T + 4600 \quad (5\text{-}3)$$

Where,

ΔT= Difference of the minimum loop temperature and freezing point temperature of the fluid (^oC)

If the minimum temperature over the course of the year is lower than fluid freezing temperature plus 3^oC (margin of safety), it is used to calculate the value of the penalty, which is then added to the objective function value to give the penalized value of the objective function.

For the case studied in this chapter, the restrictions in design parameters were identified as the following:

- Nominal U-tube size: the manufacturers set the standard increments of pipe sizes. This study follows the ¼ increment from ¾ in to 1½ in.
- Borehole radius: it was assumed that drilling contractors either drill 4.5 in (0.114 m), 5 in (0.127 m), or 6 in (0.152 m) diameter bores.

- Antifreeze type: aqueous mixtures of propylene glycol, ethylene glycol, ethanol, or methanol are the available options.

- Borehole depth: borehole drilling cost increases significantly over 300 ft (91 m), if the length of borehole required is greater than 300 ft (91 m) it might be cheaper to drill another borehole in most cases instead of going deeper (except if there are space constraints). The borehole depth is constrained by setting the upper bound for the variable to '91' in the GenOpt command file.

5.3 Optimization Methodology

The example building chosen for analysis is the same as that described in Chapter 4. Life cycle cost analysis of the system was also done using the same assumptions as explained in Chapter 4; a present value basis with an assumed life of 20 years and an annual interest rate of 6 % was used. First costs and operating costs were determined based on the unit costs shown in Table 4.1 in Chapter 4. Annual electricity consumption for the heat pump and circulating pump were used to determine the annual operating cost. Operating cost for one year was multiplied by the net present value factor to get the present value of 20 years of operation. The penalty function is calculated and applied for the one-year operation.

In practical applications, the operating cost of the system may increase from one year to the next. It is computationally infeasible to run an optimization using a 20-year simulation with an hourly time step (about 300 days on a P4 2.6GHz system). Therefore, in this study only a one year simulation was performed. The system studied has a significant imbalance between the heat extracted and heat rejected with the annual

heating load being about three times the annual cooling load. However, because the optimal solution has only two boreholes, long term net heat extraction effects are relatively minimal so the first year operating cost is assumed representative of the subsequent years operating cost.

5.3.1 GenOpt

GenOpt (Wetter 2000), a generic optimization program, was used to optimize the design. GenOpt minimizes an objective function with respect to multiple parameters. The objective function is intended to be evaluated by a simulation program that is iteratively called by GenOpt. GenOpt can be coupled to any simulation program that has text-based I/O.

GenOpt automatically generates input files for the simulation program based on input template files. GenOpt was originally developed to then call the intended simulation program to calculate the objective function, then read the output (objective function) from the simulation result file and check for errors and then determine a new set of parameters for the next run. The process is repeated iteratively until a minimum of the objective function is found. Figure 5-1 (Wetter 2001) shows the interface between GenOpt and any simulation program.

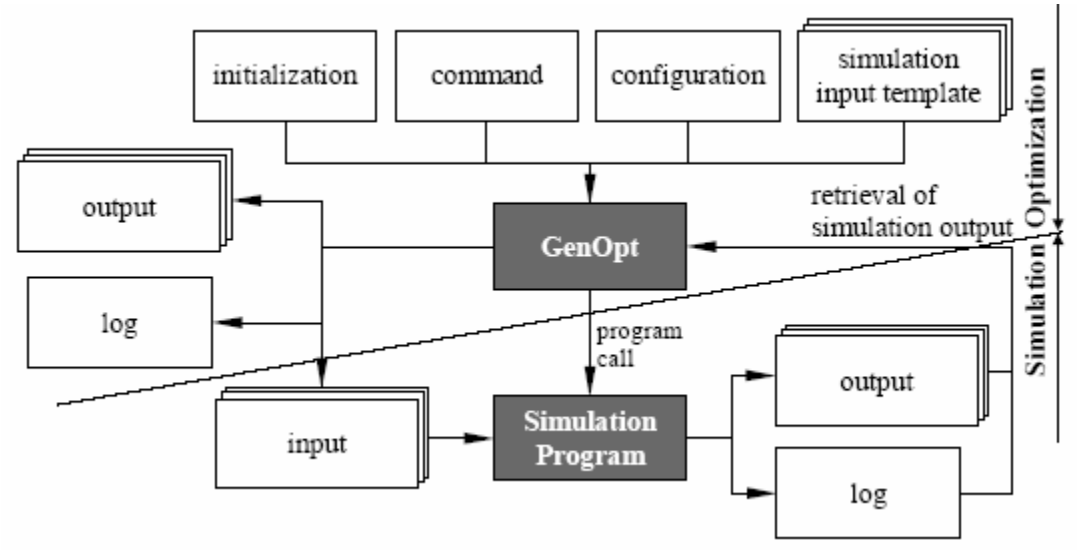

Figure 5-1. Interface between GenOpt and Simulation Program

The description of the GenOpt input files shown in Figure 5-1 is as follows.

Initialization: Specification of file location (input files, output files, log file, etc.)

Command: Specification of parameter names, initial values, bounds, optimization algorithm, etc.

Configuration: Configuration of simulation program (error indicators, start command, etc.)

Simulation input template: Templates of simulation input files

5.3.2 Buffer Program

A modification was necessary to the structure of GenOpt, as models used in the simulation require calculation of large number of input parameters. These calculations may require other programs. For example, the GLHE model requires calculation of g-functions for each geometric configuration selected by GenOpt. In addition, the HVACSIM+ program writes output for each time-step, but calculates neither operating cost nor first cost. A buffer program was developed to circumvent this problem. Instead

of GenOpt directly calling HVACSIM+, it calls the buffer program which calculates other parameters required by models in the simulation and then calls HVACSIM+. At the end of simulation call, the buffer program reads the output file and calculates the objective function based on the costs given in Table 4.1 and the life cycle cost assumptions given above. The objective function value is written to a file which is read by GenOpt. Figures 5-2 and 5-3 give the modified interface and the I/O of the buffer program respectively.

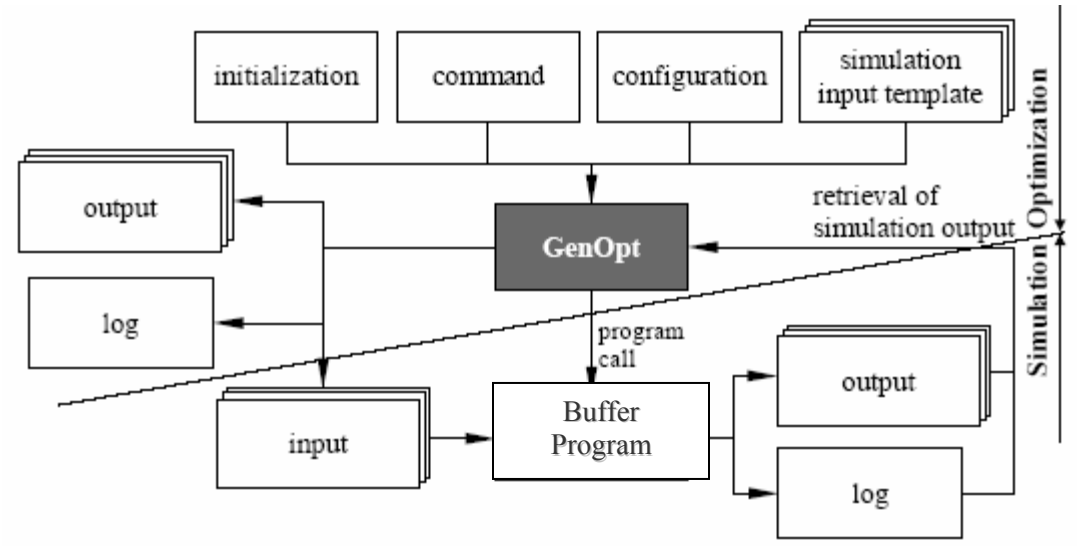

Figure 5-2. Modified interface between GenOpt and HVACSIM+

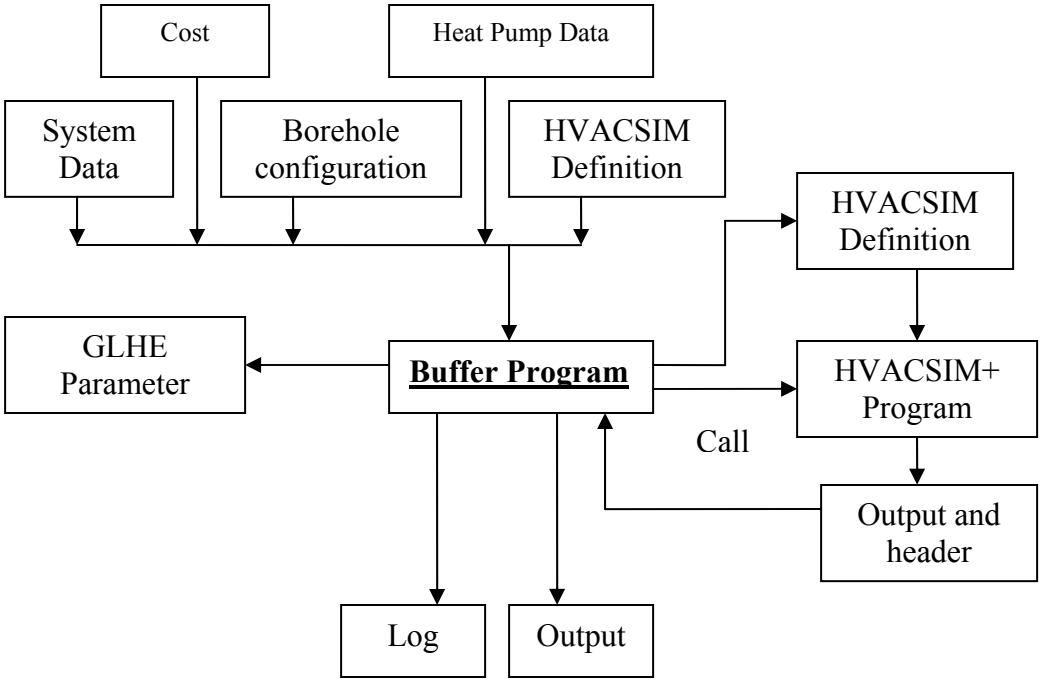

Figure 5-3. I/O of the buffer program

The description of the files associated with the buffer program shown in Figure 5-3 is as follows:

System Data (systemdata.dat): contains location and name data of input files to the buffer program (cost, HVACSIM+ definition, Borehole configuration, etc.).

HVACSIM+ Definition (GSHP.dfn): this is the input file to HVACSIM+ program. It is edited by GenOpt to change design parameters. The buffer program uses the file to recalculate the g-functions based on the parameters related to GLHE that are changed by GenOpt.

Borehole configuration (gfuncCreator.txt): contains data needed for calculating g-functions.

Output and Header (GSHP.out/.hdr): output and header files generated by HVACSIM+, containing hourly electrical energy consumption. Read by buffer program to calculate the objective function value.

GLHE Parameter (GLHEconfig.par): Parameters file containing the g-functions, written for debugging purposes.

Output (GSHPobj.out): contains the objective function value.

The flow of the buffer program is shown in Figure 5-4:

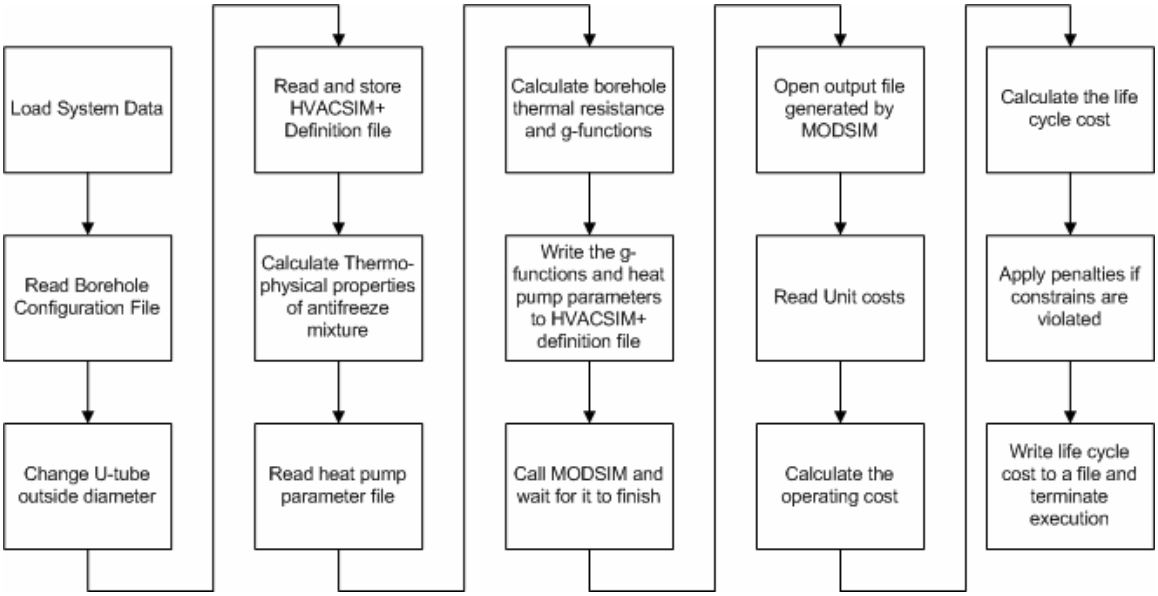

Figure 5-4. Flow of the buffer program

The structure of the buffer program is explained as follows:

- The system data file containing the location of files needed by the buffer program is loaded in the global data-structure.

- The borehole configuration file is read to get the value of parameters required to calculate the g-functions. The borehole configuration file also contains a discrete variable for the type of heat pump selected.
- The U-tube inside diameter is a design parameter and is changed by GenOpt. The outside U-tube diameter is changed according to the inside diameter selected by GenOpt (pre-selected outside U-tube diameters corresponding to the inside diameters are hard coded in the buffer program)
- HVACSIM+ definition file (an input for the MODSIM) is opened for input and the parameters for all models are read into a data-structure.
- Thermophysical properties of the antifreeze mixture are calculated using the models described in Chapter 2. (An average temperature variable read from the borehole configuration file is used to calculate the properties, for this study; $0^{o}C$ was used as the average temperature).
- A file containing heat pump parameters is opened and the parameters are read into a data-structure.
- The borehole thermal resistance is calculated, followed by the g-function calculation. Borehole thermal resistance is calculated as the sum of the convective resistance at the pipe wall, the conductive resistance of the pipe, and the conductive resistance of the grout. When the flow in the tubes is turbulent, the convective resistance is calculated with the Gnielinski's (1976) correlation. When the flow in the tubes is laminar, it is simplified as a constant heat flux problem, which gives an analytical solution of Nu=4.364. More detail regarding the borehole resistance and g-function calculation maybe found in Yavuzturk (1999).

- The HVACSIM+ definition file is edited by writing the calculated g-function parameters and the heat pump coefficients.
- The buffer program calls MODSIM and waits for it to finish execution.
- The output file generated by MODSIM is opened and results are read into a data-structure.
- The file containing the unit cost of equipment and electricity cost is read and stored in a data structure.
- Variables of interest (power consumption, unmet loads, runtime fraction, loop temperature) are extracted from the output data-structure; power consumption is used to calculate the operation cost of the system; loop temperatures are used to check for freezing and unmet loads are monitored for quality assurance.
- The objective function (life cycle cost) is calculated.
- A penalty function is applied to the objective function if freezing of the working fluid occurs and/or unmet space heating/cooling loads are present.
- The objective function is written to a file and execution of buffer program is terminated.

5.3.3 Optimization Algorithm

The Particle Swarm Optimization (PSO) algorithms in GenOpt (Wetter 2000) are population-based probabilistic optimization algorithms first proposed by Kennedy and Eberhart (1995) to solve continuous variables. Kennedy and Eberhart (1997) introduced a binary version of the algorithm to solve discrete variables. A hybrid of the pattern search Hooke-Jeeves algorithm and PSO algorithm was used to get the minimum life cycle cost of the GSHP system, which has both continuous and discrete variables. This algorithm

starts with a PSO algorithm for user specified number of generations with all variables set at discrete variables (GLHE length and antifreeze concentration were assumed as discrete variable with a step size of 1 m and 1%, respectively). The pattern search Hooke-Jeeves algorithm is than called with all the discrete variables fixed at the values that are associated with the optimal value of the objective function found by PSO algorithm. The GLHE length and antifreeze concentration are now assumed as continuous variables with starting values set as found to be associated with the lowest life cycle cost by the PSO algorithm.

PSO is a global optimization algorithm and does not require computation of the gradient of the cost function. PSO was developed as an analog to social models such as bees swarming, bird flocking and fish schooling. PSO is based on the idea that knowledge is optimized by social interaction. Due to the simple rules assumed to be used by birds to set their direction and velocity. Each bird tries to stay in the middle of the birds next to it while also trying not to collide. A bird pulling away from the flock in order to land at the perch would result in nearby birds moving towards the perch. As these birds discover the perch, they would land there, pulling more birds towards it, and so on until the entire flock has landed. The principles that the birds follow when they are flocking were revised so that particles (solution hunters, perhaps more like bees swarming rather than birds flocking) could fly over a solution space and land on the best solution. In this search procedure, ‘particles’ (each particle represents a potential solution, or can be seen as a bee in a swarm) move around in the multidimensional search space and change their position with time. The set of potential solutions in each iteration step is called a population (population is equal to the number of particles, or can be seen as the

total number of bees in a swarm). While changing their positions, each particle adjusts its position according to its own experience, and according to the experience of a neighboring particle (making use of the best position encountered by itself and its neighbor).

The neighborhood of a particle can be defined using any of the three topologies implemented in the PSO algorithm in GenOpt. These include the 'lbest', 'gbest' and the 'von Neumann' neighborhood topology. The 'lbest' neighborhood is determined by the neighborhood size, which is a user specified parameter. The 'gbest' neighborhood contains all the particles of the population and the von Neumann neighborhood is illustrated using Figure 5-5. Where each sphere is a particle and grey spheres are in one neighborhood, the numbers are the indices of the two dimensional array used to store the particle values.

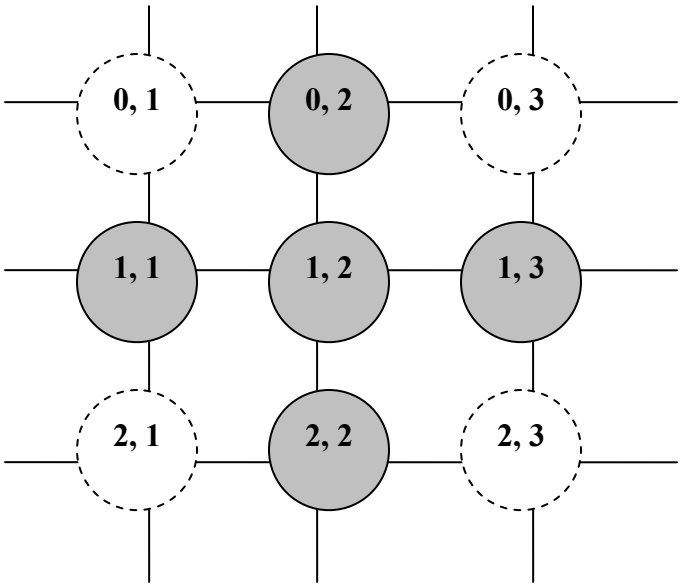

Figure 5-5. von Neumann neighborhood

PSO adheres to the five principles of swarm intelligence given by Millonas (1994)

- First is the proximity principle: the population should be able to carry out simple space and time computations.

- Second is the quality principle: the population should be able to respond to quality factors in the environment.

- Third is the principle of diverse response: the population should not commit its activities along excessively narrow channels.

- Fourth is the principle of stability: the population should not change its mode of behavior every time the environment changes.

- Fifth is the principle of adaptability: the population must be able to change behavior mode when it is worth the computational price.

The implementation of the algorithm is very simple and just a few lines of code are required. The flow of the algorithm follows initialization of particles randomly in the domain and the definition of the neighborhood of each particle. The remaining steps involve determining the local and then global best particles for the user specified number of particles, updating the particle location. Then, if the number of generations equals specified by the user stop, else determine the local and global best particles again.

5.3.4 Penalty Function Constraint

Penalty function constraints were applied to prevent both freezing of the circulating fluid and unmet loads. The penalty function constraint is applied similarly as explained in Chapter 4.

5.4 Results and Discussion

Life cycle cost with 8 independent variables was minimized as explained above using first the PSO algorithm with all variables assumed as discrete. The number of generations was taken as 1000, with the number of particles as 10. The 'gbest' neighborhood topology was chosen. The antifreeze concentration and GLHE length were assumed as discrete with a range 10-30% and 50-83 m respectively. The optimization with one-year simulation took about 10,000 iterations and 2.5 days to complete on a P4 2.6 GHz system running Microsoft Windows XP®. The starting point for each variable was set to the value in the base case, discussed in Chapter 4. The optimization results in a total borehole depth of 538 ft (164 m), grout conductivity of 0.9 Btu/h-ft.F (1.5 W/mK), U-tube inside diameter of SDR 1¼ in (0.035 m), borehole diameter of 4.5 in (0.114 m), methanol antifreeze with 13 % antifreeze concentration, and heat pump with 3.5 ton nominal heat capacity. The life cycle cost is $12,041. This is about a 3.7% reduction from the base case.

A pattern search algorithm with Hooke-Jeeves was used as the second step in minimizing the life cycle cost, with GLHE length and antifreeze concentration as continuous variables. Discrete variable values were fixed and the starting value for the continuous variables was chosen as the values resulting in least life cycle cost predicted by PSO algorithm. The following parameter values were used for Hooke-Jeeves algorithm in GenOpt:

MeshSizeDivider = 2, InitialMeshSizeExponent = 0,

MeshSizeExponentIncrement = 1, and NumberOfStepReduction = 4.

The optimization just took 10 iterations to converge and about 6 hours of computer time on P4 2.6GHz system running Microsoft Windows XP®. It results in total borehole length of 536 ft (163.4 m) and antifreeze concentration of 12.2% and slightly reduced the life cycle cost by about $10, or 3.8% from the base case.

Table 5-1 shows the comparison of the variables chosen and the life cycle cost for the optimum design as compared to the base case design.

Table 5-1: Life cycle cost and energy consumption of system with grout conductivity and U-tube diameter varied

	Base Case	**Optimum Case**
Antifreeze Type /Concentration (Wt %)	Propylene Glycol / 19%	Methanol / 12.2%
Freezing point –^{o}F (^{o}C)	19.4 (-7)	16.9 (-8.4)
Grout Conductivity – Btu/h ft ^{o}F (W/mK)	0.5 (0.8)	0.9 (1.5)
Borehole Radius – ft (m)	0.19 (0.057)	0.19 (0.057)
U-Tube Diameter– ft (m)	0.09 (0.027)	0.11 (0.035)
Total Glhe Length – ft (m)	748 (228)	536 (163.4)
Heat Pumps Annual Energy Consumption (Kwh)	6551	6523
Circulating Pump Annual Energy Consumption (Kwh)	124	131
Total Annual Operating Cost ($)	484	482
20 Years Net Present Value Of Operating ($)	5,551	5,534
First Cost Of The System ($)	6,953	6,499
Total Net Present Value Of The System ($)	12,503	12,032

The effect of change in U-tube diameter on the results is explained by an increase in the average mass flow rate by about 12%, which results in better performance of the heat pump. Even though the circulating pump power consumption rises as it operates to provide higher mass flow rate, it is insignificant as compared to the savings in the heat pump power consumption.

The optimization algorithm found methanol antifreeze mixture as the circulating fluid associated with optimal life cycle cost because the combination of higher viscosity of propylene and ethylene glycol antifreeze mixture as compared to methanol and lower mass flow rate result in flow dropping into laminar regime in the GLHE, which results in lower heat transfer.

The other reason the optimization algorithm found methanol antifreeze mixture to be associated with the optimal life cycle cost is that a lower concentration (12% by weight) provides the same freeze protection as propylene glycol concentration of 19% and is about 6 times cheaper. A savings (excluding the extra heat extraction/rejection) of about $50 in the first cost is seen when methanol antifreeze mixture is used instead of propylene glycol.

As shown in Chapter 4 increasing the grout conductivity can help reduce the GLHE length required and the extra price of the grout can be offset by the reduction in drilling costs. It is not surprising to see the optimum lie at a point with increased grout conductivity and reduced GLHE length as compared to the base case.

5.5 Conclusions and Recommendations

An optimization of a residential GSHP system has been presented, which minimizes the life cycle cost by varying GLHE length, number of boreholes, U-tube diameter, borehole diameter, grout thermal conductivity, heat pump capacity, antifreeze type and concentration, while meeting the space heating/cooling loads and preventing freezing of the circulating fluid. A buffer program was developed that mediates between GenOpt and HVACSIM+. The buffer program also calculates the parameter required by HVACSIM+ and post processes the output file created by MODSIM. The hybrid PSO algorithm with pattern search Hooke-Jeeves algorithm was used to minimize life cycle cost. The optimum was about 4% lower than the base case. The optimum design predicted only moderate savings and in practical applications, it might not be feasible to perform a complete optimization for all the independent variables.

It is the recommendation of the author if a complete optimization study is beyond the scope for a GSHP system design, at the least an optimization with grout conductivity and GLHE length as design parameters should be conducted. The results of this study show the objective function value was reduced most when an optimization was carried out with grout conductivity and GLHE length as design parameters while keeping other design parameters fixed.

In this study, the operating cost of the first year was used for calculating the net present value of 20 years of operation. The penalty function is calculated and applied for the one-year operation. In practical applications, the operating cost of the system may increase from one year to the next. In order to predict the life cycle cost, the total operating cost for the life cycle or the operating cost for the last year of the intended life

should be used for analysis. It is computationally expensive to run an optimization using a 20-year simulation with an hourly time step (about 300 days on a P4 2.6GHz system). The simulation time can be reduced by modifying the HVACSIM+ simulation so that the time steps are much longer for most of the simulation. Perhaps a scheme where for the first 18 years, a monthly time step is used, then for the next year a weekly time step is used, and for the final year an hourly time step is used, might be feasible.

CHAPTER 6

Design of Hybrid Ground Source Heat Pump That Use a Pavement Heating System as a Supplemental Heat Rejecter

6.1 Introduction

The term hybrid ground source heat pump (HGSHP) system is used for ground source heat pump systems that use a supplemental heat rejecter or a supplemental heat source. A cooling tower, shallow cooling pond, or pavement heat rejecter can be used as a supplemental heat rejecter. The HGSHP system is useful where the conventional GSHP system would require a large loop length due to imbalance in annual heat extraction/rejection.

In warmer climates, commercial buildings are usually cooling dominated. The cooling dominance results in an annual imbalance between heat extracted from the ground and heat rejected to the ground. Over time, this imbalance raises the loop temperatures and reduces the heat pump COP in cooling mode. To rectify this problem, either the ground loop heat exchanger size can be increased and/or a supplemental heat rejecter can be added. Increasing the size of the ground loop heat exchanger (GLHE) increases the capital cost and may exceed space constraints. The use of a supplemental heat rejecter may allow the GLHE size to be kept relatively small, and also allow for lower fluid temperatures, and, hence, higher heat pump COP in cooling mode.

Design of HGSHP systems is complicated by the large number of degrees-of-freedom. The GLHE size, supplemental heat rejecter size, equipment capacity, control strategy, etc. all affect the design. The continuously changing environmental conditions and building loads combined with the very large time constant of the GLHE make it very difficult to do any near-optimal design without the aid of system simulation. Two previous studies that utilized TRNSYS investigated performance of HGSHP systems with cooling towers (Yavuzturk and Spitler 2000) and cooling ponds (Ramamoorthy et al. 2001).

In this study, the performance of an HGSHP system that utilizes a pavement heating system as a supplemental heat rejecter is analyzed.

6.2 System Description

The example building has an area of is 14,205 ft^2 (1,320 m^2) and is located in Tulsa, OK. The hourly annual building heating loads (+) and cooling loads (-), shown in Figure 6-1, were calculated using BLAST (1986) by Yavuzturk (1999). The following approach was taken:

i) Eight different thermal zones were identified in the building. For each zone, a single zone draw through fan system is specified. The total coil loads obtained are assumed equal to the loads to be met with the heat pumps.

ii) The occupancy is 1 person per 100 ft^2 (9.3 m^2) with a heat gain of 450 Btu/hr (131.9 W), 70% of which is radiant, on an office occupancy schedule.

iii) Equipment heat gains are 1.1 W/ft^2 (12.2 W/ m^2), lighting heat gains are 1 W/ft^2 (11.1 W/ m^2), both on an office schedule.

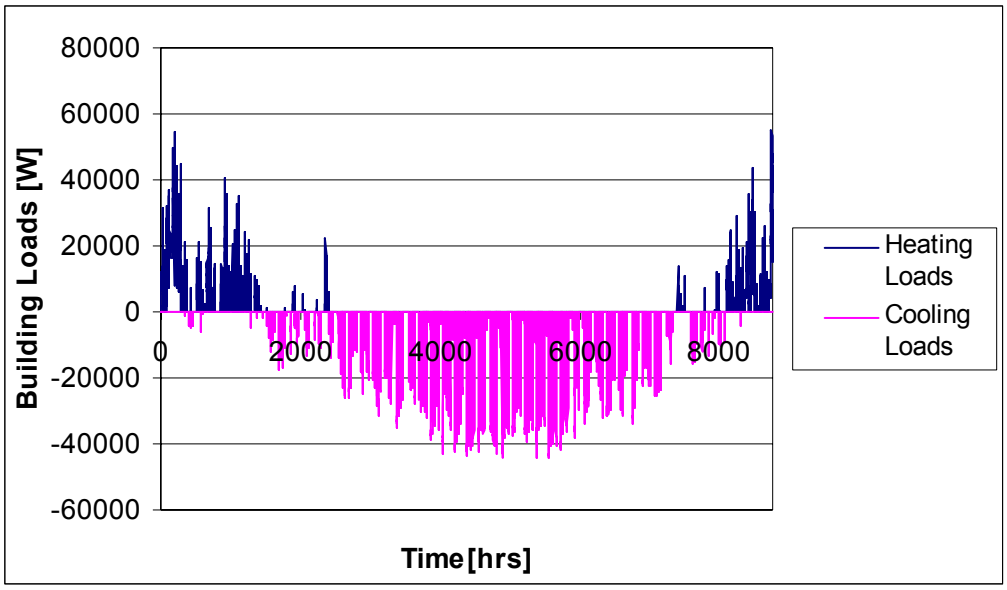

Figure 6-1. Annual hourly building loads for the example building

Figure 6-2 shows a schematic of the hybrid GSHP system. The system uses a pavement heating system (Chiasson et al. 2000a) as a supplemental heat rejecter. The pavement heating system would consist of hydronic tubing embedded in the concrete parking lot or sidewalk. The only additional capital cost is the cost of the tubing, its installation, an additional circulating pump, and additional controls.

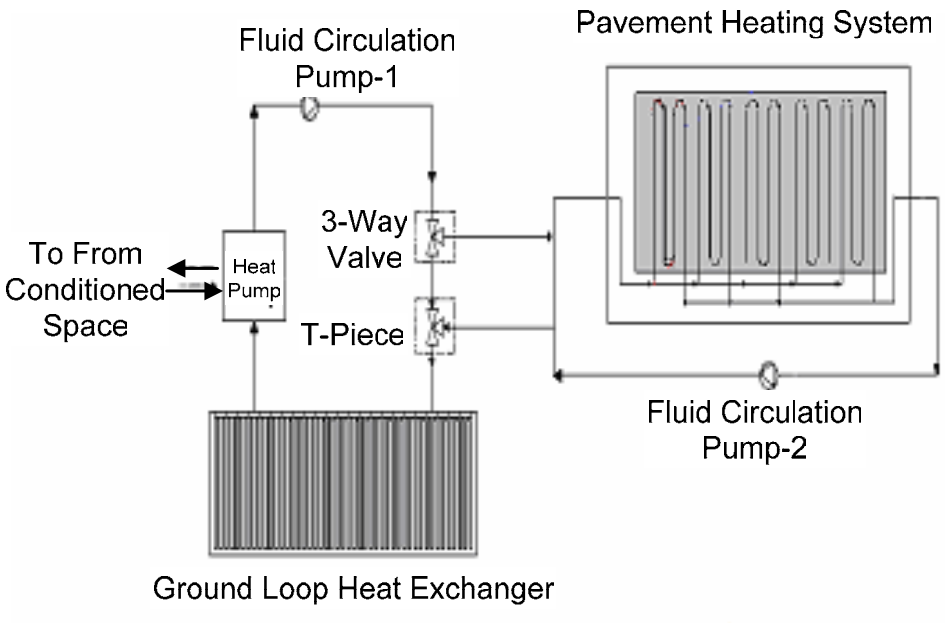

Figure 6-2. Hybrid ground source heat pump system component configuration diagram

An equation fit model, based on manufacturer's catalog data, was used for the heat pump, a Trane GEHA 180. The model determines exiting fluid temperature and power consumption based on the entering fluid temperature, cooling or heating load, and the fluid flow rate. A correction factor provided by the manufacturer for antifreeze was taken into account in calculating the coefficients for the heat pump.

The ground loop heat exchanger (GLHE) model is described in Chapter 3. Ground conductivity, borehole diameters, U-tube diameters, and grout thermal conductivity values were taken from Yavuzturk and Spitler (2000). Ground thermal conductivity was taken as 1.2 Btu/hr ft °F (2.08 W/m-K), borehole radius of 3.5 in (88.9 mm), U-tube diameter of 1.25 in (31.75 mm) and grout thermal conductivity of 0.85 BTU/hr-ft-F (1.47 W/m-K) were used.

The number of boreholes and length of the ground loop heat exchanger for the base case was determined so that the maximum entering fluid temperature would not exceed 97^{o}F (36ºC).

The circulating pump was sized to maintain a flow of approximately 3.5 gpm (0.22 kg/s) in each borehole. This flow rate was chosen to maintain turbulent flow over the expected range of temperatures.

For cases where a supplemental heat rejecter was used, the cross-linked polyethylene hydronic tubing was embedded in a 7.9 in (200 mm) thick concrete slab, at a depth of 3 in (76 mm), spaced 6 in (152 mm) apart. The number of circuits and length per circuit vary depending on the size of the supplemental heat rejecter.

For the preliminary HGSHP system design, the GLHE has been reduced in size to be approximately correct if the annual heat extraction were to remain the same, but with the annual heat rejection artificially reduced to balance the heat extraction.

The decision to turn on the supplemental heat rejecter is based on the differential control strategy developed and shown to perform well for HGSHP systems with cooling towers by Yavuzturk (1999). The controller turns on the secondary loop when the difference between the heat pump exiting fluid temperature and pavement exiting fluid temperature exceeds 46 ^{o}F (8 ºC), and is turned off when the difference falls below 37 ^{o}F (3 ºC). It was observed that if the lower set point was chosen equal to zero, redirection of flow to the supplemental heat rejecter occurred when the weather conditions were not advantageous. Care must be taken to choose a lower set point such that redirection of flow to supplemental heat rejecter takes place only when it is advantageous.

6.3 Life Cycle Cost Analysis

Life cycle cost analysis of the system was done on a net present value basis (as in previous chapters) with an assumed life of 20 years and an annual interest rate of 6%. Operating costs were determined based on unit electricity costs of $0.0725 per kWh. Annual electricity consumption for the heat pump and circulating pump were used to determine the annual operating cost. The annual operating cost was multiplied by the net present value factor to get the present value of operating cost for 20 years. First cost was determined based on GLHE installation cost (drilling, pipe, and grout inclusive) of $6 per ft ($19.7 per m) and the incremental cost (does not include the cost of the pavement, just the incremental cost for adding hydronic tubing, controls, and a second circulating pump) of pavement heat rejecter is taken as $14 per ft^2 ($150 per m^2).

6.4 Simulation

Three cases were simulated to predict the system performance over a period of 10 years and to evaluate the impact of using different size pavement heating systems as a supplemental heat rejecter. Each case is discussed below, along with the associated simulation issues.

6.4.1 Case 1 (base case)

The base case is a GSHP system with no supplemental heat rejecter. Based on the 95^{o}F (35ºC) maximum design EFT, a square borehole field with 16 boreholes, each 240 ft (73.2 m) deep and spaced 12.1 ft (3.7 m) apart was selected. The heat transfer fluid was water. In an earlier study (Khan et al. 2003), it was shown that modeling the HGSHP system with variable flow rate might be unnecessarily complex as only a 1.5% change in

heat pump power consumption was seen when the system was modeled with variable flow rate. For this study, the flow rate was simply set and assumed fixed at 55.5 gpm (3.5 kg/sec). In the visual modeling tool, the entire system is configured as shown in Figure 6-3.

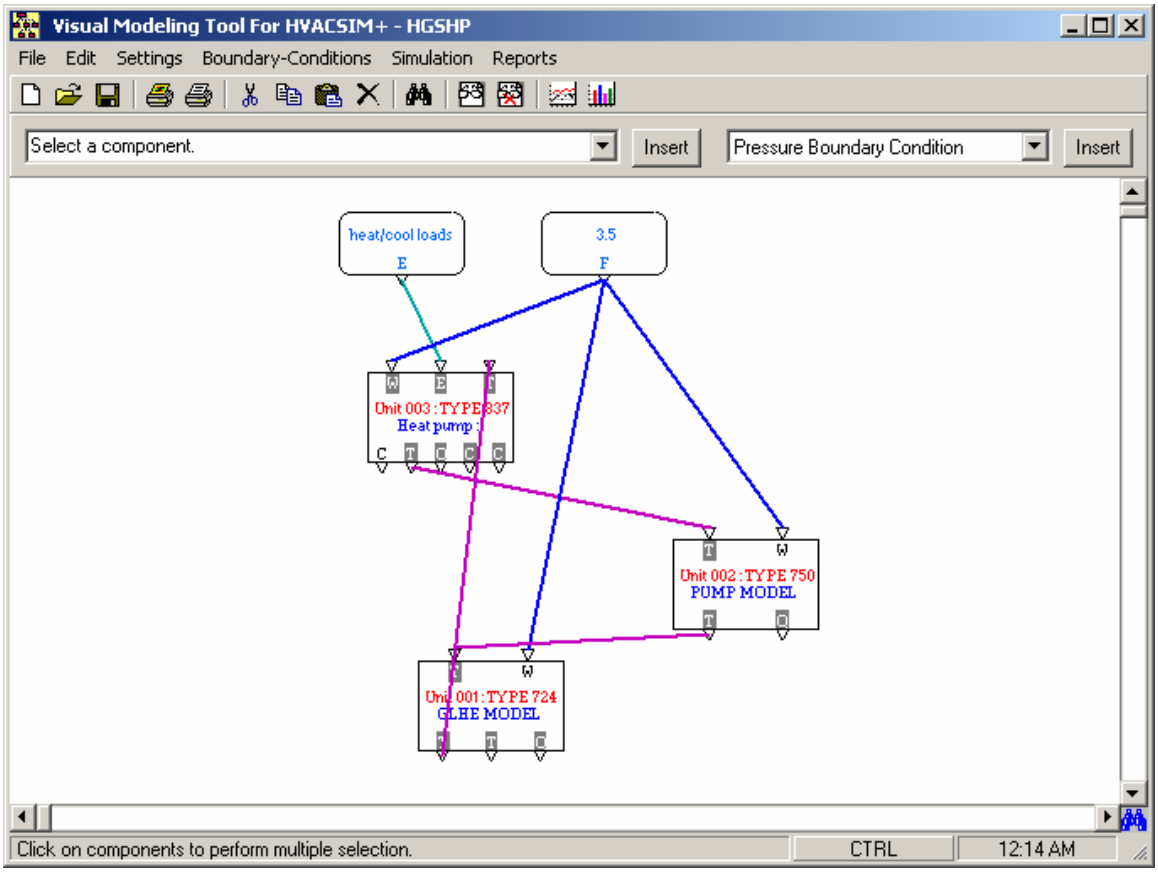

Figure 6-3. System configuration in the visual modeling tool- Case1

6.4.2 Case 2

The system was simulated with a reduced GLHE size (a square 9 borehole field with the same spacing and depth as Case 1) and a pavement heating system. The pavement fluid circuit is turned on by switching fluid circulation pump 2 (shown in Figure 6-2 and Figure 6-4 as Unit4, Type750). whenever the difference between the heat

pump exiting fluid temperature and the outlet fluid temperature of the slab hit an upper setpoint of 46 °F (8 ºC) and is turned off when this difference hits a lower setpoint of 37 °F (3 ºC). The heat transfer fluid was water with 30% propylene glycol as antifreeze, necessary to prevent the water in the slab from freezing if the system is turned off. The system was setup using the visual modeling tool as shown in Figure 6.4.

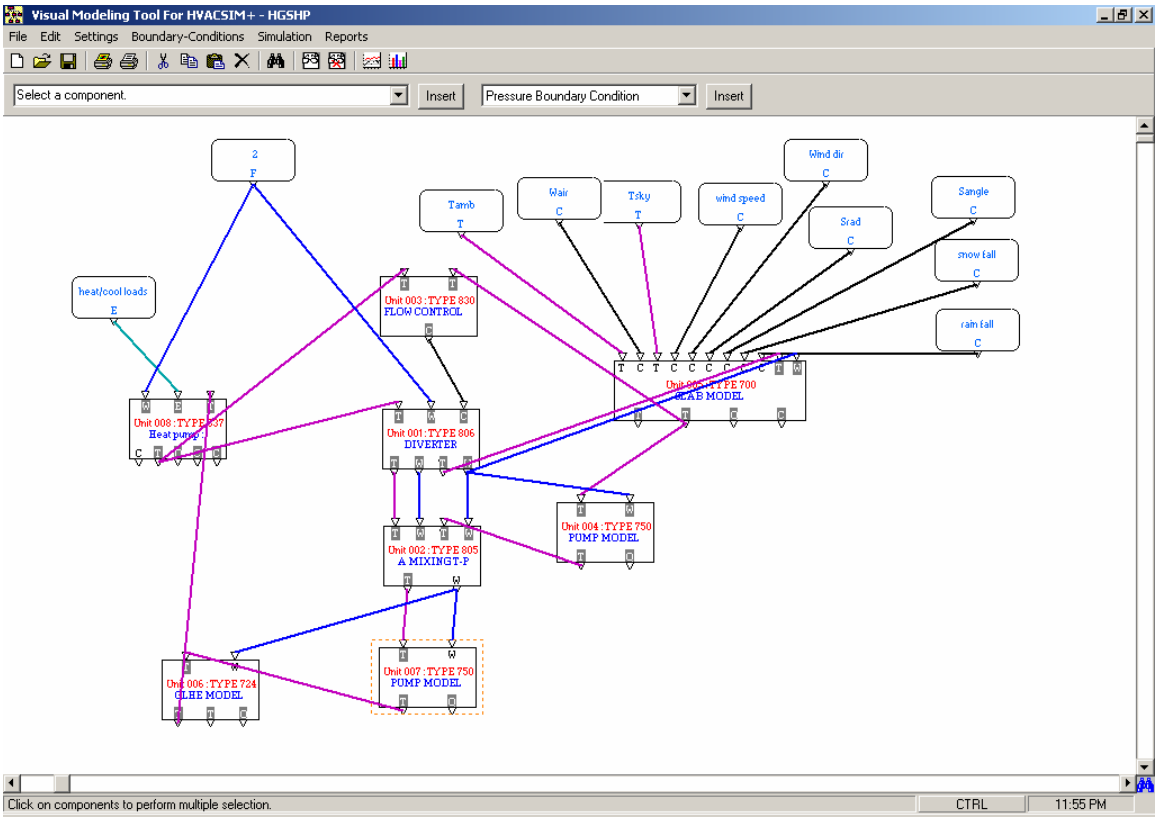

Figure 6-4. System Configuration- Case 2 and 3

6.4.3 Case 3

The size of the pavement was increased to see the effect of providing additional supplemental cooling on the heat pump power consumption. The pavement area was increased to 689 ft^2 (64 m^2) with 4 flow circuits.

Table 6-1: Summary of design parameters for each simulation case

Case	No Of Boreholes	Borehole Depth ft (m)	Pavement Area ft^2 (m^2)	Flow Circuits /Pipe Length Per Circuit - ft (m)
Case1	16 (4x4)	240 (73.2)	N/A	N/A
Case2	9 (3x3)	240 (73.2)	388 (36)	3 / 263 (80)
Case3	9 (3x3)	240 (73.2)	689 (64)	4 / 348 (106)

6.5 Simulation Results

Table 6-2 summarizes the power consumption of the heat pump and the circulating pump for each case. Since the heat pump power varies somewhat from year to year, both the first year and tenth power consumptions are given. Since the circulating pump power varies negligibly, only the average value is given.

Table 6-2: Heat pump and circulating pump power consumption.

	Annual Heat Pump Power Consumption (Kwh)		Annual Average Circulating Pump Power Consumption (Kwh)	
	1^{ST} YEAR	10^{TH} YEAR	CIRCUIT 1	CIRCUIT 2
Case 1	14,058	14,394	7,750	N/A
Case 2	16,859	16,870	4,317	296
Case 3	16,582	16,602	4,308	289

6.5.1 Case 1 (base case)

Figure 6-5 shows the variation of heat pump EFT over the ten-year simulation period. The maximum EFT for the first year is 88 ^{o}F (31 ^{o}C) and rises to 93 ^{o}F (34 ^{o}C) for the 10^{th} year.

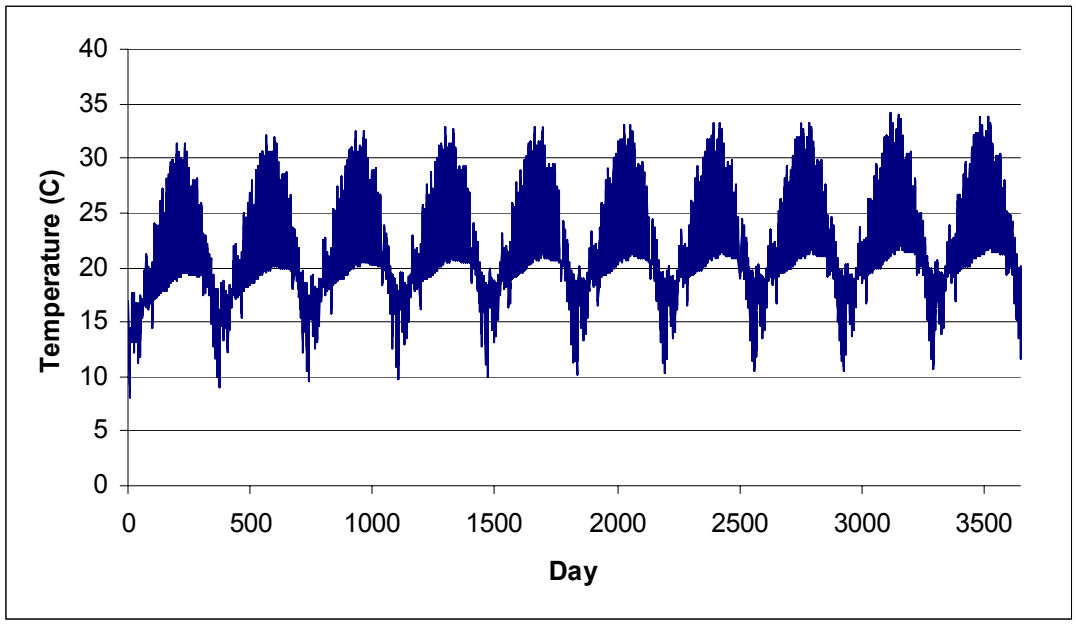

Figure 6-5. Entering fluid temperature to the Heat Pump(^{o}C) - Case1

6.5.2 Case 2

The EFT for the heat pump is shown in Figure 6-6. The EFT is somewhat higher than for Case 1, indicating the supplemental heat rejecter does not fully compensate for the reduction in GLHE size. However, the total power costs are somewhat lower than for Case 1 – because the smaller GLHE has a smaller total flow rate, the pumping costs are significantly reduced. On the other hand, the heat pump performance is also reduced by the lower flow rate.

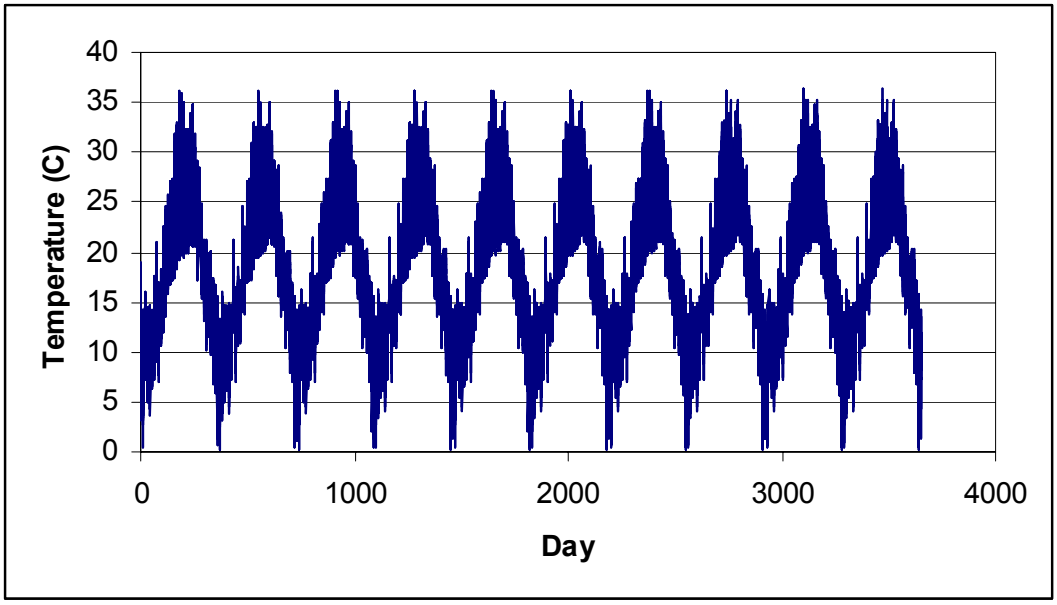

Figure 6-6. Entering fluid temperature to the Heat Pump(°C) - Case 2

6.5.3 Case 3

An increase of a third in the pavement heating system leads to slight decrease in the EFT and a negligible decrease in heat pump power consumption.

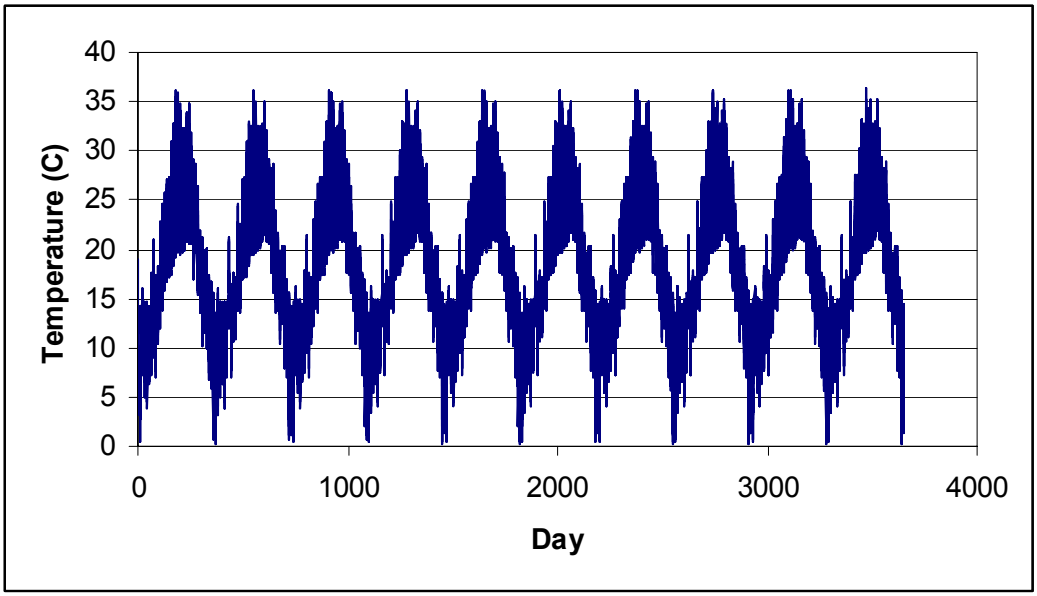

Figure 6-7. Entering fluid temperature to the Heat Pump(°C) – Case 3

Using the life cycle cost analysis assumptions explained above, the reduction in first cost is approximately $5,000 when a supplemental heat rejecter is used. In addition, a small annual savings in electricity is also obtained. The life cycle cost analysis is summarized in Table 6-3. It can be inferred from the result of case 3 that there is a point of diminishing returns when increasing the size of the supplemental heat rejecter.

Table 6-3: Life Cycle Cost Analysis Summary for each Case.

	Case 1	Case 2	Case 3
Borehole depth - ft (m)	3842 (1,171)	2162 (659)	2162 (659)
Cost of GLHE installation ($)	$23,052	$12,972	$12,972
Pavement Area - ft^2 (m^2)		388 (36)	689 (64)
Pavement construction cost ($)		$5,400	$9,600
First Cost of Equipment ($)	$23,052	$18,372	$22,572
Savings in first cost ($)		$4,680	$480
Annual operating cost ($) Circulating pump 1 Circulating pump 2 Heat Pump	 $561 $1,019	 $313 $22 $1,222	 $312 $21 $1,221
Total annual operating cost ($)	$1,580	$1,557	$1,554
Present value of 20 year operation($)	$18,122	$17,858	$17,824
Total	$41,174	$36,230	$40,396

6.6 Comparison to Previous Studies

A comparison was made to previous studies of HGSHP system, which utilize cooling tower (Yavuzturk 1999) and cooling pond as the supplemental heat rejecter (Ramamoorthy 2001). The HGSHP systems in these studies were designed for the same building and weather data as studied in this chapter; also, the same assumptions were used for borehole configuration of conventional GSHP system (base case). A larger capacity heat pump with better COP was chosen for this study, which leads to a lower operating cost when compared to that of HGSHP systems with cooling tower or pond.

For the case with the cooling tower used as a supplemental heat rejecter, the optimum design had a life cycle cost of $35,443 and when a cooling pond is used, the minimum life cycle cost was found to be $35,082.

Even though, as shown in the results in Table 6-3, the minimum life cycle cost calculated for the HGSHP system with pavement heat rejecter as supplemental heat rejecter is higher than that of HGSHP systems with cooling tower or pond, an additional benefit of snow melting is achieved when a pavement heating system is used as supplemental heat rejecter.

6.7 Conclusions and Future Recommendations

The hybrid ground source heat pump system used a pavement heating system as a supplemental heat rejecter. Compared to the standard GSHP system, the HGSHP system has significantly lower first cost and slightly lower operating cost. Some snow-melting is also obtained as a side benefit.

As the HGSHP design problem offers ample opportunity for design optimization, this should be an area of further study.

Lower set point of the differential set point controller should be chosen such that redirection of flow towards the supplemental heat rejecter is avoided when it is not advantageous. It should always be higher than zero.

CHAPTER 7

Conclusions and Recommendations

7.1 Conclusions

The design of GSHP systems is complicated by the large number of degrees of freedom. Computer simulations prove to be a useful tool in evaluating various design parameters.

The choice of antifreeze mixture can be a factor in attaining optimal design of ground source heat pump systems. Chapter 2 explains the modeling technique used to model the thermophysical properties of the antifreeze mixtures. The models developed give satisfactory results and a root mean square error of below 4% was observed for all thermophysical properties, except ethyl alcohol viscosity, for which it was below 10%.

Accurate and efficient mathematical models are required for system simulation. Chapter 3 explains the various mathematical models developed for GSHP system simulation. Development of system simulation in HVACSIM+ using the Visual Modeling Tool is also explained.

Chapter 4 investigates the various parameters in GSHP design to check for sensitivity. The GSHP design shows some sensitivity to all of the variables tested. Changing one variable at a time did not lead to significant change in the life cycle cost. The maximum saving in life cycle cost was predicted when the design was optimized with GLHE length and grout conductivity as design parameters, with all other design

parameters fixed. Methanol antifreeze mixture gave the minimum life cycle cost for all the mixtures tested.

The GSHP design developed in Chapter 4 is optimized with all the specified design parameters varied at the same time to get a global optimal value in Chapter 5. Only a 4% reduction in the life cycle cost from base case was observed. While the percentage reduction is dependent on how far off the base case design is from the optimal design, at this point in time, the optimization has not been shown to give substantial improvement.

An HGSHP system with a hydronic heated pavement system as the supplemental heat rejecter was studied in Chapter 6. Compared to the standard GSHP system, the HGSHP system has significantly lower first cost and slightly lower operating cost. Some snow-melting is also obtained as a side benefit.

7.2 Recommendations

In order to successfully use or replicate the findings of this thesis some recommendations are made as follows:

- It is recommended that good initial guesses be given as outputs to the models when fluid flow network is modeled to get the fluid mass flow rate at the operating condition.

- It was observed that heat imbalance occurs if the system is not setup correctly in HVACSIM+. It is recommended to check the heat balance of a system if more than one SUPERBLOCK is used.

- For optimization studies, the slope of the penalty function should be small.

- The initial guess for optimization should be such that the penalty function is not applied. In other words, the optimization should start with initial point in the feasible region.

Additional recommendations for future work are as follows:

- For GSHP system simulation looking at the results of varying Reynolds number over the year, it is recommended that a model of GLHE that takes into account the varying convection coefficient be used.

- Viscosity effects on the performance of the circulating pump when antifreeze mixtures are used should be modeled.

- The refrigerant property subroutines should be modified to have better exception handling.

- The cooling tower model should be modified to calculate the power consumption.

- The fluid flow network components should be modified so that they can account for the temperature rise due to fluid frictional losses.

- A scheme should be developed to handle bad initial guesses of flow rates in HVACSIM+. This could take the form of an algorithm for modifying

the initial flow rate guesses or otherwise coming up with a consistent set of initial guesses.

- The optimization is a time consuming task and may take up to several days to finish. It would be worthwhile to have ability to pause and restart GenOpt; for example if a power outage is imminent, the optimization can be paused and restarted when conditions are normal. This could be possible by editing the GenOpt code to store all the optimization results for each step.

- The time required to run an optimization study can be reduced by coupling GLHEPRO (GLHEPRO requires very little time to run a simulation) with an external optimization program or adding optimization algorithms within the program. GLHEPRO with an optimization engine can effectively be used in the GSHP system design development.

- A scheme should be developed to run an optimization with 20-year simulation using HVACSIM+. One way of doing this would be to change the HVACSIM+ simulation time step control so that the simulation time steps are longer for much of the simulation. This would require modifications to the heat pump component model, which currently expects an hourly time step, so that it can run with variable time steps.

References

Abaszade, A., N.A. Agaev, and A.M. Kerimov. 1971. Viscosity of ethyl alcohol aqueous solutions at high pressures in the 30–200.deg. range. Zhurnal Fizicheskoi Khimii 45 (10): 2672-2673.

Angell, C.A., M. Ogunl, and W.J. Sichina. 1982. Heat capacity of water at extremes of supercooling and superheating. Journal of Physical Chemistry 86: 998-1002.

ASHRAE. 1995. *ASHRAE Handbook-Applications*. Chapter 29,14-25. American Society of Heating, Refrigerating and Air-Conditioning Engineers.

ASHRAE. 2001. *ASHRAE handbook-fundamentals*, Chapter 21. American Society of Heating, Refrigerating and Air-Conditioning Engineers.

Assael, M.J., J.P.M. Trusler, and T.F. Tsolakis. 1996. Thermophysical properties of fluids: an introduction to their prediction. Imperial College Press, London.

Bates, O.K., G. Hazzard, and G. Palmer. 1938. Thermal conductivity of liquids. Ind. Eng. Chem 10 (6) : 314- 318.

Bearce, H.W., G.C. Mulligan, and M.P. Maslin. 2003. Density of certain aqueous organic solutions. International Critical Tables of Numerical Data, Physics, Chemistry and Technology. Knovel.

Bell M., and M.C. Pike. 1966. Remark on algorithm 178. Comm. ACM, (9):685-686.

Blacet, F. E., P.A. Leighton, and E.P. Bartlett. 1931. The specific heat of five pure organic liquids and of ethyl alcohol-water mixtures. Journal of Physical Chemistry 35: 1935-1943.

Bulone, D., I.D. Donato, M.B. Palma-Vittorelli, and M.U. Palma. 1991. Density, structural lifetime, and entropy of hydrogen-bond cages promoted by monohydric alcohols in normal and supercooled water. Journal of Chemical Physics 94(10), 6816-6826.

Bulone, D., C. Spinnato, F. Madonia, and M.U. Palma. 1989. Viscosity of aqueous solution of monohydric alcohols in the normal and supercooled states. Journal of Chemical Physics 91(1): 408-415.

BLAST. 1986. BLAST (Building Loads and System Thermodynamics). University of Illinois, Urbana-Champaign.

Cane, R.L.D., A. Morrison, and C.J. Ireland. 1998. Maintenance and Service Costs of Commercial Building Ground-Source Heat Pump Systems. ASHRAE Transactions, 104(2): 699-706.

Chaney, J.F., V. Ramdas, C.R. Rodriguez, and M.H. Wu. 1982. Thermophysical properties research literature retrieval guide, 1900-1980, Vol. 6. Purdue Research Foundation. Lafayette, IN.

Chaney, J.F., V. Ramdas, C.R. Rodriguez, and M.H. Wu. 1982. Thermophysical properties research literature retrieval guide, 1900-1980, Vol. 2. Purdue Research Foundation. Lafayette, IN.

Chen, X., Y. Zhu, S. Nakahara. 1999. Improvement of the fluid network's module construction for HVACSIM+. Proceedings of Building Simulation '99, Volume 3: 1229-1236.

Chiasson, A.D. 1999. Advances in Modeling of Ground-Source Heat Pump Systems. M.S. Thesis. Oklahoma State University. December. www.hvac.okstate.edu/pdfs/chiasson_thesis.pdf

Chiasson, A.D., J.D. Spitler, S.J. Rees, M.D. Smith. 2000a. A Model For Simulating The Performance Of A Pavement Heating System As A Supplemental Heat Rejecter With Closed-Loop Ground-Source Heat Pump Systems. ASME Journal of Solar Energy Engineering. November 2000. 122(4):183-191.

Chiasson, A.D., J.D. Spitler, S.J. Rees, M.D. Smith. 2000b. A Model For Simulating The Performance Of A Shallow Pond As A Supplemental Heat Rejecter With Closed-Loop Ground-Source Heat Pump Systems. ASHRAE Transactions. 106(2):107-121.

Churchill, S.W. 1977. Friction-factor equation spans all fluid flow regimes. Chem. Eng. 7: 91-92.

Clark, D. R. 1985. HVACSIM+ Building Systems and Equipment Simulation Program Reference Manual. NBSIR 84-2996. National Bureau of Standards, January.

Clark, D. R. and W.R. May. HVACSIM+. 1985. Building Systems and Equipment Simulation Program Users Guide. NBSIR 85-3243. National Bureau of Standards, September.

Commercial Solvent Corporation, 1960. Synthetic Methanol.

Daubert, T.E., and R.P. Danner. 1989. Physical and thermodynamic properties of pure chemicals: data compilation. Hemisphere Pub. Corp, New York.

Dimoplon, W. Jr. 1972. Estimating specific heat of liquid mixtures. Chem. Eng. 79 (22): 64-66.

Dizechi, M., and E. Marschall. 1982. Viscosity of some binary and ternary liquid mixtures. Journal of Chemical and Engineering Data 27 (3): 358-363.

DOE. 1997. Geothermal Energy… power from the depths. Energy Efficiency and Renewable Energy Clearinghouse.

DOE. 2004. http://www.eere.energy.gov/buildings/tech/index.html

Downing, R.C. 1974. Refrigerant Equations. ASHRAE Transactions, 80(2):158.

Dul'nev, G.N., and Y.P. Zarichnyak. 1966. Thermal conductivity of liquid mixtures. Inzhenerno-Fizicheskii Zhurnal. 11(6): 747-50.

Dunstan, A.E., and F.B. Thole. 1909. The Relation between Viscosity and Chemical Constitution. Part IV. Viscosity and chemical constituents. Journal of the Chemical Society 95: 1556-1561.

Eskilson, P. 1987. Thermal Analysis of Heat Extraction Boreholes. Doctoral Thesis, University of Lund, Department of Mathematical Physics. Lund, Sweden.

ESRU 2000. The ESP-r System for Building Energy Simulations: User Guide Version 9 Series, ESRU Manual U00/1, University of Strathclyde, Glasgow UK.

Everett, W.H., and R.E. Tapscott. 1996. Assessment of antifreeze solutions for ground source heat pump systems. Final Report. ASHRAE 908-TRP.

Filippov, L.P. 1968. Liquid thermal conductivity research at Moscow University. Int. J. Heat Mass Transfer 11: 331-345.

Filippov, L.P., and N.S. Novoselova. 1955. Vestnik Moskov. Univ., ser. Fiz.-Mat. Estestven.Nauk, no.3, 37.

Gillam, D.G., and O. Lamm. 1955. Precision measurements of thermal conductivity of certain liquids using hot wire method. Acta. Chem. Scan 9: 657-660.

Grunberg, L., and A.H. Nissan. 1949. Mixture law for viscosity. Nature 164: 799-800.

Halfpap, B.L., 1981. An investigation of some properties of supercooled fluids using photon correlation spectroscopy. M.S. Thesis. Kansas State University. Manhattan, KS.

Halfpap, B.L., and C.M. Sorensen. 1982. The viscosity of supercooled aqueous solutions of ethanol and hydrazine. Journal of Chemical Physics 77(1): 466-471.

Hare, D.E., and C.M. Sorensen. 1987. The density of supercooled water. II. Bulk samples cooled to the homogeneous nucleation limit. Journal of Chemical Physics 87(8): 4840-4845.

Heinonen, E.W., M.W. Wildin, A.N. Beall, R.E. Tapscott. 1997. Assessment of antifreeze solutions for ground-source heat pump systems. ASHRAE Transactions, 103(2): 747-756.

Hooke R., and T.A. Jeeves. 1961. 'Direct search' solution of numerical and statistical problems. J. Assoc. Comp. Mach., 8(2):212-229.

Hodge B.K., and R. P. Taylor. 1998. Analysis and design of energy systems. New Jersey: Prentice Hall, Inc.

Ivin, A.A., and S.P. Sukhatme. 1967. Specific heat of methanol solutions using a calorimeter with adiabatic shell. Indian. J. Technol. 5: 249- 250.

Jamieson, D.T., and G. Cartwright. 1978. Properties of binary liquid mixtures: heat capacity. Nat. Eng. Lab. Glasgow, Rep. 684.

Jin, H. 2002. Parameter Estimation Based Models of Water Source Heat Pumps. PhD. Thesis. Oklahoma State University.
http://www.hvac.okstate.edu/pdfs/Hui_Jin_Thesis.pdf

Jin, H., and J.D. Spitler. 2002. A parameter estimation based model of water-to-water heat pump for use in energy calculations programs. ASHRAE Transactions, 108: 3-17.

Jin, H., and J.D. Spitler. 2003. Parameter estimations based model of water-to-water heat pumps with scroll compressors and water/glycol solutions. Building Serv. Eng. Res. Technol. 24(3): 203-219.

Kennedy J., and R.C. Eberhart. 1995. Particle swarm optimization. In IEEE International Conference on Neural Networks, Perth, Australia, (IV):1942-1948.

Kennedy J., and R.C. Eberhart. 1997. A discrete binary version of the particle swarm algorithm. In Proc. of Systems, Man, and Cybernetics, (5):4104-4108.

Khan, M.H., A. Varanasi, J.D. Spitler, D.E. Fisher, R.D. Delahoussaye. 2003. Hybrid Ground Source Heat Pump System Simulation Using Visual Modeling Tool For Hvacsim+. Proceedings of Building Simulation, Eindhoven, Netherlands, August 11-14, 641-648.

Kurata, F., T.W. Yergovich, and G.W. Swift. 1971. Density and viscosity of aqueous solutions of methanol and acetone from the freezing point to 10.deg. Journal of Chemical and Engineering Data 16 (2): 222-226.

LeBrun J., J.P.Bourdouxhe, and M. Grodent. 1999. HVAC 1 Toolkit: A Toolkit for Primary HVAC System Energy Calculation. ASHRAE.

Li, C. C. 1976. Thermal conductivity of liquid mixtures. AIChE Journal 22 (5): 927-930.

Liu, X. 2004. Modeling and simulation of hydronic snow melting systems. PhD Qualifying report. Oklahoma State University.

Liu, X., S.J. Rees, and J.D. Spitler. 2003. Simulation of a Geothermal Bridge Deck Anti-icing System and Experimental Validation. Proceedings of the Transportation Research Board 82nd Annual Meeting. Washington, D.C. January 12-16, 2003.

Losenicky, Z. 1968. Thermal Conductivity of binary liquid solutions. J. Phys. Chem 72 (12): 4308-4310.

Mandal, B. P., M. Kundu, and S.S. Bandyopadhyay. 2003. Density and viscosity of aqueous solutions of (N-Methyldiethanolamine + monoethanolamine), (N-Methyldiethanolamine + diethanolamine), (2-amino-2-methyl-1-propanol + monoethanolamine), and (2-amino-2-methyl-1-propanol + monoethanolamine). Journal of Chemical and Engineering Data 48: 703-707.

Miller, L. M. 1995. Centrifugal circulating pumps, Plant Engineer, 39(3): 18-29.

Melinder, A. 1997. Thermophysical properties of liquid secondary refrigerants. International institute of refrigeration.

Mikhail, S.Z., and W.R. Kimel. 1961. Densities and viscosities of methanol-water mixtures. Journal of Chemical and Engineering Data 6: 533-537.

Millonas M.M. 1994. Swarms, phase transitions, and collective intelligence. In C. G. Langton, Ed., Artificial Life III. Addison Wesley, Reading, MA.

Misra, B.N., and Y.P. Varshni. 1961. Viscosity-temperature relation for solutions. Journal of Chemical and Engineering Data 6: 194-196.

Nishi, Y., X. Chen, and S. Nakahara. 1999. Development Of A Visual Tool For Dynamic Simulation Program HVACSIM+. Proceedings of Building Simulation '99, Volume 2: 669-674.

Noda, K., M. Ohashi, and K. Ishida. 1982. Viscosities and densities at 298.15 K for mixtures of methanol, acetone, and water. Journal of Chemical and Engineering Data 27 (3): 326-328.

Park, C., D.R. Clark, and G.E. Kelly. 1985. An Overview of HVACSIM+, a Dynamic Building/HVAC/Control Systems Simulation Program. Building Energy Simulation Conference, Seattle, Washington. August 21-22.

Perry, Chemical Engineering Handbook, 4th Edition. 1963. McGraw-Hill, New York. 3-133.

Purdy, J. 2004. Private communication.

Rackett, H.G. 1971. Calculation of the Bubble-Point Volumes of Hydrocarbon Mixture. J. Chem. Data 16 (3); 308-310.

Rafferty, K.D. 1995. A capital cost comparison of commercial ground-source heat pump systems. ASHRAE Transactions. 101(2).

Ramamoorthy, M. 2001. Applications of Hybrid Ground Source Heat Pump Systems to Buildings and Bridge Decks. M.S. Thesis. Oklahoma State University.

http://www.hvac.okstate.edu/pdfs/Ramamoorthy_Thesis.pdf

Ramamoorthy, M., H. Jin, A.D. Chiasson, J.D. Spitler. 2001. Optimal Sizing of Hybrid Ground-Source Heat Pump Systems that use a Cooling Pond as a Supplemental Heat Rejecter – A System Simulation Approach. ASHRAE Transactions. 107(1):26-38.

Rao, S.S. 1996. Engineering optimization. New York: John Wiley & Sons.

Rastorguev, Yu.L., and Yu.A. Ganiev. 1966. Thermal conductivity of aqueous solutions of organic liquids. Russ. J. Phys. Chem 40 (7): 869-871.

Rastorguev, Y.L., and Y.A. Ganiev. 1967. Thermal conductivity of non-electrolyte solutions. Russ. J. Phys. Chem 41 (6): 717-720.

Rastorguev, Y.L., and Y.A. Ganiev. 1967. Thermal conductivity of solutions of non-electrolytes. Russ. J. Phys. Chem 41 (11): 1557-1561.

Reid, R.C., J.M. Prausnitz, and T.K. Sherwood. 1977. The properties of gases and liquids. New York: McGraw-Hill.

Reidel, L. 1951. Chem. Ing. Tech 23 (19): 465- 484.

Robert W.G. 1966. Physical Properties of Hydrocarbons, Part 8. Hydrocarbon Processing 45 (10): 171-182.

Smith Lyle.B. 1969. Remark on algorithm 178. Comm. ACM, (12):638.

Sorensen, C.M. 1983. Densities and partial molar volumes of supercooled aqueous solutions. Journal of Chemical Physics 79(3): 1455-1461.

Spitler, J. 2001. Using the Earth for Energy Storage. Heat Transfer Engineering. An International Journal. Vol. 22, No. 6. Nov-Dec.

Spitler, J.D. 2000. GLHEPRO- A design tool for commercial building ground loop heat exchangers. Proceedings of the Fourth International Heat Pumps in Cold Climates Conference, Aylmer, Quebec. August 17-18.

Spitler, J.D., and C. Underwood. 2003. UK Application of Direct Cooling Ground Source Heat Pump Systems. Proceedings of ASHRAE-CIBSE Conference, Edinburgh, Scotland, September 24-26.

Stewart, W.E., and K.R.Stolfus. 1993. Predicted heat transfer characteristics of some working fluids for ground source heat pumps. Heat Pump and Refrigeration Systems Design, Analysis, and Applications. 29: 83-88.

Stephan, K., and T. Heckenberger. 1988. Thermal conductivity and viscosity data of fluid mixtures. DECHEMA, Chemistry Data Series, Vol. X, part. 1.

Stephan, K., and H. Hildwein. 1987. Recommended data of selected compounds and binary mixtures. DECHEMA, Chemistry Data Series, Vol. IV, part. 1+2.

Swardt C.A. and J.P. Meyer. 2001. A performance comparison between an air-source and a ground-source reversible heat pump. Int. J. Energy Res. 25:899-910.

Touloukian, Y.S., and T. Makita. 1970. Specific heat, non metallic liquids and gases, thermophysical properties of matter, Vol 6, TPRC data series. IFI/Plenum, New York.

Touloukian, Y.S., P.E. Liley, and S.C. Saxena. 1970a. Thermal Conductivity, non metallic liquids and gases, thermophysical properties of matter, Vol 3, TPRC data series. IFI/Plenum, New York.

Touloukian, Y. S., S.C. Saxena, , and P. Hestermans. 1970b. Viscosity, thermophysical properties of matter, Vol 11, TPRC data series. IFI/Plenum, New York.

Varanasi, A. 2002. Visual Modeling Tool for HVACSIM+. M.S. Thesis. Oklahoma State University. www.hvac.okstate.edu/pdfs/THESIS_AdityaV.pdf

Vogelaere R.De. 1968. Remark on algorithm 178. Comm. ACM, (11):498.

Wagenbreth, H. 1970. Density of ethanol-water mixtures at -20.deg. to +20.deg. PTB-Mitteilungen 80 (2): 81-86.

Wang, J., and M. Fiebig. 1996. Determination of the thermal diffusivity of aqueous solutions of methanol in an extended range of temperature by a laser-induced thermal grating technique. Experimental Thermal and Fluid Science 13: 38-43.

Waterfurnace International Technical Bulletin, 1985. Antifreeze Methods. TB8502. Fort Wayne, Indiana.

Westh, P., and A. Hvidt. 1993. Heat capacity of aqueous solutions of monohydric alcohols at subzero temperatures. Biophys. Chem. 46: 27-35.

Wetter, M. 2000. GenOpt Generic Optimization Program. Lawrence Berkeley National Laboratory.

Wetter, M. 2001. GenOpt – A Generic Optimization Program. Proceedings of seventh international IBPSA conference, Rio de Janeiro, Brazil, August 13-15, 601-608.

Yano, R., Y. Fukuda, and T. Hashi. 1988. Thermal conductivity measurement of water-ethanol solutions by the laser-induced transient grating method. Chemical Physics 124: 315-319.

Yavuzturk, C. 1999. Modeling of Vertical Ground Loop Heat Exchangers for Ground Source Heat Pump Systems. PhD. Thesis. Oklahoma State University. www.hvac.okstate.edu/pdfs/Yavuzturk_thesis.pdf

Yavuzturk, C., and J.D. Spitler. 1999. A Short Time Step Response Factor Model for Vertical Ground Loop Heat Exchangers. ASHRAE Transactions. 105(2): 475-485.

Yavuzturk, C., and J.D. Spitler. 2000. Comparative Study to Investigate Operating and Control Strategies for Hybrid Ground Source Heat Pump Systems Using a Short Time-step Simulation Model. ASHRAE Transactions. 106(2):192-209.

Yusa, M., G.P. Mathur, and R.A. Stager. 1977. Viscosity and compression of ethanol-water mixtures for pressures up to 40,000 psig. Journal of Chemical and Engineering Data 22 (1): 32-35.

Zanker, A.. 1981. Get thermal conductivity of liquid mixes quickly. Hydrocarbon Processing (3): 165-167.

Appendix A

Description of Component Models

A.1. TYPE 900: Water-to-Air Heat Pump (Equation Fit)

Component Description

This model simulates the water-to-air heat pump. The model can simulate the heat pump performance in both heating and cooling mode.

Nomenclature

$\dot{m}$ = Mass Flow Rate	(kg/sec)
Load = Space heating (+) or cooling load (-)	(W)
EFT = Entering Water Temperature	(^{o}C)
Ratio = Ratio of Heat rejected to cooling provided in cooling mode Ratio of Heat extracted to Heating provided in heating mode	(-)
ExFT = Exiting Water Temperature	(^{o}C)
Power = Power consumed	(kW)
minEFT = Minimum Entering Water Temperature	(^{o}C)
maxEFT = Maximum Entering Water Temperature	(^{o}C)
COP = Coefficient of performance	(-)
C_1 to C_5 = Coefficients for COP in heating mode	(-)
C_6 to C_{10} = Coefficients for COP in cooling mode	(-)
CoolCap = Cooling capacity	(W)
HeatCap = Heating Capacity	(W)
CC_1 to CC_2 = Coefficients for cooling capacity calculation	(-)
HC_1 to HC_2 = Coefficients for heating capacity calculation	(-)
Runtime = Runtime fraction	(-)
Unmet = Unmet loads	(-)
Fluid = antifreeze mixture type	(-)
N = weight concentration of organic liquid in antifreeze mixture	(%)

Subscript: h = Heating mode
c= Cooling mode

Mathematical Description

The entering fluid temperature input is checked to see if it lies in the fitted range by comparing to the maximum and minimum entering fluid temperature parameter.

The mode of operation (heating or cooling) is determined by checking the space heating/ cooling loads (positive for heating, negative for cooling), then the coefficient of performance in heating mode or cooling mode is calculated using Equations A.1-1a or A.1-1b.

$$COP_h = C_1 + C_2 * EFT + C_3 * EFT^2 + C_4 * \dot{m} + C_5 * EFT * \dot{m} \quad \text{(A.1-1a)}$$

$$COP_c = C_6 + C_7 * EFT + C_8 * EFT^2 + C_9 * \dot{m} + C_{10} * EFT * \dot{m} \quad \text{(A.1-1b)}$$

The heat pump power consumption is than calculated using the Equation A.1-2.

$$Power = Load / COP \quad \text{(A.1-2)}$$

The ratio of heat extracted to heating provided is calculated using Equation A.1-3a or the ratio of heat rejected to cooling provided is calculated using Equation A.1-3b.

$$Ratio_{(HE/Heating)} = 1 - 1/COP \quad \text{(A.1-3a)}$$

$$Ratio_{(HR/Cooling)} = 1 + 1/COP \quad \text{(A.1-3b)}$$

The exiting fluid temperature is calculated using the Equation A.1-4

$$ExWT = EFT - Load * RATIO / (\dot{m} * C_P) \quad \text{(A.1-4)}$$

The heating or cooling capacity is calculated using Equation A.1-5a or A.1-5b, respectively.

$$Heatcap = HC_1 * EFT + HC_2 \quad \text{(A.1-5a)}$$

$$Coolcap = CC_1 * EFT + CC_2 \quad \text{(A.1-5b)}$$

Runtime fraction is calculated by Equation A.1-6a or A.1-6b.

$$Runtime = Load / Heatcap \quad \text{(A.1-6a)}$$

$$Runtime = -Load / Coolcap \quad \text{(A.1-6b)}$$

Unmet loads are calculated by Equation A.1-7

$$Unmet = Load - HeatCap \quad \text{(A.1-7a)}$$

$$Unmet = Load + CoolCap \quad \text{(A.1-7b)}$$

Component configuration

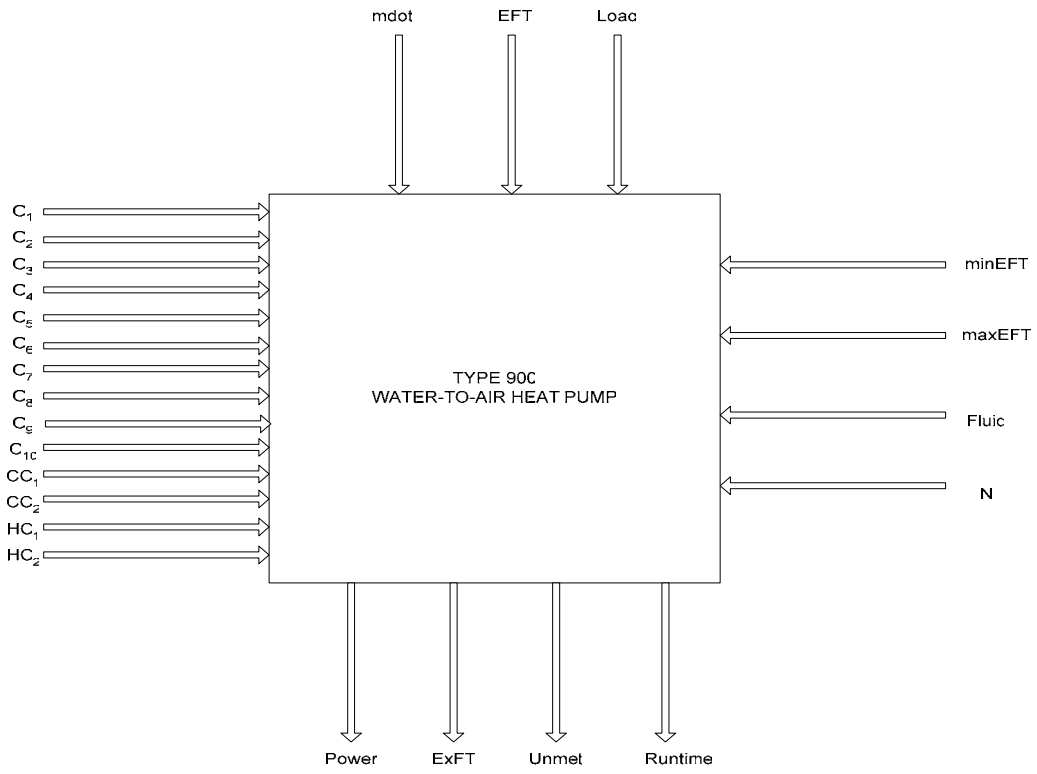

A.2. TYPE 901: Water-to-Air Heat Pump (Parameter Estimation)

Component description

This steady state component model simulates the performance of a water-to-air heat pump. This parameter estimation model can simulate the heat pump performance in both heating and cooling modes with the performance degradation caused by using antifreeze mixture as circulating fluid. A detailed description of the model can be found in Jin (2000).

Nomenclature

C = Clearance factor	(-)
C_p = specific heat of fluid	(kJ/(kg-C)
h = enthalpy	(kJ/(kg)
m = load side mass flow rate	(kg/s)
m = refrigerant mass flow rate	(kg/s)
m = source side mass flow rate	(kg/s)
$Minflow$ = Minimum mass flow rate of the heat pump	(kg/s)
$P_{suction}$ = suction pressure	(kPa)
$P_{discharge}$= discharge pressure	(kPa)
T_{SH}= superheat	(C)
T_c = condensing temperature	(C)
T_{min} =Minimum entering fluid temperatures	(C)
T_{max} =Minimum entering fluid temperatures	(C)
TL_i = load side entering fluid temperature	(C)
TL_o= load side exiting fluid temperature	(C)
TS_i = source side entering fluid temperature	(C)
TS_o= source side exiting fluid temperature	(C)
V_{cd} = specific volume of saturated vapor at condensing pressure	(m^3/kg)
V_{ev} = specific volume of saturated vapor at evaporating pressure	(m^3/kg)
V_{sh} = specific volume of superheated vapor from evaporator	(m^3/kg)
W = heat pump power consumption	(kW)
W_{loss} = constant part of the electromechanical losses	(kW)
Q_l = load side heat transfer rate	(kW)
Q_s = source side heat transfer rate	(kW)
ε_l = thermal effectiveness of the heat exchanger on load side	(-)

ε_s = thermal effectiveness of the heat exchanger on source side (-)
h = electromechanical loss factor proportional to power consumption (-)
S= Space heating/ cooling loads *(W)*
ΔP = pressure drop across suction and discharge valves (kPa)
Runtime= runtime fraction of the heat pump (-)

Mathematical description

The load side and source side heat exchangers in the heating mode and the source side heat exchanger in the cooling mode are defined as sensible heat exchangers. The Effectiveness of the heat exchanger is determined using the Equation (A.2-1) and (A.2-2):

$$\varepsilon_s = 1 - e^{\left(\frac{-UA_s}{\dot{m}_s Cp}\right)} \quad \text{(A.2-1)}$$

$$\boldsymbol{\varepsilon_l = 1 - e^{\left(\frac{-UA_l}{\dot{m}_l Cp}\right)}} \quad \text{(A.2-2)}$$

Where, UA_s and UA_l represent the overall heat transfer coefficient of the source and load sides respectively.

In the cooling mode, the split of latent and sensible heat transfer must be calculated in the load side heat exchanger. The sensible heat transfer is calculated using Equation A.2-3.

$$\dot{Q}_{Sens} = \varepsilon' \dot{m}_a Cp_a (T_{a,t} - T_{se}) \quad \text{(A.2-3)}$$

The latent heat transfer can be calculated using Equation A.2-4.

$$\dot{Q}_{latent} = \dot{Q}_{total} - \dot{Q}_{sens} \quad \text{(A.2-4)}$$

The evaporating temperature T_e and condensing temperature T_c are computed using equation (A.2-5) and (A.2-6) in the heating mode.

$$T_e = TS_i - \frac{Q_s}{\varepsilon_s \dot{m}_s Cp} \tag{A.2-5}$$

$$T_c = TL_i + \frac{Q_l}{\varepsilon_l \dot{m}_l Cp} \tag{A.2-6}$$

Guess values of Q_s and Q_l are used during the first iteration. The heat transfer rates are updated after every iteration until the convergence criteria are met.

The suction pressure and discharge pressure of the compressor is computed from the evaporator and condenser temperatures as shown in equations (A.2-7) and (A.2-8):

$$P_{suction} = P_e - \Delta P \tag{A.2-7}$$

$$P_{discharge} = P_c + \Delta P \tag{A.2-8}$$

Where, ΔP represents the pressure drops across the suction and discharge valves of the compressor respectively.

The refrigerant mass flow rate is found using the relation given by (A.2-9):

$$\dot{m}_r = \frac{PD}{Vsuc}\left[1 + C + C\left(\frac{P_{discharge}}{P_{suction}}\right)^{1/\gamma}\right] \tag{A.2-9}$$

Where, γ is the isentropic exponent and V_{suc} is the specific volume of at suction pressure.

The power consumption of the compressor for an isentropic process is computed as in Equation A.2-10.

$$W_T = \frac{\gamma}{\gamma - 1} \dot{m}_r P_{suc} \vartheta_{suc} \left[\left(\frac{P_{dis}}{P_{suc}} \right)^{\frac{\gamma-1}{\gamma}} - 1 \right] \quad \text{(A.2-10)}$$

The actual power consumption is the sum of electromechanical losses W_{loss} and the isentropic work times the loss factor η. The condenser side heat transfer rate Q_l is then the sum of power consumption W and the heat transfer rate in the evaporator Q_s.

For a given set of inputs, the computation is repeated with the updated heat transfer rates until the heat transfer rate of the evaporator and condenser converge within a specified tolerance.

Runtime fraction is calculated by Equation A.2-11a or A.2-11b.

$$Runtime = Load / Heatcap \quad \text{(A.2-11a)}$$

$$Runtime = -Load / Coolcap \quad \text{(A.2-11b)}$$

Unmet loads are calculated by Equation A.2-12a or A.2-12b

$$Unmet = Load - HeatCap \quad \text{(A.2-12a)}$$

$$Unmet = Load + CoolCap \quad \text{(A.2-12b)}$$

The runtime is multiplied by the power consumption to get the part load power consumption.

Component configuration

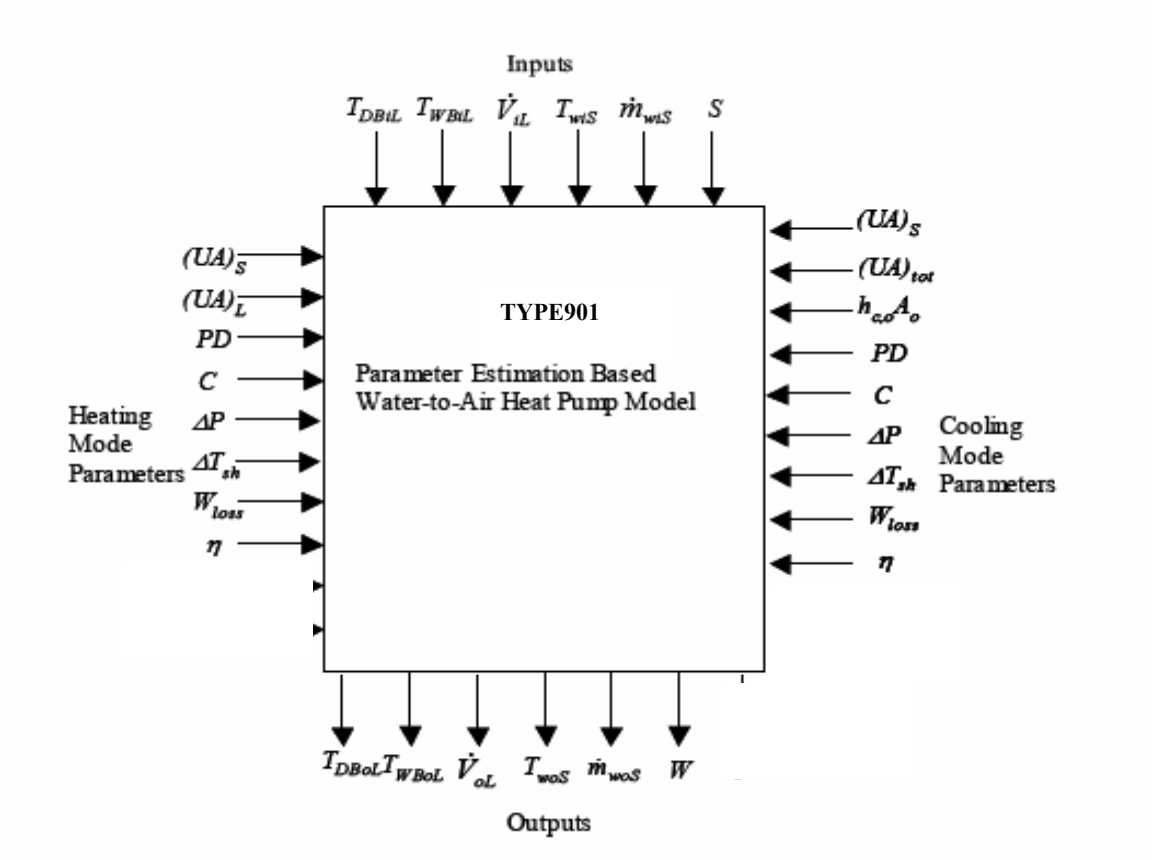

A.3. TYPE 724: Vertical Ground Loop Heat Exchanger Model

Component description

The ground loop heat exchanger (GLHE) model considered here is an updated version of that described by Yavuzturk and Spitler (1999), which is an extension of the long-time step temperature response factor model of Eskilson (1987). It is based on dimensionless, time-dependent temperature response factors known as "g-functions", which are unique for various borehole field geometries. The model includes a hierarchical load aggregation algorithm that significantly reduces computation time.

Nomenclature

$C_{\_Ground}$	= volumetric heat capacity of ground	(J/(m^{3}K))
C_{fluid}	= specific heat capacity of fluid	(J/(kgK))
$g( )$	= g-function	(--)
H	= borehole length over which heat extraction takes place	(m)
K_{Ground}	= thermal conductivity of the ground	(W/(mK))
$\dot{m}$	= mass flow rate of fluid	(kg/s)
N_b	= number of boreholes	(--)
$NPAIRS$	= number of pairs of g-function data	(--)
QN	= normalized heat extraction rate for ith hour	(W/m)
RAD_b	= borehole radius	(m)
R_b	= borehole thermal resistance	(^{o}K per W/m)
t	= current simulation time	(s)
T_{fluid_avg}	= average fluid temperature	(^{o}C)
T_{fluid_in}	= inlet fluid temperature	(^{o}C)
T_{Ground}	= undisturbed ground temperature	(^{o}C)
T_{fluid_out}	= outlet fluid temperature	(^{o}C)
t_s	= steady-state time	(s)

Mathematical Description

The g-function value for each time step is pre-computed and stored in an array. The initial ground load, which has been normalized to the active borehole length, is given by (A.3-1):

$$QN_n = \dot{m}\, C_{fluid}\,(T_{fluid\_out} - T_{fluid\_in})/(H\, N_b) \qquad \text{(A.3-1)}$$

The outlet fluid temperature is computed from average fluid temperature using equation (A.3-2):

$$T_{fluid\_out} = T_{fluid\_avg} + \frac{QN_n \cdot H \cdot N_b}{2\dot{m}C_{fluid}} \qquad \text{(A.3-2)}$$

The average fluid temperature T_{fluid_avg} is computed using the relation:

$$T_{fluid\_avg} = T_{Ground} + \sum_{i=1}^{n} \frac{(QN_i - QN_{i-1})}{2 \cdot \pi \cdot k_{Ground}} g\left(\frac{t_n - t_{i-1}}{t_s}, \frac{R_{borehole}}{H}\right) + QN_n R_b \qquad \text{(A.3-3)}$$

There are 3 unknowns T_{fluid_out}, QN_n and T_{fluid_avg} that can be solved simultaneously. The explicit solutions of T_{fluid_out}, QN_n and T_{fluid_avg} have been derived and implemented in the model.

Component Configuration

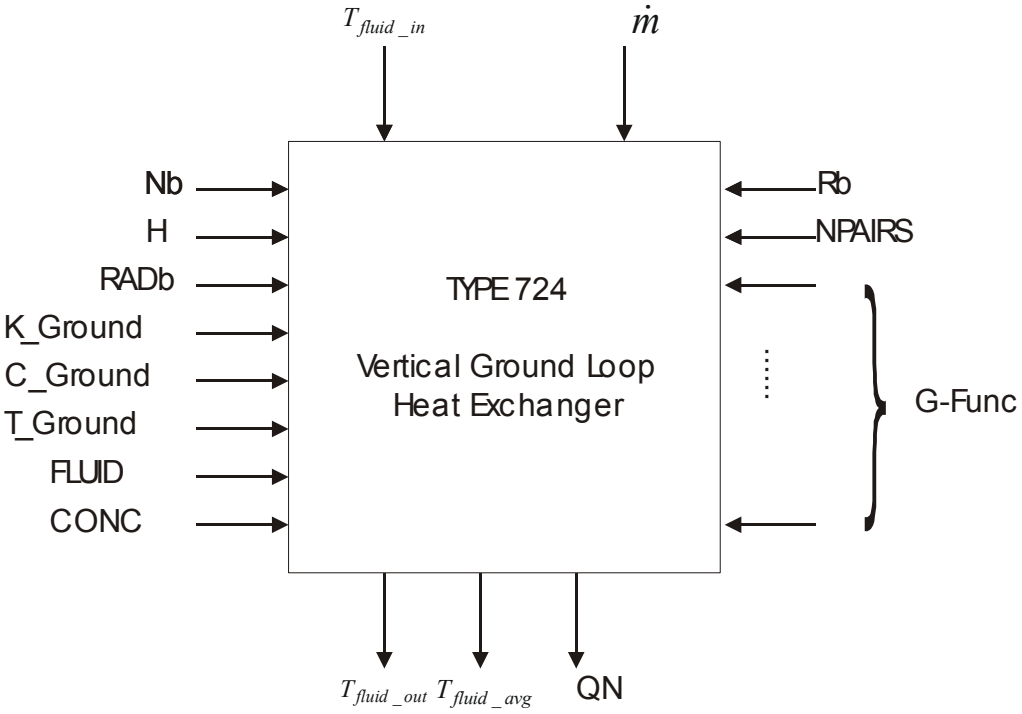

A.4 TYPE 700: Hydronically-Heated Pavement Model

General Description

This component model is developed by (Liu 2004) from a previous model described in detail by Chiasson et al. (2000). It can simulate heat transfer mechanisms within a hydronically-heated pavement. The heat transfer mechanisms within the hydronically-heated pavement include several environmental factors as well as convection due to the heat transfer fluid.

Nomenclature

α	= thermal diffusivity of pavement material	(m^2/s)
α_{solar}	= solar absorptance of pavement	(--)
Δt	= size of time step	(s)
Δx	= grid size in x direction	(m)
Δy	= grid size in y direction	(m)
ε	= emissivity coefficient	(--)
ρ	= density	(kg/m^3)
σ	= Stephan-Boltzmann constant = 5.67 x 10^{-8}	(W/m^2-$K^{4)}$
c_p	= specific heat	(J/(kg-K))
Delta	= x and y grid spacing	(m)
D_{AB}	= Binary mass diffusion coefficient	(m^2/s)
D_{pipe}	= Pipe diameter	(m)
Fo	= Fourier Number	(--)
h_c	= convection heat transfer coefficient at pavement top surface	(W/m^2-K)
h_d	= mass transfer coefficient	(kg/m^2-s)
h_{fg}	= heat of evaporation	(J/kg)
h_{if}	= latent heat of fusion of water	(J/kg)
h_{fluid}	= convection heat transfer coefficient for fluid	(W/m^2-K)
I	= solar radiation incident on the pavement surface	(W/m^2)
k	= thermal conductivity	(W/(m-°C))
l	= length	(m)
Le	= Lewis number	(--)
m''	= accumulated snow or ice per unit area	(kg/ m^2)
$\dot{m}''$	= mass flux	($kg/ s\text{-}m^2$)

mdot	= fluid mass flow rate	(kg/s)
mdott	= fluid mass flow rate per flow circuit	(kg/s)
Nu	= Nusselt Number	(--)
P	= pressure	(atmospheres)
Pr	= Prandtl Number	(--)
$q''_{cond,surface}$	= conductive heat flux at the pavement top surface	(W/m^2)
q''_{conv}	= convective heat flux from pavement surface	(W/m^2)
q''_{evap}	= heat flux due to evaporation	(W/m^2)
q''_{fluid}	= heat flux from heat carrier fluid	(W/m^2)
q_{fluid}	= heat transfer rate per unit length of pipe	(W/m)
q''_{melt}	= heat flux for melting snow	(W/m)
q''_{rad}	= solar radiation heat flux	(W/m^2)
q''_{sen}	= sensible heat for melting snow	(W/m^2)
$q''_{thermal}$	= thermal radiation heat flux from pavement surface	(W/m^2)
Re	= Reynold's Number	(--)
Snowfall	= snowfall rate	(mm of water equivalent per hr)
t	= time	(s)
T	= temperature	(°C or K)
$T_{(m,1)}$	= surface node temperature	(°C)
$T_{(x,y)}$	= non-surface node temperature	(°C)
U	= overall heat transfer coefficient for fluid	(W/m^2-°C)
w	= humidity ratio	(kg water /kg d.a.)
wallt	= pipe wall thickness	(m)

Subscript :

amb	= ambient air
avg	= average
circuit	= per circuit of flow
evap	= evaporation
fl	= fluid
in	= inlet
out	= outlet
pipe	= pipe
pv	= pavement
r	= thermal radiation
sky	= sky
snow	= snow
wt	= water

Mathematical Description

The governing equation of model is the two-dimensional form of the transient heat diffusion equation given in Equation A.4-1:

$$\frac{\partial^2 T}{\partial x^2} + \frac{\partial^2 T}{\partial y^2} = \frac{1}{\alpha}\frac{\partial T}{\partial t} \tag{A.4-1}$$

Appearing in all nodal equations is the finite-difference form of the Fourier number as given in Equation (A.4-2).

$$Fo = \frac{\alpha \Delta t}{(\Delta x)^2} \tag{A.4.2}$$

One disadvantage of the fully explicit finite difference method employed in this model is that the solution is not unconditionally stable. For a 2-D grid, the stability criterion is:

$$Fo \leq \frac{1}{4} \tag{A.4.3}$$

For the prescribed values of α and Δx, the appropriate time step can be determined with Equation (A.4.3).

Heat Flux Calculation Algorithm

To provide the finite-difference equations with the appropriate heat flux term at the boundaries, the heat fluxes considered in the model are as follows.

Solar radiation heat flux

Convection heat flux at the pavement surfaces

Thermal radiation heat flux

Heat flux due to evaporation of rain and melted snow

Heat flux due to melting of snow

Convection heat transfer due to internal pipe flow

Solar Radiation Heat Flux

$$q''_{solar} = \alpha_{solar} I \tag{A.4-4}$$

Convection Heat Flux at the pavement Surface

$$q''_{convection} = h_c (T_{amb} - T_{(m,1)}) \tag{A.4-5}$$

The convection coefficient (h_c) is then computed by following equation:

$$h_c = \frac{Nuk}{L} \tag{A.4-6}$$

Thermal Radiation Heat Flux

This model uses a linearized radiation coefficient (h_r) defined as given in Equation A.4-7.

$$h_r = 4\varepsilon\sigma\left(\frac{T_{(m,1)} + T_2}{2}\right)^3 \tag{A.4-7}$$

where, $T_{(m,1)}$ is the surface node temperature in absolute units, and T_2 represents the sky temperature or ground temperature in absolute units. If the bottom of the bridge is exposed, T_2 represents the ground temperature in absolute units, which is approximated as

the air temperature. The thermal radiation heat flux at each surface node ($q''_{thermal}$) is then computed by:

$$q''_{thermal} = h_r (T_2 - T_{(m,1)}) \tag{A.4-8}$$

Heat Flux Due to Evaporation of Rain and Melted Snow

Heat flux due to evaporation is considered only if the temperature of a specified top surface node is not less than 32 °F (0 °C) and there is no snow layer covered on the surface. This model uses the j-factor analogy to compute the mass flux of evaporating water at each pavement top surface node ($\dot{m}''_{evap}(m,1)$):

$$\dot{m}''_{evap}(m,1) = h_d (w_{air} - w_{(m,1)}) \tag{A.4-9}$$

where, w_{air} is the humidity ratio of the ambient air, and $w_{(m,1)}$ represents the humidity ratio of saturated air at the top surface node, which is calculated with the psychrometric chart subroutine PSYCH companied with HVACSIM+ package. The mass transfer coefficient (h_d) is defined using the Chilton-Colburn analogy by Equation A.4-10.

$$h_d = \frac{h_c}{c_p Le^{\frac{2}{3}}} \tag{A.4-10}$$

The heat flux due to evaporation ($q''_{evap(m,1)}$) is then given by Equation A.4-11.

$$q''_{evap}(m,1) = h_{fg} \dot{m}''_{evap} \tag{A.4-11}$$

Heat Flux Due to Melting of Snow

The heat required to melt snow includes two parts: one is the amount of sensible heat needed to raise the temperature of the snow to 0 °C, the other is the heat of fusion. The temperature of freshly fallen snow is assumed to be the air temperature T_{air} in this model.

The heat flux for melting snow q''_{melt} is determined with heat and mass balance on a specified top surface node. In this model, snow is treated as an equivalent ice layer. The heat available for melting the snow on a specific node can come from the conductive heat flux from its neighbor nodes and the heat stored in the cell represented by the node.

Convection Heat Transfer Due to Internal Pipe Flow

Since the outlet temperature at any current time step is unknown, it is determined in an iterative manner. The heat flux transferred from the heat carrier fluid through the pipe wall (q''_{fluid}) is computed by EquationA.4-12:

$$q''_{fluid} = U(T_{fl\_avg} - T_{(x,y)}) \tag{A.4-12}$$

where, U is the overall heat transfer coefficient between the heat carrier fluid and pipe wall, which is expressed as:

$$U = \frac{1}{\frac{1}{h_{fluid}} + \frac{l}{k_{pipe}}} \tag{A.4-13}$$

The convection coefficient due to fluid flow in the pipe (h_{fluid}) is determined using correlations for the Nusselt Number in flow through a horizontal cylinder. For laminar flow in the pipe (Re<2300), the Nusselt Number is a constant equal to 4.36. For transition and turbulent flow, the Gnielinski correlation is used to compute the Nusselt Number given in Equation A.4-14.

$$Nu_{TranTurb} = \frac{(f/2)(\mathrm{Re}-1000)\,\mathrm{Pr}}{1+1.27(f/2)^{\frac{1}{2}}(\mathrm{Pr}^{\frac{2}{3}}-1)} \tag{A.4-14}$$

Where, the friction factor f is given by Equation (A.4-15).

$$f = \left[1.58\ln(\mathrm{Re}) - 3.28\right]^{-2} \tag{A.4-15}$$

The gap between 4.36 (the Nu number for laminar flow) and the value calculated from the Gnielinski correlation for transition flow could result in discontinuities in the value of convection coefficient. It will introduce problem for the iterative process to obtain a converged solution for the outlet temperature. In order to avoid this problem, the gap of the Nu number is "smoothed" by following equation:

$$Nu = \sqrt{4.36^2 + Nu_{TranTurb}{}^2} \tag{A.4-16}$$

Finally, the convection coefficient due to fluid flow in the pipe (h_{fluid}) is given by Equation A.4-17.

$$h_{fluid} = \frac{Nu \cdot k_{fl}}{L} \tag{A.4-17}$$

Where, the characteristic length (L) is defined as the inner diameter of the pipe.

Component configuration

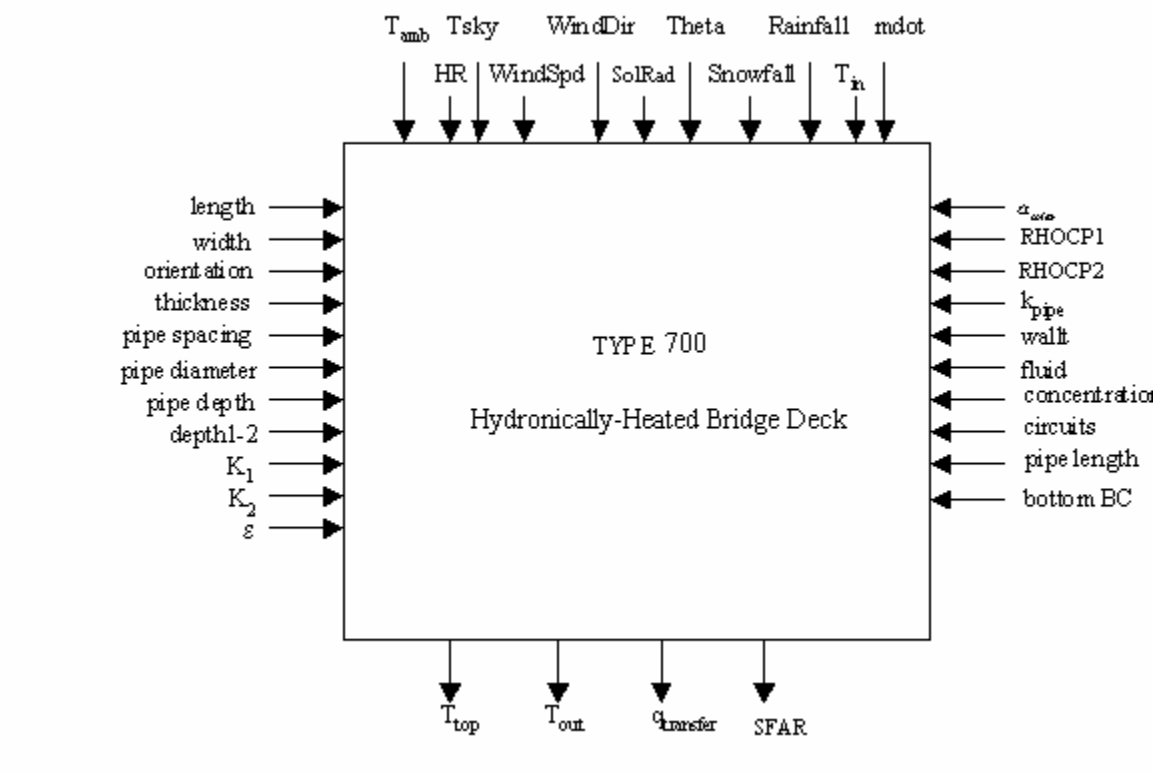

A.5 TYPE 902: Counter Flow Heat Exchanger Model

Component Description

This is a simple counter flow heat exchanger model based on the ε-NTU method.

Nomenclature

$\dot{m}_1$ = Mass Flow Rate of fluid 1	(kg/sec)
$\dot{m}_2$ = Mass Flow Rate of fluid 2	(kg/sec)
Q = Heat Transfer Rate	(kW)
C_{P1} = Specific heat of fluid 1	(kJ/kg k)
C_{P2} = Specific heat of fluid 2	(kJ/kg k)
UA = Overall heat transfer co-efficient times the Area	(kW/K)
$C_{\min}$ = Minimum of the two heat capacities	(kW/K)
$C_{\max}$ = Maximum of the two heat capacities	(kW/K)
NTU = Number of transfer units	(-)
ε = Effectiveness	(-)
T_h = Temperature of the hot fluid	(^{o}C)
T_c = Temperature of the cold fluid	(^{o}C)

Subscript:

In = Inlet
Out = Outlet
1 = Fluid 1
2 = Fluid 2

Mathematical Description

Effectiveness of the heat-exchanger is defined as the ratio of the actual rate of heat transfer to the maximum possible rate of heat exchange.

Effectiveness of a counter flow heat exchangers is used calculated using Equation A.5-1

$$\varepsilon = \frac{1 - \exp\left[-\mathrm{NTU}(1-\mathrm{C})\right]}{1 - \mathrm{C}\ \exp\left[-\mathrm{NTU}*(1-\mathrm{C})\right]} \qquad \text{(A.5-1)}$$

NTU is calculated using Equation A.5-2

$$NTU = \frac{UA}{C_{\min}} \tag{A.5-2}$$

Heat transfer is calculated using Equation A.5-3

$$Q = \varepsilon C_{\min}(T_{h_{in}} - T_{c_{in}}) \tag{A.5-3}$$

The temperature of the exiting fluid is calculated by Equation A.5-4a and A.5-4b

$$T_{h_{out}} = T_{h_{in}} - q\left(\frac{C_{\max}}{C_{\min}}\right) \tag{A.5-4a}$$

$$T_{c_{out}} = T_{c_{in}} + q\left(\frac{C_{\max}}{C_{\min}}\right) \tag{A.5-2b}$$

Component configuration

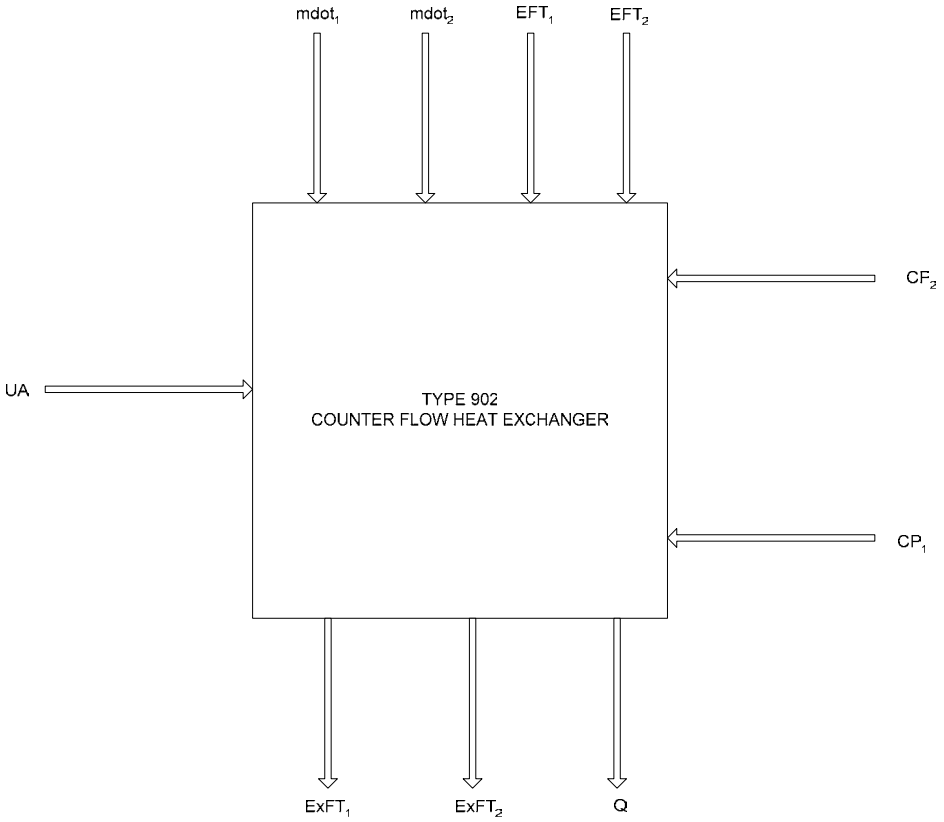

A6. TYPE 903: Cooling Tower Model

General Description

The cooling tower is modeled as a counter flow heat exchanger with water as one of the fluids and moist air treated as an equivalent ideal gas as the second fluid.

Component Configuration

UA= Overall heat transfer co-efficient times the Area	(W/K)
C_{min}= Minimum of the two heat capacities	(kW/K)
C_{max}= Maximum of the two heat capacities	(kW/K)
C= ratio of minimum and maximum heat capacity	(-)
NTU = Number of transfer units	(-)
ε = Effectiveness	(-)
T= Temperature	(C)
C_P= Specific heat	(kJ/kg K)
h= Saturated air enthalpy	(kJ/kg)

Subscript:

e = equivalent
in = Inlet
out = Outlet
wb = wet bulb
w = water

Mathematical Description

The saturated air enthalpy is calculated as a function of entering air wet bulb temperature using A.6-1.

$$h = \sum_{i=0}^{3} C_i T^i{}_{wb} \qquad \text{(A.6-1)}$$

An iterative process is used to calculate the T_{wbout}. The effective specific heat is calculated as in Equation A.6-2 with a guess value of T_{wbout}.

$$C_{pe} = \frac{h_{out} - h_{in}}{T_{wbout} - T_{wbin}} \tag{A.6-2}$$

The effective heat transfer coefficient-area product is:

$$UA_e = UA\frac{C_{pe}}{C_p} \tag{A.6-3}$$

The heat exchanger effectiveness is calculated as given in Equation A.6-4.

$$\varepsilon = \frac{1 - \exp[-NTU(1-C)]}{1 - C\exp[-NTU(1-C)]} \tag{A.6-4}$$

Water-air heat transfer rate is calculated using Equation A.6-5.

$$Q = \varepsilon C_{\min}(T_{w_{in}} - T_{wb_{in}}) \tag{A.6-5}$$

The leaving air wet bulb temperature and leaving water temperature are calculated by Equation A.6-6 and A6-7 respectively.

$$T_{wb_{out}} = T_{wb_{in}} + \left(\frac{Q}{C_e}\right) \tag{A.6-6}$$

$$T_{w_{out}} = T_{w_{in}} - \left(\frac{Q}{C_w}\right) \tag{A.6-7}$$

Component configuration

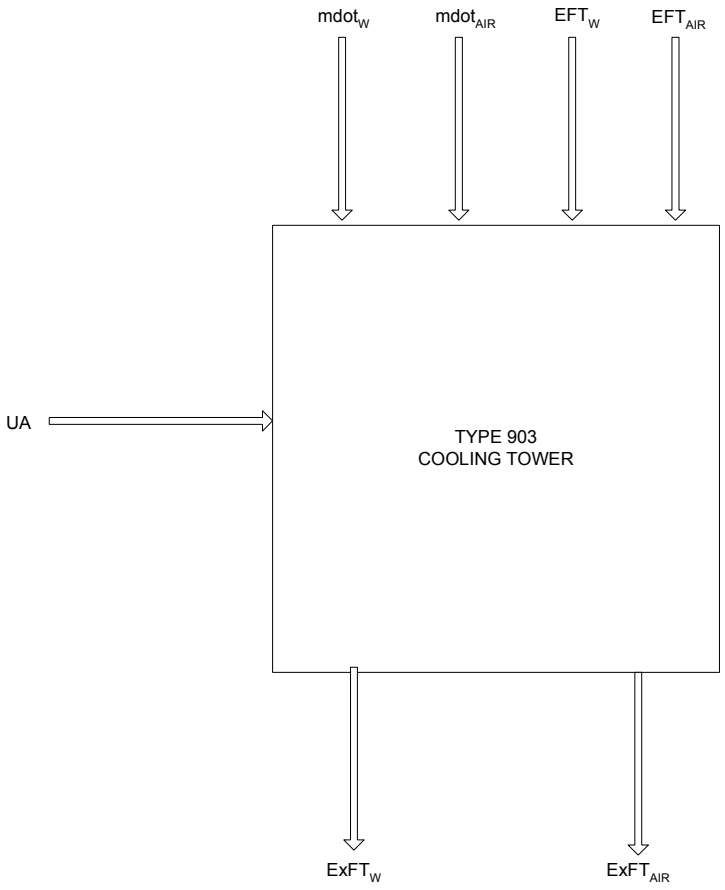

A8. TYPE 905: Ideal Circulating Pump Model

General description

This pump model computes the power consumption and the temperature rise of the fluid using the parameters of fluid mass flow rate, pressure rise across the pump, and the pump efficiency.

Nomenclature

$\dot{m}_{out}$ = actual fluid mass flow rate	(kg/s)
P = pump power consumption	(kW)
T_{in} = inlet fluid temperature	(°C)
T_{out} = outlet fluid temperature	(°C)
ΔP = pressure drop across the pump	(kPa)
η = pump efficiency	(-)
ρ = density of the fluid	(kg/m^3)
C_p= Specific heat of the fluid	(kJ/kg K)

Mathematical description

The pump power consumption P and the outlet fluid temperature T_{out} are computed using relation (A.8-1) and (A.8-2) respectively.

$$P = \frac{\Delta P \dot{m}_{out}}{\rho \cdot \eta} \tag{A.8-1}$$

$$T_{out} = T_{in} + \Delta P \left(\frac{\frac{1}{\eta} - 1}{\rho \cdot C_p} \right) \tag{A.8-2}$$

Component configuration

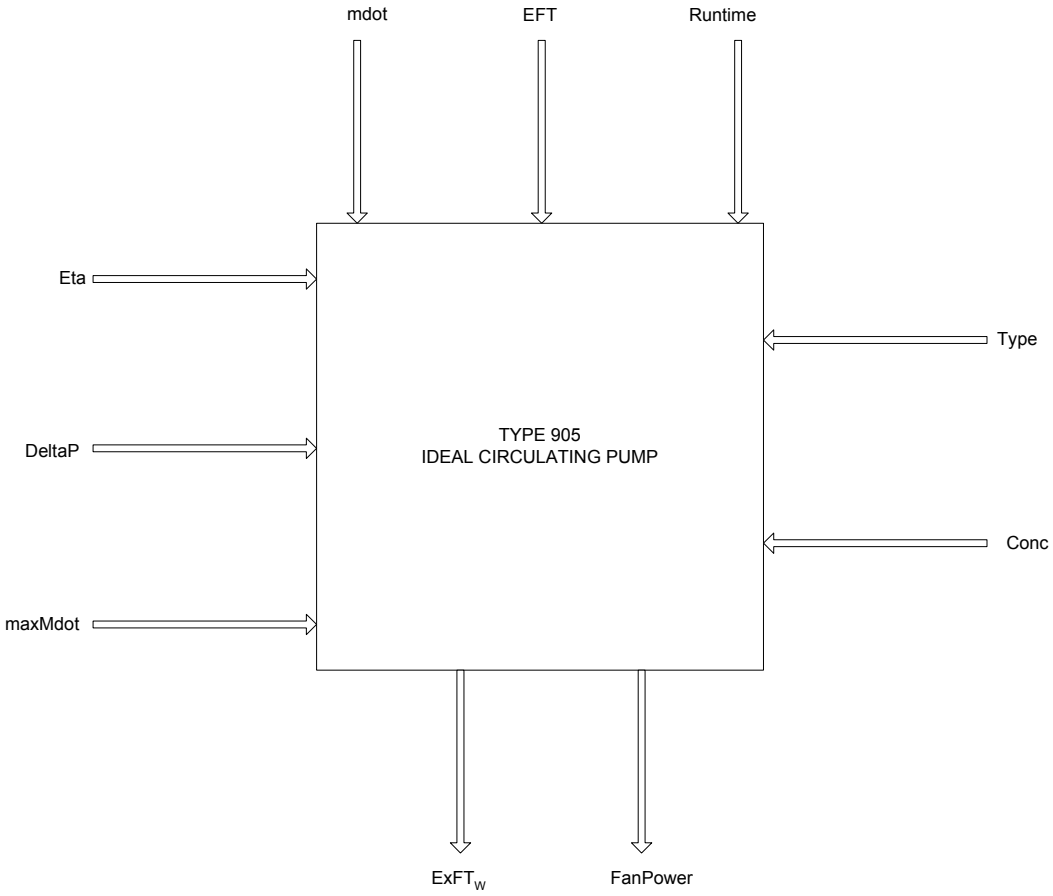

A9. TYPE 906: Detailed Circulating Pump Model

Component description

The detailed model determines the fluid flow rate for a pressure drop input. Coefficients for the equation fit on the dimensionless mass flow rate as a function of dimensionless pressure rise and the coefficients for the efficiency as a function of dimensionless pressure rise are provided by the user. As the model is an equation fit so the max and the min pressure rise given in the catalog data should be provided to limit the power and mass flow rate calculations.

Nomenclature

$\dot{m}$ = mass flow rate	(kg/s)
ρ= density	(kg/m^3)
D = Impeller Diameter	(m)
EFT = entering fluid temperature	(C)
ΔP = Pressure Rise	(kPa)
φ = dimensionless mass flow rate	(-)
Ψ = dimensionless pressure rise	(-)

Mathematical description

The model is based on similarity considerations the dimensionless flow variable and the dimensionless pressure rise are calculated as follows

$$\varphi = \frac{\dot{m}}{\rho \mathrm{N} D^3} \tag{A.9-1}$$

$$\psi = \frac{\Delta P}{\rho \mathrm{N}^2 D^2} \tag{A.9-2}$$

Given the catalog data the and are estimated as a 4th order polynomial of the following form

$$f(\varphi) = \sum_{i=0}^{4} C_i \psi^i \qquad \text{(A.9-3)}$$

Component configuration

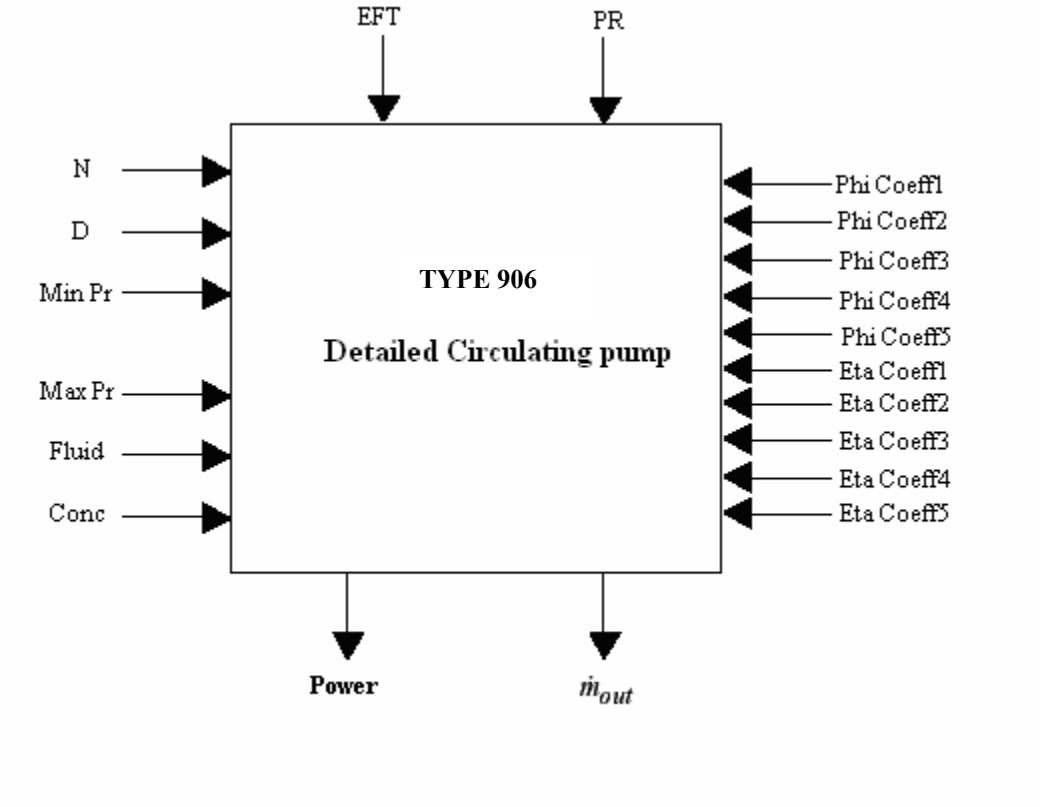

A10. TYPE 907: Fluid Mass Flow Rate Divider Model

Component description

The model divides the input mass flow rate by a user-defined factor to get a number of flow rate outputs. The model in HVACSIM+ has the maximum number of outputs set to six.

Nomenclature

$\dot{m}_{out}$ = outlet mass flow rate	(kg/s)
$\dot{m}_{in}$ = inlet mass flow rate	(kg/s)
factor = mass flow rate fraction	(-)

Mathematical Description

The exiting mass flow rates are calculated by Equation (A.10-1)

$$\dot{m}_{out} = \dot{m}_{in} * factor \qquad \text{(A.10-1)}$$

Component configuration

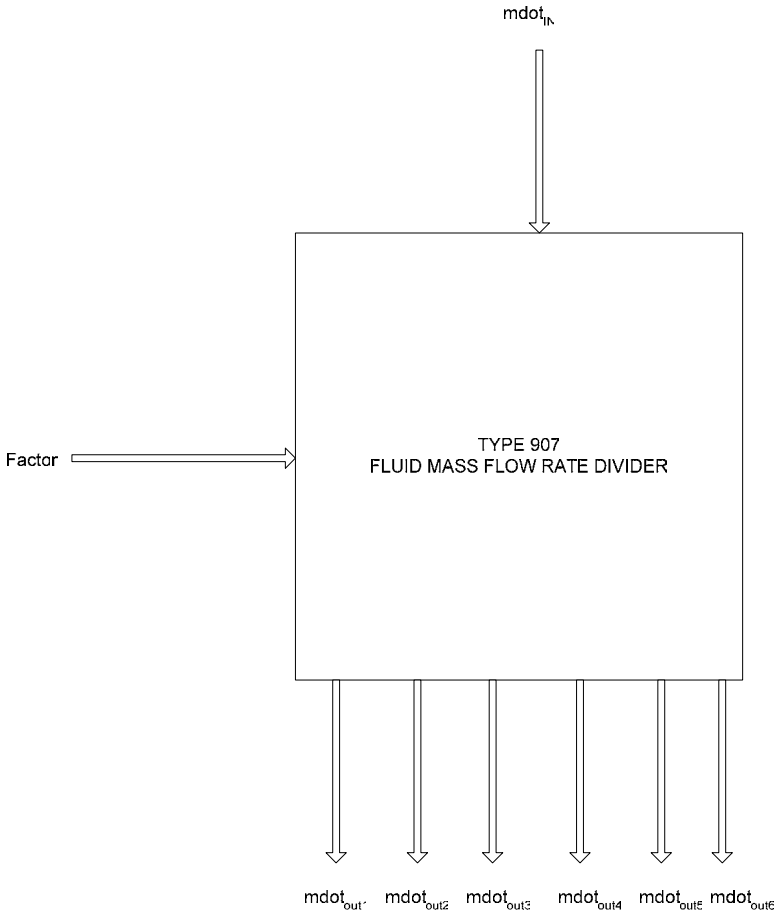

A11. TYPE 908: Pressure Drop Adder Model

Component description

This model sums up the input pressure drops and gives the sum as an output. The maximum number of inputs is set to six in HVACSIM+.

Nomenclature

Δp_{out} = outlet mass flow rate (kPa)
Δp_{in} = inlet mass flow rate (kPa)

Mathematical Description

The pressure drop sum is given by Equation A.11-1.

$$\Delta p_{out} = \sum_{i=0}^{5} \Delta p_{in} \tag{A.11-1}$$

HVACSIM+ does not allow any model without a parameter so a dummy variable is defined as the parameter

Component configuration

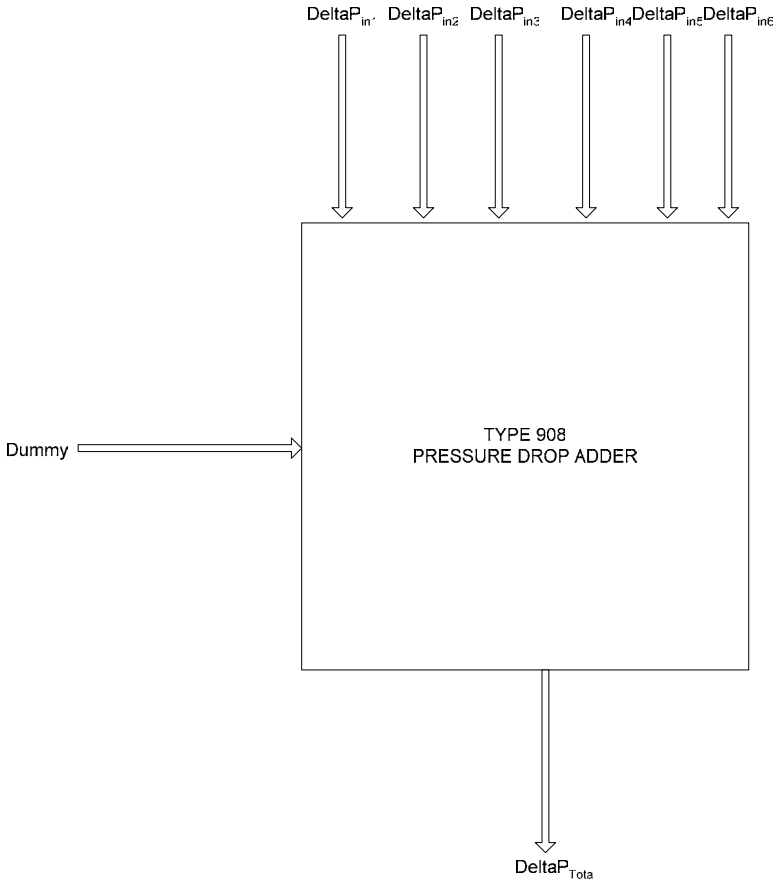

A12. TYPE 909: Pipe Pressure Drop Model

Component description

The model calculates the pressure drop in a pipe. The friction factor is calculated using the Churchill correlation (Churchill 1977).

Nomenclature

ΔP_{pipe} = pressure drop through a straight pipe	(Pa)
f = friction factor	(-)
g_c = constant of proportionality = 1	(kg m/ N s^2)
A = Area	(m^2)
L = Length of pipe	(m)
ρ= Density of the fluid	(kg/m^3)
$\dot{m}$ = mass flow rate	(kg/sec)
D = pipe Diameter	(m)
Re=Reynolds number	(-)
rr= roughness ratio	(-)

Mathematical description

The pressure drop is calculated the using the Equation A.12-1.

$$\Delta P_{pipe} = \frac{f\dot{m}^2 L}{2A^2 D\rho g_c} \qquad \text{(A.12-1)}$$

Friction factor is calculated using the Churchill correlation given in Equation A.12-2.

$$f = 8\left[\left(\frac{8}{\mathrm{Re}}\right)^{12} + (\mathrm{a}+\mathrm{b})^{-1.5}\right]^{\frac{1}{12}} \qquad \text{(A.12-2)}$$

Where,

$$a = \left(2.457 \, \mathrm{Ln} \left[\frac{1}{\left(\frac{7}{\mathrm{Re}} \right)^{0.9} + 0.27 * \mathrm{rr}} \right] \right)^{16}$$

$$b = \left[\frac{37530}{\mathrm{Re}} \right]^{16}$$

rr = roughness ratio (-)

$$\mathrm{Re} = VD/\nu$$

Component configuration

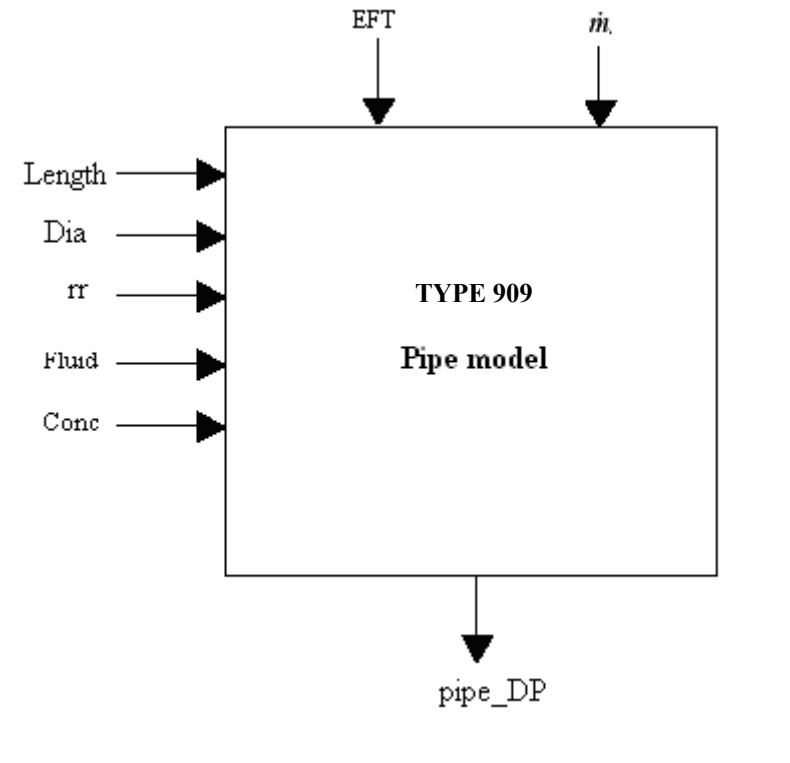

A13. TYPE 910: Fitting Pressure Drop Model

Component description

The model calculates the pressure drop in fittings.

Nomenclature

ΔP_{fit} = Fitting Pressure Drop	(kPa)
K= the loss coefficient	(-)
V= velocity	(m/s)
g_c = constant of proportionality = 1	(kg m/ N s^2)

Mathematical description

The pressure drop is calculated the using the Equation A.13-1.

$$\Delta P_{fit} = K \frac{V^2}{2g_c} \qquad \text{(A.13-1)}$$

Component configuration

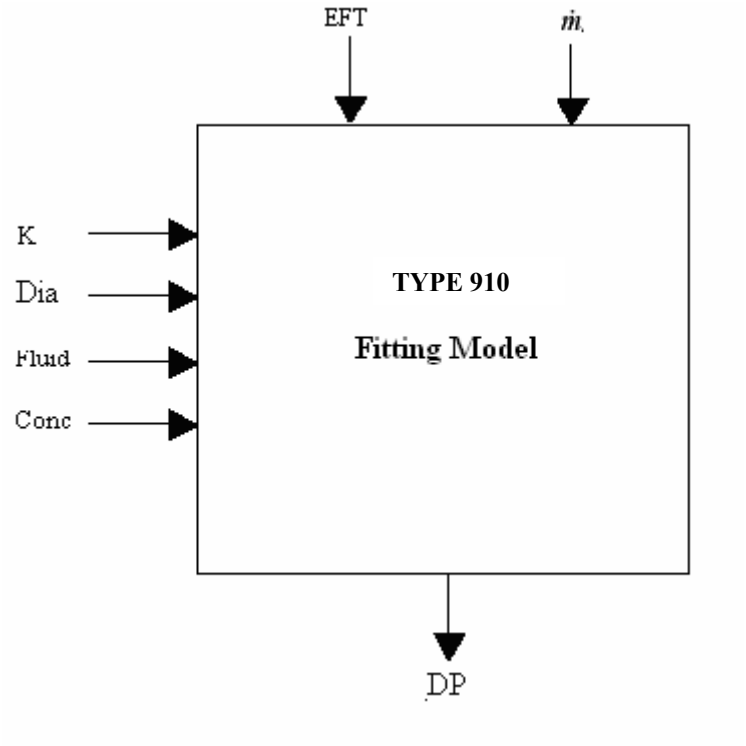

Appendix B

Cooling Tower UA Calculator Description and Step-By-Step Instructions

The purpose of the program is to determine the overall heat transfer coefficient – area associated with a given specified mass flow rate based on one operating point in steady-state operating conditions (LeBrun et al. 1999).

The program requires entering water mass flow rates, entering air mass flow rate, range (difference between entering and leaving water temperatures), approach (difference between the leaving water temperature and entering air wet-bulb temperature), and the entering air wet bulb temperature as inputs.

The program follows the following algorithm:

- Calculates the leaving and entering water temperatures
- Calculates the entering moist air enthalpy, water heat capacity flow rate and water-air heat transfer rate
- Iterative process : first guesses the leaving air wet-bulb temperature
    - Calculates the leaving moist-air enthalpy, the effective specific heat and the effective fluid heat capacity flow rate
    - Recalculates the leaving air wet-bulb temperature
- Calculates the effective heat transfer coefficient-area product
- Calculates the actual heat transfer coefficient-area product

STEP-BY-STEP INSTRUCTIONS:

1. Copy “coolingtowerUA.jar” from D:\Utilities\coolingtowerModelUA to working directory (assuming D:\ is the device name for the CDROM).
2. Open the command prompt window to run “coolingtowerUA.jar” by using the following command “java -jar coolingtowerUA.jar” (do not double click the file to open it). The JAVA Runtime Environment (JRE) should be installed to run the command. If it is not installed, go to http://java.sun.com/ website and download JRE.
3. After running the above command, the interface appears as shown in Figure B-1. Enter the required parameter and then press calculate UA button. The over heat transfer coefficient time the area is calculated and shown.

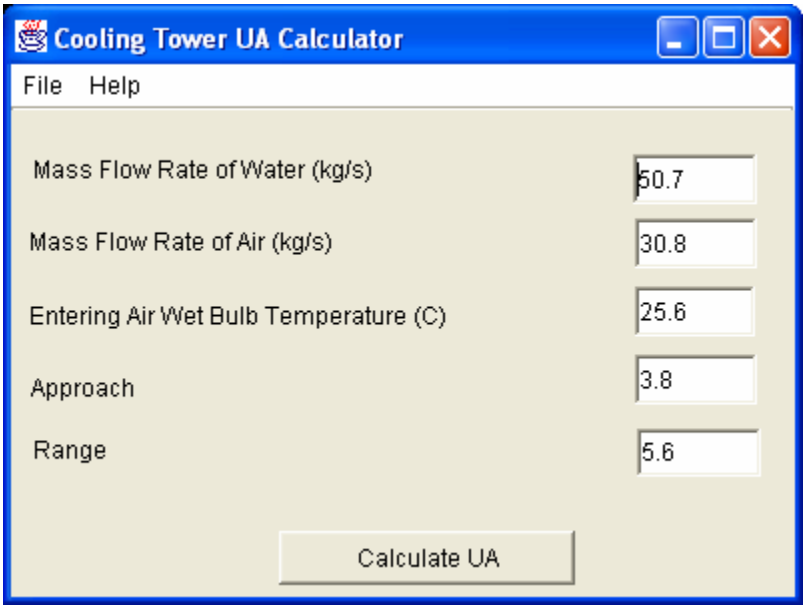

Figure B-1 graphical user interface of the UA calculator

Appendix C

Multiyear Simulation Step-By-Step Instructions

1. Copy “output.jar” from D:\Utilities\bnd_out_processor to working directory (assuming D:\ is the device name for the CDROM).
2. Copy all the necessary files required by MODSIM to your working directory, this includes the .dfn, .bnd, .sum, .fin, .out, .ini and the inputfile.dat files.
3. Open the command prompt window to run “output.jar” by using the following command “java -jar output.jar” (do not double click the file to open it). The JAVA Runtime Environment(JRE) should be installed to run the command. If it is not installed, go to http://www.java.com/ website and download it. The main interface of the program is displayed as shown in Figure C-1.

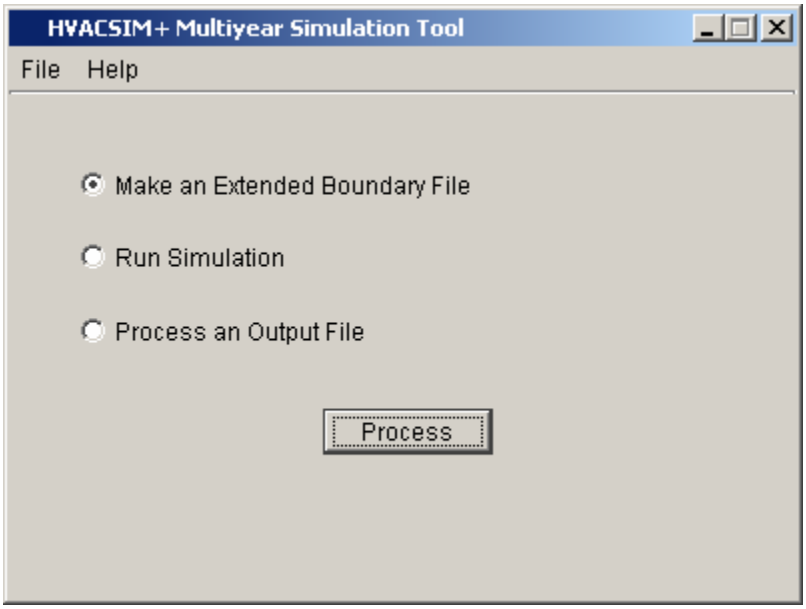

Figure C-1 main form

4. Select option 1 (make an extended boundary file) from the GUI and click on the “process” button. Another form will open showing two buttons as shown in Figure C-2.

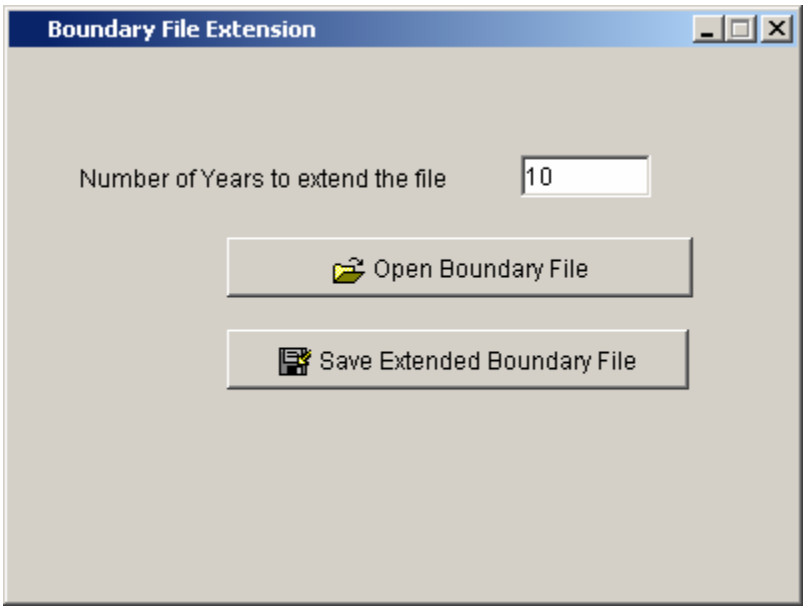

Figure C-2 Boundary file extension form.

“open boundary file” opens a dialog box for the location of the boundary file to be extended, and “save boundary file” opens a dialog box for the location to save the extended boundary file.

5. The second option “Run simulation” open a form as shown in Figure C-3.

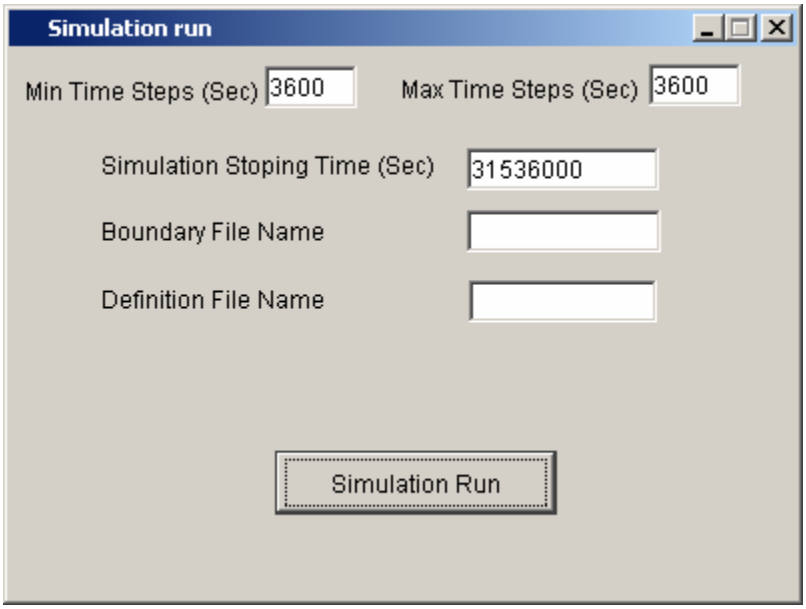

Figure C-3 Simulation run form

The simulation time step and running time is required as an input, also the names of the files required by MODSIM are the required fields. The "simulation run" button automatically edits the inputfile.dat file according the user inputs and calls MODSIM to start the simulation.

6. At the end of the simulation a file with ".out" extension is created which can be processed selecting the option 3 (process an output file) in the main form. Figure C-4 shows the output file processor form.

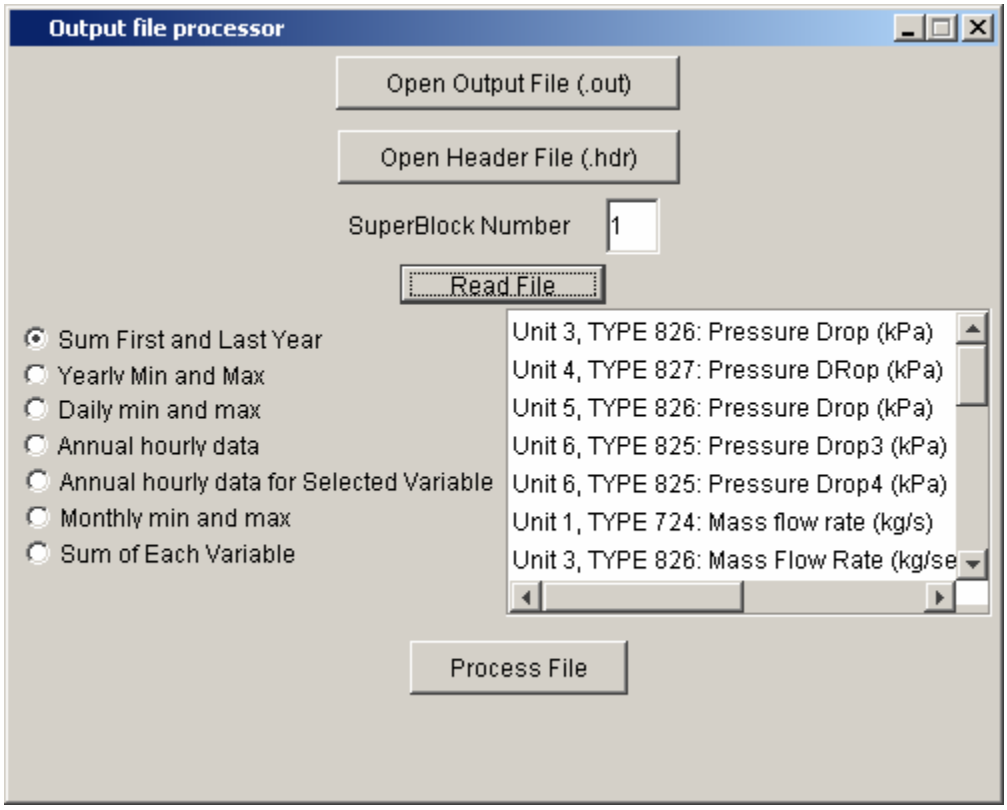

Figure C-4 Output file processor form

The output file generated at the end of simulation is opened along with the associated simulation header file (header file created by Visual Modeling Tool only). “read file” button opens the file and reads it, the file is now ready for processing, any of the processes shown in Figure C-4 can be used as desired.

VITA

Muhammad Haider Khan

Candidate for the Degree of

Master of Science

Thesis: MODELING, SIMULATION AND OPTIMIZATION OF GROUND SOURCE HEAT PUMP SYSTEMS

Major Field: Mechanical Engineering

Biographical:

Personal: Born in Karachi, Pakistan, on May 18, 1977, to Muhammad Imtiaz Khan and Shahida Begum.

Education: Received Bachelor of Science in Mechanical Engineering from University of Engineering and Technology, Lahore, Pakistan in August 2000. Completed the requirements for the Master of Science degree with a major in Mechanical Engineering at Oklahoma State University in December, 2004

Experience: Employed by Oklahoma State University, Department of Mechanical Engineering as a graduate Research assistant March 2002 to date.

Professional Memberships: Student Member ASHRAE.